STRESS, A MATTER OF BALANCE

Hypothalamic glucocorticoid receptor in CRF neurons is essential for HPA axis habituation to repeated stressor

Dissertation
der Fakultät für Biologie
der Ludwig-Maximilians-Universität München

November, 2020

Dournes, Carine
dournes.carine@gmail.com

Diese Dissertation wurde angefertigt
unter der Leitung von Prof. Dr Alon Chen, im Bereich von Max Planck Institute of Psychiatry
an der Ludwig-Maximilians-Universität München

Tag der Abgabe: 02.11.2020
Tag der mündlichen Prüfung: 16.03.2021

Erstgutachter: PD Dr. Schmidt
Zweitgutachterin: Prof. Dr. Busse

Supervisors:

Prof. Dr. Alon Chen

Stress Neurobiology and Neurogenetics,
Max Planck Institute of Psychiatry,
Munich, Germany

The Ruhman Family Laboratory for Research on the Neurobiology of Stress, Department of Neurobiology, Weizmann Institute of Science, Rehovot, Israel

Dr. Jan M. Deussing

Stress Neurobiology and Neurogenetics,
Max Planck Institute of Psychiatry,
Munich, Germany

1st appraiser:

PD Dr. Schmidt
Neurobiology of Stress Resilience, Max Planck Institute of Psychiatry, Munich, Germany

2nd appraiser:

Prof. Dr. Busse

Division of Neurobiology, Department Biology II, Ludwig-Maximilians-Universität München, Munich, Germany

Prof. Dr. Horn-Bochtler
Anatomische Anstalt, Ludwig-Maximilians-Universität München,
Munich, Germany

Prof. Dr. Nägele
Plant Sciences, Departement Biology I
Fakultät für Biologie
Ludwig-Maximilians-Universität
München, Munich, Germany

“The three great essentials to achieve anything worthwhile are: hard work, stick-to-itiveness, and common sense.”

Thomas Edison, 1818, inventor

Table of contents

1 ABSTRACT I

2 PREAMBLE IV

3 INTRODUCTION 1

3.1 Stress and psychiatric disorders 1
  3.1.1 What is stress? 1
  3.1.2 Stress and Major Depressive Disorders 2
  3.1.3 Preclinical animal models in psychiatric research 3
3.2 The stress response systems 8
  3.2.1 Sympathetic nervous system and Hypothalamic-Pituitary-Adrenal axis 8
  3.2.2 Development of the HPA axis 12
  3.2.3 PVN: The bandmaster of the HPA axis 13
3.3 CRF system: the starting point of the HPA axis cascade 16
  3.3.1 The corticotropin-release factor system 17
  3.3.2 CRF Expression 19
  3.3.3 CRF Regulation 21
3.4 GR: the finishing actor of the stress response 22
  3.4.1 Nr3c1 gene structure, expression and function 22
  3.4.2 GC-induced negative feedback on CRF neurons of the PVN 28
3.5 Habituation to stress 28
3.6 Aim of the thesis 33

4 METHODS 34

4.1 Animals and animal care. 34
4.2 Experimental design: Effects of GR KO in CRF expressing neurons in mice 35
  4.2.1 Anatomical characterization of GRs neurons expressing CRF and cKO validation 35
  4.2.2 Deletion of GRs from CRF neurons towards stress susceptibility 38
  4.2.3 Effect of GRs deletion on Circadian HPA activity 40
  4.2.4 Effect of GRs deletion on HPA responsiveness 42
  4.2.5 Effect of acute and repeated homotypic stress in $GR^{CRF\text{-}CKO}$ mice 43
  4.2.6 Impact of GR deletion in CRF+ neurons on the stress-induced excitation / inhibition balance needed for the habituation of the HPA axis 45
4.3 Microbiological methods 48

4.3.1 Genotyping *48*
4.3.2 Polymerase Chain Reaction (PCR) *49*
4.3.3 Assessment of DNA/RNA concentrations *50*
4.3.4 Preparation, analysis of plasmid DNA and cloning steps *50*
4.3.5 RNA isolation and quantitative real-time PCR (qRT-PCR) *53*
4.3.6 Preparation of brain slices and immunohistochemistry *54*
4.3.7 In situ hybridization (ISH) *54*
4.3.8 Stress reactivity and CORT measurement *56*

5 RESULTS 58

5.1 Anatomical characterization of GRs neurons expressing CRF and cKO validation58
5.2 Impact of GRs from CRF neurons on stress susceptibility 64
5.3 Effect of GRs deletion on circadian HPA activity 67
5.4 HPA responsiveness 73
5.4.1 Dex/CRF test *73*
5.4.2 Effect of acute stress in GR$^{CRF\text{-}cKO}$ mice *75*
5.5 HPA habituation 77
5.5.1 Effect of repeated stress in GR$^{CRF\text{-}cKO}$ mice *77*
5.5.2 Rescue experiment *78*
5.6 Impact of GR deletion in CRF+ neurons needed for the habituation of the HPA axis 85
5.6.1 Impact of GR deletion in CRF neurons regarding cell activity *85*
5.6.2 GRs deletion does not affect intrinsic electrical properties or the excitability of CRF-expressing neurons of the PVN *86*
5.6.3 GR deletion in CRF neurons impairs the RRS-induced shift in excitation / inhibition balance *87*

6 DISCUSSION 97

6.1 PVN anatomy 100
6.2 Effect of GRs deletion in CRF-expressing neurons in mice 101
6.3 Response to acute stress in GR$^{CRF\text{-}cKO}$ mice 102
6.4 Role of GRs in habituation of the HPA axis 104
6.4.1 Effect of repeated homotypic stress in cKO mice *104*
6.4.2 Targeted re-expression of GRs can restore HPA habituation in GR$^{CRF\text{-}cKO}$ mice *105*
6.5 Electrophysiological characterization of GR / CRF neurons and impact on HPA habituation 106
6.6 Conclusion and future directions 109

7 REFERENCES 110

8 APPENDIX 134

8.1 Abbreviations 134
8.2 Acknowledgements 148
8.3 Affidavit 150
8.4 Declaration of author contributions 150
8.5 Curriculum vitae 151

1 Abstract

Modern society is a dynamic plot pervaded by cultural, social, emotional, and biological experiences, some of which ultimately endanger our lifestyle and affect our physiology and behaviour. For health and survival, adequate regulatory control of the HPA stress axis is required. Over the years, chronic stress has been frequently implicated in altered brain function. Current evidence shows that the habituation of HPA axis response is more complex than previously thought. The adaptive reduction of repeated stress-induced responses seems to involve complex crosstalk between negative feedback mechanisms induced by the release of GCs under repeated stress, response habituation processes produced by repetitive exposure to the stress stimulus, and likely more complex learning and memory encoding information regarding previous stressful events. We directed our research towards two major problems that currently impede advances in modeling HPA habituation in mice and mechanisms leading to it. By doing so, we contribute to a better understanding of normal behavior and mechanisms. Here, we show that glucocorticoid receptors in the hypothalamic paraventricular nucleus in CRF neurons are essential for HPA axis habituation. When re-exposed to the same stressor, glucocorticoid receptors led to essential cellular modulation and dampened HPA axis activation by increasing inhibitory tone onto CRF neurons. The current research study provides a new set of data that confidently positions the GR-CRF system as a crucial player in the executive function following repeated stress exposure, thus offering a molecular mechanism through which this effect occurs. Hence, it shows a possible pharmacological target that could support the production of active measures to mitigate the deleterious effects of repeated stress exposure.

Zusammenfassung

Die moderne Gesellschaft ist ein dynamischer Prozess, der von kulturellen, sozialen, emotionalen und biologischen Erfahrungen geprägt ist. Diese Erfahrungen beeinflussen ständig unsere Physiologie und unser Verhalten, und können letztlich auch unseren Lebensstil gefährden. Für Gesundheit und Überleben ist eine angemessene regulatorische Kontrolle der HPA-Stressachse erforderlich, denn chronischer Stress, über Jahre hinweg, trägt zu einer veränderten Gehirnfunktion bei. Aktuelle Erkenntnisse aus Studien zeigen, dass der Gewöhnungseffekt des Körpers auf die Reaktion der HPA-Achse komplexer ist als bisher angenommen. Die adaptive Limitierung wiederholter stressinduzierter Reaktionen scheint ein komplexes Zusammenspiel zwischen negativen Rückkopplungsmechanismen (durch die Freisetzung von GCs unter wiederholtem Stress, Gewöhnungsprozessen (durch wiederholte Exposition des Stressreizes, und wahrscheinlich auch komplexen Lern- und Gedächtniscodierungsinformationen (durch frühere stressige Ereignisse zu sein. Wir haben unsere Forschung auf zwei zentrale Themen fokussiert, die ausschlaggebend für Fortschritte bei der Modellierung der HPA-Gewöhnung bei Mäusen und der zugrundeliegenden Mechanismen sind. Auf diese Weise tragen wir auch zu einem besseren Verständnis des normalen Verhaltens und der entsprechenden Mechanismen bei. Hier zeigen wir, dass Glukokortikoidrezeptoren in CRF-Neuronen im paraventrikulären Kern des Hypothalamus für die Gewöhnung der HPA-Achse essentiell sind. Bei wiederholter Exposition desselben Stressors führten Glukokortikoidrezeptoren zu einer zellulären Modulation: Sie dämpften die Aktivierung der HPA-Achse, indem sie den inhibitorischen Tonus auf CRF-Neuronen erhöhten. Die aktuelle Forschungsstudie liefert einen neuen Datensatz, der das GR-CRF-System bei wiederholter Belastung als einen entscheidenden Akteur in der Exekutivfunktion identifiziert und somit einen molekularen Mechanismus bietet, durch den dieser Effekt auftritt. Daher zeigen unsere Daten ein mögliches Ziel für einen pharmakologisches Ansatz der zur Abschwächung der schädlichen Auswirkungen wiederholter Belastung beitragen könnte.

2 Preamble

"It's not stress that kills us, it is our reaction to it"

Figure 1: Hans Selye (Pioneer of stress physiology 1907-1982).

Stress is a part of life, wherever you are and whatever you do. Stress cannot be avoided, but it is possible to learn how to manage it, so it does not manage you. When stress events repeatedly occur across the full lifespan, their incidence have significant impact. It is interesting to see the differences across gender, countries, civilization, socioeconomic status… Therefore, it is crucial to study the mechanisms underlying the stress response and understand the coping strategies that can help safely and effectively reduce the vulnerability to experiencing severe negative stress.

3 Introduction

3.1 Stress and psychiatric disorders

3.1.1 What is stress?

In our society, "stress" ubiquitously refers to a situation, a feeling, or a state that is perceived as stressful. The psychiatric field of research defines it more precisely to avoid confusion and redundancy. Therefore, the Austrian-Canadian physician Hans Selye defined "stress" as “the nonspecific response of an organism to a stressor” (Selye, 1976, Fig. 1). The stressor may be any potential menace to homeostasis, from a real physical threat or psychological danger. It can be perceived or real. Notably, acute stress can exert a broad variety of beneficial outcomes, as it primes the brain towards optimum resilience, vigilance, behavioural and cognitive performances to increase the chance of survival. Health, well-being, physical, and psychological adaptation are required. The problems start when the stress response system delivers maladaptive processes (Selye, 1980).

3.1.2 Stress and Major Depressive Disorders

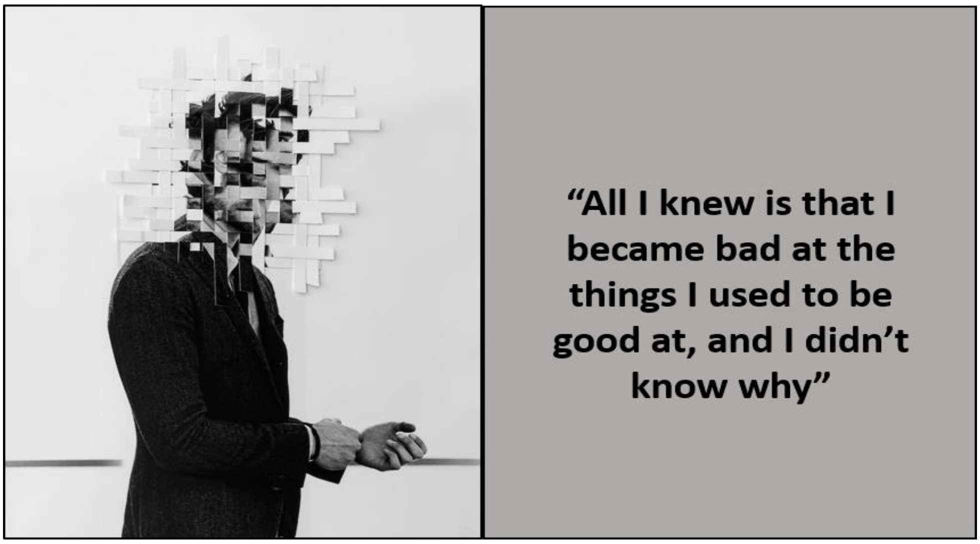

“All I knew is that I became bad at the things I used to be good at, and I didn’t know why”

Figure 2: - Edward Honaker (Photographer documenting his own depression).

In the past several decades, growing literature has linked stressful life events to various pathologies, such as metabolic dysfunctions, cardiovascular disease, inflammation, and most importantly, neurodegenerative and psychiatric disorders (Zorn *et al.*, 2017. Prolonged stress exposure, such as child abuse, poor social/psychological surroundings, devastating socioeconomic status, has been shown to increase the likelihood to develop the previously cited disorders (Gill et al., 2020. However, we will also see that stress per se, is not always bad and a tuneable regulation of this mechanism is vital for mental and physical homeostasis.

For people that have never experienced depression, it is difficult to fathom what it feels. The above quote tries to illustrate what patients suffering from Major Depressive Disorder (MDD experience (Fig. 2. It is a very subjective pain that each patient undergoes in their own way and own words. MDD is characterized by an immense sadness, a feeling of distress, a loss of motivation, and a decrease in feeling happiness (ICD-10-CM, 2018, replacing DSM-5. Patients describe a feeling of incapability of moving and acting, together with a perception of pain or being hurt (Joiner and Metalsky 2001. MDD negatively affects sleeping and eating habits to a point where social and work life are negatively impacted. MDD is the leading cause of disability worldwide with more than 264 million people of all ages affected according to the most recent estimates from the World Health Organization (WHO 2017) with an increase of more than 18% between 2005 and 2015. Depression is on the rise globally, and as such, it is responsible for a substantial economic burden (Greenberg, Fournier et al. 2015). A crucial distinction is also made between depression in individuals with or without a history of manic episodes. All forms of depression may be chronic (i.e., over a longer period) with relapses, particularly if they are not treated. The last report from WHO aimed to act as a wake-up call for all governments in the hope they will change the way mental health is perceived and treated, with a recent interest for workers and perinatal depression. About half of people suffering from MDD in high-income countries do not receive any treatment, even though those countries have the highest antidepressant (AD) consumption. People are misdiagnosed and AD are overprescribed. Worldwide, between 0.5 and 5% of government health budgets are invested in mental health (low income and high-income countries, respectively) with an average of 3%. Stress, along with adverse life experiences, is recognized as being the principal factor for developing MDD. It initiates biological and cognitive processes (Beck, De Bosscher et al. 2011) that can trigger a latent onset of depression (Kendler, Karkowski, & Prescott, 1999; Kendler et al., 1995). People who have gone through significant and persistent stressful life events such as physical abuse, becoming unemployed, grief, or psychological trauma are more at risk to develop MDD.

However, stress *per se* is not always bad. What is problematic is the inability for the organism to adapt and deliver a suitable response. Decades of research have examined cognitive processes mediating the link between depression and stress (Cooney, Joormann, Eugene, Dennis, & Gotlib, 2010; Fritzsche et al., 2010; Joormann, Gilbert, & Gotlib, 2010), but the cognitive and affective processes due to stress, that lead to depression remain unknown. Moreover, it is nowadays still unclear why individuals react differently to the same type of stress: some people becoming resilient, and others being more vulnerable.

3.1.3 Preclinical animal models in psychiatric research

The definition of illness as an objective and distinct cause is a central question in clinical diagnosis in psychiatry. The foundation for the modern nosology of psychiatric disorders was developed by Emil Kraepelin (Kraepelin, 1893, Kraepelin, 1896). A strong distinction between nosological entities and the other can be made in the latest international Statistical Classification of Diseases and Associated Health Conditions (ICD-10, 1989, http:/www.who.int/classifications/icd/en/) and the Mental Illness Manual on Diagnostics and Statistics (DSM-5, 2013), http:/www.dsm5.org/Pages/Default.aspx). Psychopathologies diagnosis is generally based on the identification of deviant behaviour in patients. The RDoC concept was developed as an alternative method for categorization of psychopathological conditions by NIMH experts (Cuthbert, 2014, Cuthbert & Island, 2010, Insel et al., 2010). At the present time the classification matrix is based on five behavioural domains: (1) positive valence systems, (2) negative valence systems, (3) excitement/regulation systems, (4) social process systems and (5) cognitive systems. These five domains and their respective structures can be used to profile behaviour comprehensively. The novelty in the RDoC framework is the connection with the established five behavioural domains of changes at all neurobiological levels, from molecules to neuronal networks and behaviours. The suggested units of research are: genes, molecules, cells, circuits, physiology, behaviour, self-reports and paradigms. The definition of neuronal networks underlying fundamental behavioural domains and advancing in functional diagnosis and imaging supported the development of the RDoC diagnostic criteria. For more details, refer to Anderzhanova et al. (2017).

Most of our expertise in the MDD analysis is extracted from case studies of human patients and epidemiological research. Human studies are essential in the study of human disorders, but have the downside that, due to a number of important ethical and practical concerns, causality and mechanistic evidence at the level of neurobiological processes are hard to acquire from human patients (Nestler & Hyman, 2010). A lot of work on the neurobiological underpinnings of MDD is therefore performed using animal models. MDD is a highly complicated disorder, affecting higher-order memory, mood, vegetative behaviour, cognition, general health, and many of the main symptoms of MDD cannot be convincingly modelled in animals. Nevertheless, an opportunity to make effective use of animal models in the study of psychiatric disorders is given by concentrating on individual endophenotypes. Throughout the last decades, the laboratory mouse (*Mus musculus*) has been the main mammalian animal model for biomedical research. This is partly due to the availability of its complete genome allowing the development of mouse-specific genetic engineering techniques (such as gene-targeted mutagenesis) that have enabled the creation of mouse models for a wide range of human diseases. Researchers have devoted a lot of efforts to develop and study mouse models of nervous system diseases, including psychiatric disorders. See section 3.1.3.3 Genetic animal models.

Strategies used to model disease include targeted genetic engineering, selective breeding, optogenetics, brain lesions, and environmental manipulation. In order to be an effective research tool, the animal model should show high levels of etiological, construct, face, and predictive validity (Chadman, Yang, & Crawley, 2009). Etiological validity refers to the origin or cause of the disease to be modelled, which should be comparable in the model and real-life cases. Construct validity relates to the process through which the phenotype was achieved, which should be plausibly linked to the causal process of the phenotype in humans. Face validity implies that a model recreates key features of the target endophenotype. Predictive validity confirms that the animal model responds to medication (e.g., pharmacotherapy) in the same manner as human patients do. The optimal model should comply to a high degree with all of these criteria. Nevertheless, some animal models may be beneficial and useful although not all criteria are fully met (Belzung & Lemoine, 2011).

3.1.3.1 Stress in mice

Adverse early life events, acute and chronic stressors challenge an organism's ability to cope. If coping approaches fail, different occurrences result in a long-lasting state of distress, reflected in inappropriate stress responses and altered limbic functions. According to the time of exposure, stress can be split into acute (single exposure, short-lasting) or chronic (long-lasting continuous or chronic repeated exposures) affecting physiological mechanisms differently. A wide range of stress models is used in laboratory animals to study stress responsiveness. Models of acute and chronic stress can comprise homotypic (same) or heterotypic (various) stressors.

Most chronic stress models are based on an individual's exposure to several weeks of daily restraint, a choice of daily randomized stressors or repetitive social stressors, for instance, daily exposure to a dominant aggressive male (chronic social defeat, especially in our laboratory, adapted from Berton and colleagues (Berton et al., 2006 ; Nestler &

Hyman, 2010)). While these processes do not have comparable results for all stress parameters, they trigger severe hippocampus-dependent memory deficiencies (Sandi & Pinelo-Nava, 2007). Besides, chronically stressed-animals exhibit increased fear-motivated behaviour. Repeated restraint stress promotes fear conditioning and has been shown to cause dendritic atrophy of hippocampal CA3 pyramidal neurons (Conrad, LeDoux, Magarinos, & McEwen, 1999).

The hippocampus, the amygdala and the prefrontal cortex have revealed neural correlates of behavioural deficits, including elements of structural remodelling and cell proliferation, as well as modifications in amine, neuropeptide and corticosteroid systems (Woolley, Gould, Frankfurt, & McEwen, 1990). Chronic stress continually leads to a decrease in the branching and length of CA3 pyramidal apical dendrites, together with a decrease in synaptic contacts. Prolonged exposure to glucocorticoids (GC) decays adult hippocampal pyramidal neurons' dendritic morphology. If stress is rapidly retracted, a loss of synapses in the CA3 subfield of the hippocampus may be observed, for example, after water maze training, in rats (Woolley et al., 1990).

3.1.3.2 Restraint stress

The first review on restraint stress (RS) was published in 1986. Several studies have since explored RS itself or coupled it with other pharmacological, physiological, or pathological events. The primary use of RS was to induce stress reactions in animals and, more specifically, to investigate drug impacts, especially since they affect typical stress-related pathology — gastrointestinal, neuroendocrine, and immunological agents were widely investigated. RS, in which an animal is prevented from moving or turning around, is one of the most widely used physical stressors in animal research (Glavin, Pare, Sandbak, Bakke, & Murison, 1994). RS consists of the placement of the animal in a cylindrical, aired plastic tube for a period of time that varies from five minutes to hours. Various research laboratories have extensively investigated the impacts of repeated exposure to RS (Natelson et al., 1988). It is established that individuals exhibit variations (high responders vs. low responders), independently of the intensity of the stressor. On the other hand, an attenuation of the stress response is also found, depending on the intensity of the stressor. Studies on both physiological and behavioral components of the stress response are needed to reveal more profitable results (Glavin et al., 1994). It is fundamental to understand why some people are susceptible, while others are resilient to stress in order to diagnose and treat better stress-associated disorders. Over the years, it has become evident that various neurochemical and neuroanatomical pathways, particularly those related to the stress responses, respond differently to stress in resistant and susceptible individuals. Thus, RS provides an animal model for investigating individual differences in stress reactivity that may be associated with such resilient and susceptible phenotypes to chronic stress of relevance to stress-related psychiatric disorders.

3.1.3.3 Genetic animal models

Genetic engineering, i.e., direct manipulation of the genome by targeting particular candidate genes, is a powerful method that promises high construct validity to delineate the function of particular genes and their contribution to physiology and behavior in a bottom-up strategy (Nestler & Hyman, 2010). For example, using molecular gene editing, scientists can generate "transgenic" lines in which DNA sequences are inserted, resulting in downstream functional changes, or "knock-in / knockout" lines in which the expression of specific genes is regulated, thereby producing animals with targeted genetic variants of interest. Overall, the higher the human penetration of a genetic variant (i.e., the percentage of people carrying a specific variant that also expresses the related phenotype), the more probable it is that the required phenotype will also be reproduced by a mouse model carrying this version (Cox, 2015). Regrettably, few or no alleles corresponding to this criterion have been identified for most affective illnesses (Klengel & Binder, 2015). Moreover, the genetic pathway leading to a disease phenotype may differ in distinct people, and vice versa, based on its interaction with other genes, epigenetic variables, and environmental influences, the same genetic variant may result in distinct phenotypes (Nestler & Hyman, 2010). This makes the process of building and validating genetic animal models for MDD much more complicated. Nevertheless, genetic models are used to recreate particular endophenotypic changes connected with MDD with excellent achievement. In animal models, for instance, impaired or enhanced feedback inhibition of the Hypothalamic-Pituitary-Adrenal (HPA) axis was genetically engineered by knocking out or overexpressing glucocorticoid receptors (GR) in chosen brain areas (Howell & Muglia, 2006 ; Muller & Holsboer, 2006) or conflicting with the Corticotropin-Releasing Factor (CRF system (Dedic et al., 2012 ; Wang et al., 2013). Genetically manipulated mice were also used to investigate the involvement of different monoamine and neuropeptide systems, the neurotrophic system, and the immune system to MDD-related endophenotypes (see Urani, Chourbaji, & Gass, 2005).

3.2 The stress response systems

3.2.1 Sympathetic nervous system and Hypothalamic-Pituitary-Adrenal axis

Upon detection of adverse events designated as “stressors”, two endocrine systems are quickly initiated to allow the organism to cope and restore homeostasis: First, the sympathetic nervous system (SNS) sends signals to the adrenal medulla to launch the release of catecholamines (epinephrine and norepinephrine) into the bloodstream. Those transmitters function in the periphery where they enhance cardiovascular rhythm and blood supply to internal organs and skeletal muscles, and stimulate energy metabolism from lipids and glucose (Fig. 3, left side). In the meantime, catecholamine signalling focuses the body on survival function and decreases appetite, digestive functions, and sexual drive. The individual concentrates on necessary actions in order to survive (the so-called "fight-or-flight" response; Cannon, 1929). Centrally, norepinephrine is released from the locus coeruleus (LC) and binds to receptors in limbic areas, such as the amygdala and the hippocampus, where it can influence cognitive functions (Valentino & Van Bockstaele, 2008).

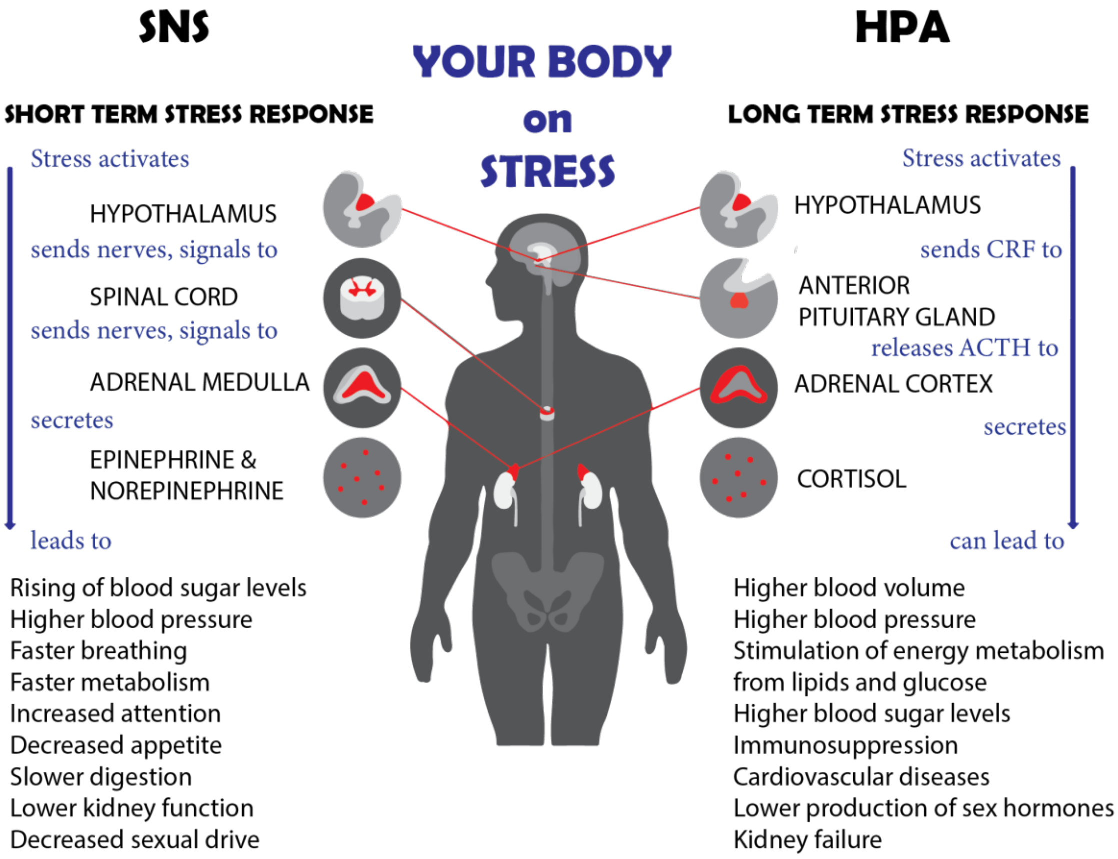
SNS
YOUR BODY
on
STRESS
HPA
SHORT TERM STRESS RESPONSE
Stress activates
HYPOTHALAMUS
sends nerves, signals to
SPINAL CORD
sends nerves, signals to
ADRENAL MEDULLA
secretes
EPINEPHRINE &
NOREPINEPHRINE
leads to
Rising of blood sugar levels
Higher blood pressure
Faster breathing
Faster metabolism
Increased attention
Decreased appetite
Slower digestion
Lower kidney function
Decreased sexual drive
LONG TERM STRESS RESPONSE
Stress activates
HYPOTHALAMUS
sends CRF to
ANTERIOR
PITUITARY GLAND
releases ACTH to
ADRENAL CORTEX
secretes
CORTISOL
can lead to
Higher blood volume
Higher blood pressure
Stimulation of energy metabolism
from lipids and glucose
Higher blood sugar levels
Immunosuppression
Cardiovascular diseases
Lower production of sex hormones
Kidney failure

Figure 3: Schematic overview of the two major arms of the stress response system showing systemic effects of stress on the neuroendocrine systems.

Perceived stressors initiate a cascade of biochemical reactions. It leads to the activation of the HPA axis, the SNS, and corresponding release of hormones and glucocorticoids from adrenal glands and nerve terminals in the periphery. HPA axis, Hypothalamic-Pituitary-Adrenal axis; SNS, sympathetic nervous system.

It secondly leads to the activation of the Hypothalamic-Pituitary-Adrenal (HPA) axis (Fig. 3, right side). Parvocellular neurons in the paraventricular nucleus (PVN) of the hypothalamus synthesize and secrete corticotropin-releasing factor (CRF) and arginine vasopressin (AVP) into the portal vein to the median eminence of the pituitary gland, where they induce adreno-corticotropic hormone (ACTH) release into the bloodstream to initiate the synthesis and release of glucocorticoids (GCs) from the cortex of the adrenal glands (De Kloet, Vreugdenhil, Oitzl, & Joels, 1998; Herman & Cullinan, 1997) (Fig. 4). GCs (cortisol in humans and corticosterone (CORT) in rodents) operate in the periphery by mobilizing glucose stocks, promote gluconeogenesis, and repress inflammation. AVP enhance vasoconstriction and water retention, which is especially essential should injuries occur (Sapolsky, Romero, & Munck, 2000). The GCs are lipophilic and therefore easily cross the blood-brain barrier. They interact with several neurotransmitter systems in the brain through their receptors (e.g., the dopaminergic, the endocannabinoid, the neurotrophic, or the noradrenergic systems) — eventually, GCs act as a negative feedback that alters HPA axis activity and influences behaviour by binding to the GC receptor family: glucocorticoid receptor (GR) and mineralocorticoid receptor (MR) (Fig. 4).

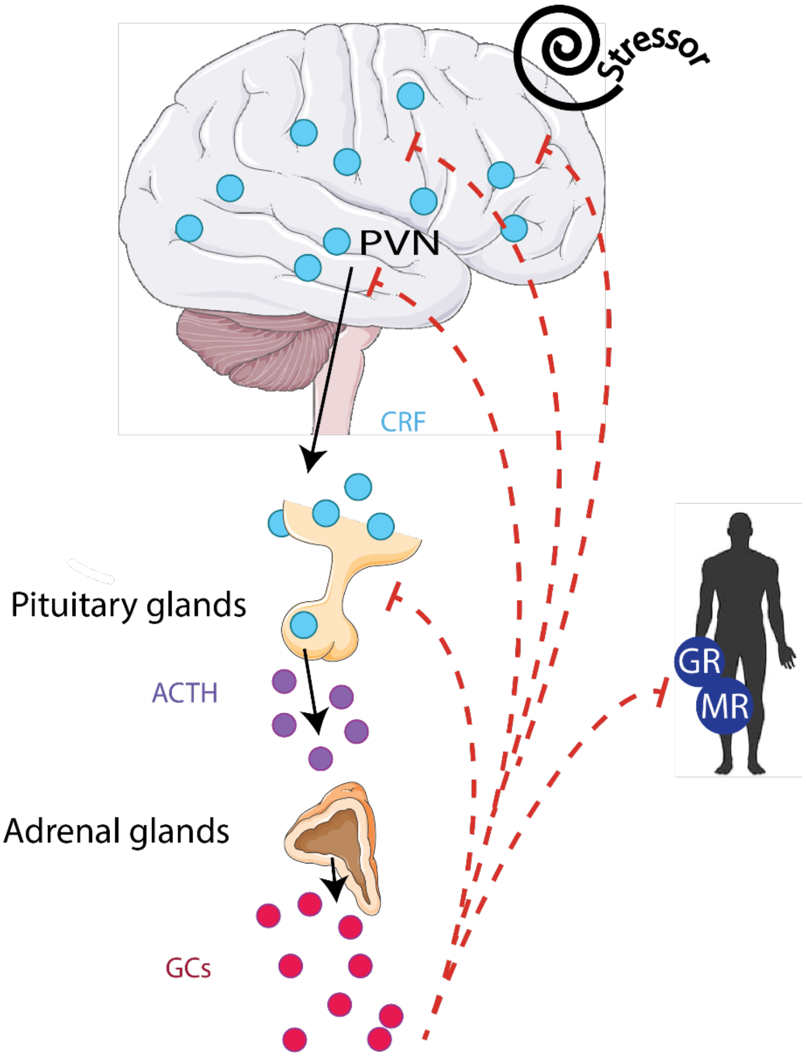

Figure 4: The HPA axis mediates neuroendocrine responses to stress via the release of CRF. CRF mediates neuroendocrine and higher-order behavioural responses to stress by acting as a secretagogue along the HPA axis and as a synaptic transmission modulator within the CNS. Adrenocorticotropic hormone (ACTH), corticotropin-releasing hormone (CRF), hypothalamic-pituitary-adrenal (HPA) axis, hypothalamic paraventricular nucleus (PVN), glucocorticoid receptor (GR), mineralocorticoid receptor (MR). Modified from Deussing and Wurst, 2005.

The GR and MR have very separate functional profiles (de Kloet, Joels, & Holsboer, 2005; Reul & de Kloet, 1985). The intracellular MR has a high affinity for GCs (~0.5 nM) and is hence preferentially bound, under basal conditions. In contrast, the GR has an about 10-fold lower binding affinity and therefore, is activated only under elevated GC levels (Joels & Baram, 2009). Both types of receptor co-expressed in several cortical and limbic brain regions, including the hippocampus, amygdala, and PVN, but the relative amounts vary among regions. MR and GR are both ligand-activated transcription factors. When bound, they translocate to the nucleus and regulate gene expression by binding to GC response elements (GREs). Thus, a biochemical cascade leading to the transcription or repression of genes is initiated (Dostert & Heinzel, 2004; Pearce, 1994). It has been shown that 10-20 % of the human genome is regulated by GR (Oakley & Cidlowski, 2011).

CRF neurons of the PVN initiate the HPA axis stress response. CRF is the primary physiological activator of the HPA axis and regulates the neuroendocrine stress response. Upon perception of physical or psychological stressor by an organism, a series of events is activated, including the release of CRF from parvocellular neuroendocrine neurons of the PVN that culminates with elevated GCs in the bloodstream. The elevated level of circulating GCs promotes their binding to GRs, which in the PVN drives a negative feedback signal straight to the CRF-releasing neurons. A negative feedback message also comes from GR activation on corticotropic cells of the anterior pituitary, blocking ACTH release, and on the hippocampus, transmitted via glutamatergic projections to the PVN, leading to a suspension of the CRF release and a return of the HPA axis to baseline (Myers et al., 2014, Joels & Baram, 2009). The circuitry is detailed further in a later paragraph (see: PVN: The bandmaster of the HPA axis). The negative feedback loop of the HPA axis is necessary to keep a fine balance between an activated stress response process, coping with potentially life-threatening situations at the cost of self-sustaining physiological and reproductive functions, and a baseline state, which is needed for recovery, rest and reproduction (McEwen, 2004). Hence, a well-controlled stress response is highly adaptive and indispensable for survival (de Kloet, 2000; Sapolsky et al., 2000).

Nevertheless, prolonged exposure to high levels of GCs can exhibit neurotoxic consequences, influencing among others, cell proliferation, synaptic plasticity, and dendritic arborization over the brain, eventually impairing brain functions and increasing the risk of developing mental illnesses, such as MDD (Collins et al., 2011; Ising & Holsboer, 2006; Lupien, McEwen, Gunnar, & Heim, 2009). Researchers use the term "allostatic load" (McEwen, 2004) to describe those effects of the stress response on cells and systems of the brain. The stress response is advantageous and highly adaptive as long as the stress balance and recovery phases are retained, but if the balance is shifted this may lead to detrimental health and well-being consequences. An inappropriate stress response is associated with various sorts of metabolic, immune and affective disorders (McEwen, 2007; Sapolsky et al., 2000) and plays a significant role in their etiology and in the pathophysiology of MDD. It is also remarkable that HPA activation does not occur only when the organism encounters an aversive stressor. For instance, a positive experience like sexual encounter, reward or social victory induces the same degree of HPA activation as an aversive stress such as foot shock, social defeat or restraint stress in rats (Koolhaas et al., 2011; Koolhaas, De Boer, De Rutter, Meerlo, & Sgoifo, 1997).

3.2.2 Development of the HPA axis

Rodents have proven to be useful models for research on HPA axis development, and function as evidence suggests that the development of the stress response system in humans follows a comparable trajectory, albeit with a different time scale (Gunnar & Donzella, 2002; Sapolsky et al., 2000). In mice, CORT levels stay stable at low concentrations until postnatal day 12 (P 12) (Schmidt et al., 2003) in reaction to most stressors. Stimuli that typically increase CORT concentrations do not result in the activation of the HPA axis during this time frame. That phenomenon is called the stress hyporesponsive period (SHRP). ACTH secretion is suppressed under basal conditions during the SHRP and demonstrates no measurable rise in reaction to stressors (Walker, Sapolsky, Meaney, Vale, & Rivier, 1986). Additionally, adrenal glands are not susceptible, and there is a significant reduction in ACTH signalling (Levine, Huchton, Wiener & Rosenfeld, 1991 ; Rosenfeld, Wetmore & Levine, 1992). It is believed that the SHRP is due to pituitary GRs that have a suppressive impact on the HPA axis (Schmidt et al., 2009). Only 50% of central GRs found in adulthood are found during

SHRP (Levine, 2001), and even if the SHRP terminates at P12, the GR-mediated negative feedback happens much later in development.

CRF concentrations in the PVN, on the other hand, are high from birth to P12, but this signal does not promote a reaction from the HPA axis (Baram & Lerner, 1991; Schmidt et al., 2003). Interestingly, since birth MRs are highly expressed, but GR concentrations are low at birth and are continuously increasing up to P12 (Rosenfeld et al., 1991). Animals demonstrate a temporary increase in basal CORT concentrations after P12, as the negative feedback loop becomes efficient and GRs are more integrated into the hippocampus (Schmidt et al., 2003). The regulation of the HPA axis progressively normalizes to concentrations comparable to adult brain levels.

Evolutionarily, the SHRP's aim is most probably protecting the brain during a sensitive developmental period from the neurotoxicity of excessive GC exposure. Due to ethical and practical constraints regarding neonate studies, the SHRP is less well defined in humans. At birth, human babies already demonstrate an increase in cortisol in reaction to mild stressors (Gunnar, 1992), but around three months of age the adrenal sensitivity to ACTH dramatically decreased (Gunnar & Nelson, 1994) and, at 12 months of age, minor stressors (vaccinations or short separation periods) do not cause a cortisol response, despite frightened or distant reactions (Gunnar & Donzella, 2002). To summarize, the SHRP is a critical stage in the growth of the brain and the HPA axis, which is strictly governed by maternal signs and can only be interrupted by severe stressors, such as interfering with the relationship between mother and infant.

3.2.3 PVN: The bandmaster of the HPA axis

In contrast to the cerebral cortex and cerebellum, the hypothalamus lacks distinct layers or other stringent anatomical, repetitive organizational principles. It is made of numerous distinct subnuclei, supervising several types of neuroendocrine and autonomic functions. The PVN is one of the CNS's most complex and heterogeneous nuclei. It lies adjacent to the third ventricle. Most of the current knowledge about the subnuclear organization of the PVN was initially investigated in rats (Swanson & Sawchenko, 1980). However, recent work has identified the same degree of complexity in these subnuclei in mice (Biag et al., 2012, Ramos et al. 2017). In general, the PVN may be separated into magnocellular and parvocellular divisions. The neurons that project from higher brain centers to the median eminence secrete neurohormones in the hypophysial portal vein that act at the level of the median eminence of the anterior pituitary gland. These projecting neurons constitute the endocrine hypothalamus (Fig. 5). The whole endocrine system is controlled by neuropeptides. The endocrine hypothalamus is influenced by direct feedback from the endocrine glands and other circulating factors. The integrated role is complex, and the networks between and amongst the neuroendocrine cells allow precise control in order to reach homeostasis.

3.2.3.1 PVN cell population

Many hypothalamic nuclei are directly engaged in regulation of the HPA axis and autonomic responses to stressful occurrences, but the PVN emerges as the main integrator of stress signals. The PVN comprises distinct neuron populations projecting onto the anterior pituitary gland and onto the brainstem and spinal cord autonomous targets. The vast majority of endocrine cells are concentrated at the anterior two-thirds of the PVN (Fig. 5 left part). The PVNam and PVNmm hold mainly oxytocin (OXY) neurons. On the other hand, the PVNpml included nearly solely vasopressin (VAS) neurons, whereas the PVNpmm includes both types of magnocellular neurons. The vast majority of somatostatin (SS) parvocellular endocrine cells are located in the PVNpv near the third ventricle, whereas two other parvocellular populations, CRF and thyrotropin-releasing hormone (TRH) are mostly located in the PVNmpd. PVN CRFR1-expressing neurons represent a distinct neuronal population within the PVN that did not colocalize with classical PVN markers such as CRF, vasopressin, oxytocin or other parvocellular neurosecretory neuronal types (Ramot et al. 2017).

By contrast, the posterior third of the PVN mainly comprises three pre-autonomic descending neuronal populations (Fig. 5. right side) that regulate sympathetic and parasympathetic outputs. These neurons are organized into four parts of the PVN with a clear spatial topological arrangement: 1) PVNdp includes mainly IML-projecting neurons and a limited number of CGS-projecting neurons. 2) PVNmpv comprises all three descending neuronal populations: DMX-projecting neurons (medially, adjacent to PVNpv and comprising the main portion of PVNmpv), CGS-projecting neurons (in the center of PVNmpv) and IML-projecting neurons (dorsolateral area adjacent to PVNpm). 3) All three descending neuronal population are present in PVNlp, where

IML-projecting neurons appear to be spread more dorsally than DMX-projecting neurons. 4) PVNf tends to comprise mainly spinal cord-projecting neurons.

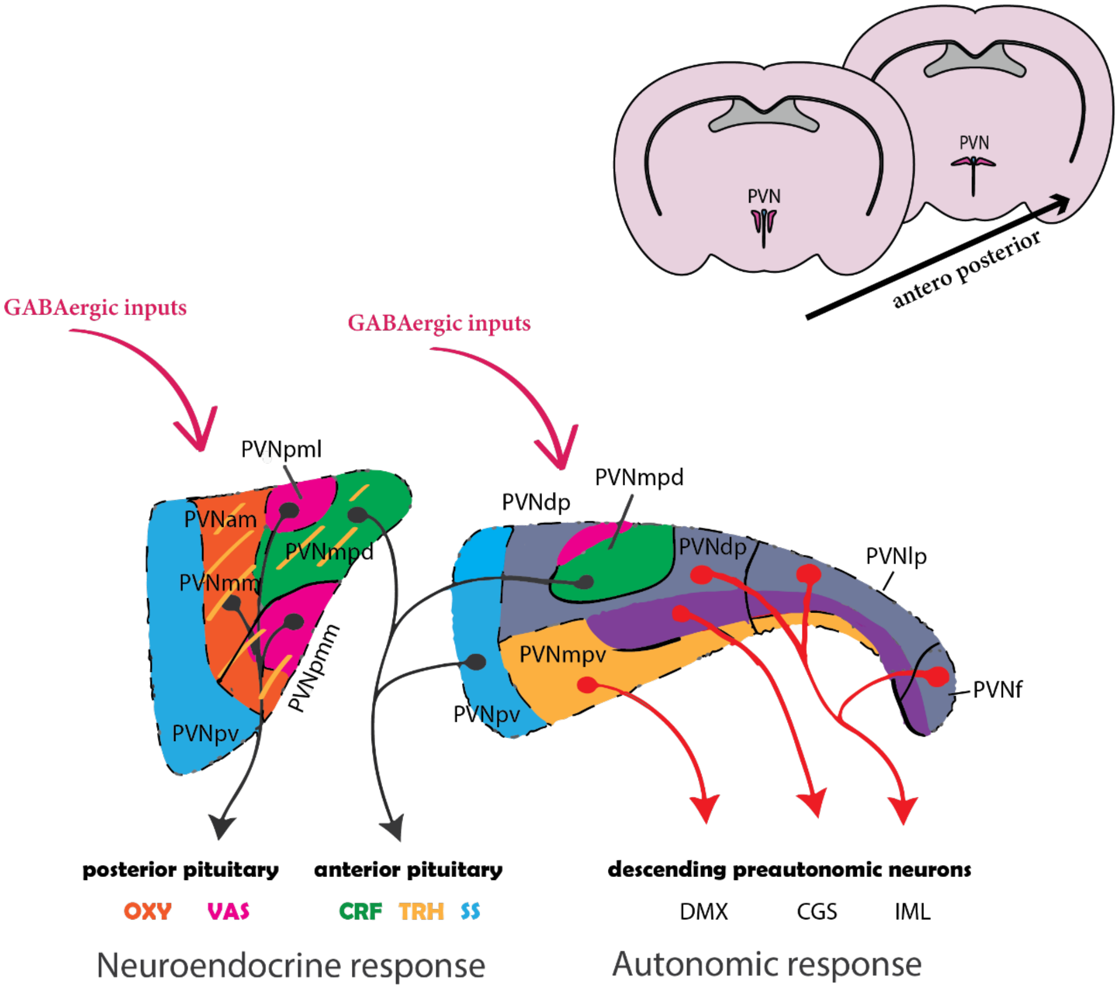
PVN
PVN
antero posterior
GABAergic inputs
GABAergic inputs
PVNpml
PVNam
PVNmpd
PVNmm
PVNpmm
PVNpv
PVNmpd
PVNdp
PVNdp
PVNlp
PVNmpv
PVNpv
PVNf
posterior pituitary
OXY VAS
anterior pituitary
CRF TRH SS
descending preautonomic neurons
DMX CGS IML
Neuroendocrine response
Autonomic response

Figure 5: Schematic model of the PVN cyto- and chemo-architecture in the mouse (adapted from Biag et al. 2012).

The anterior two-thirds of the PVN comprises the large majority of magnocellular neuroendocrine neurons that project to the posterior pituitary and parvocellular neuroendocrine neurons that project to the median eminence. The posterior one-third of the PVN contains most of the descending pre-autonomic neurons.

PVNam: paraventricular hypothalamic nucleus, anterior magnocellular part
PVNmm: paraventricular hypothalamic nucleus medial magnocellular part
PVNpmm: paraventricular hypothalamic nucleus, posterior magnocellular part, medial zone
PVNpv: paraventricular hypothalamic nucleus, periventricular part
PVNpml: paraventricular hypothalamic nucleus, posterior magnocellular part, lateral zone
PVNmpv: paraventricular hypothalamic nucleus, medial parvicellular part, ventral zone
PVNmpd: paraventricular hypothalamic nucleus, medial parvicellular part, dorsal zone
PVNlp: paraventricular hypothalamic nucleus, descending division, lateral parvicellular part
PVNf: paraventricular hypothalamic nucleus, descending division, forniceal part

PVNdp: paraventricular hypothalamic nucleus, descending division, dorsal parvicellular part
PVNam: paraventricular hypothalamic nucleus, anterior magnocellular part
IML: intermediolateral column, spinal cord
CGS: central gray, spinal cord
DMX: dorsal motor nucleus of the vagus nerve

3.2.3.2 PVN connectivity

The PVN is highly innervated by GABAergic inputs (Decavel & Van Den Pol, 1990), which provide a global inhibitory tone (Park, Skalska, Son, & Stern, 2007). Some of the GABAergic inputs to the PVN come from neurons in the peri-PVN area (Roland & Sawchenko, 1993), which in turn is targeted by several limbic brain regions, enabling the translation of limbic information into the regulation of HPA axis or autonomic activation. The dorsal portion of the medial parvocellular PVN (PVNmpd) is activated under stress by several brain areas (Fig. 5). The PVN receives noradrenergic, adrenergic, and peptidergic projections from the nucleus of the solitary tract (NTS). The dorsomedial component of dorsomedial hypothalamus (dmDMH) and arcuate nucleus supply intrahypothalamic stress excitation. The anterior part of the BNST, especially the anteroventral nucleus of the BNST (avBNST), stimulates HPA axis stress responses. The PVN also gets, among other things, stress-exciting afferences from avBNST, dorsal raphe, tuberomammillary nucleus, supramammillary nucleus, and spinal cord. Several hypothalamic circuits inhibit PVNmpd activation, including the medial preoptic region (mPOA), the ventrolateral portion of the dorsomedial hypothalamus (vlDMH), and the peri-PVN (pPVN) local neurons. The BNST's posterior areas (pBNST) provide with a majority of GABAergic inputs a significant forebrain inhibition of HPA axis reactions.

3.3 CRF system: the starting point of the HPA axis cascade

As introduced before, the neuronal population expressing CRF in the PVN initiate the stress response of the HPA axis. CRF (also referred to as corticotropin-releasing hormone CRH) is the primary physiological activator of the HPA axis and regulates the neuroendocrine stress response.

3.3.1 The corticotropin-release factor system

The discovery of CRF in 1981 (Vale, Spiess, Rivier, & Rivier, 1981) launched a wave of research that resulted in the significant accomplishments regarding what is known about stress regulation and stress-related pathologies (Bale & Chen, 2012). The mature and biologically active form of CRF is a 41-amino acid peptide generated by proteolytic cleavage from a 196-amino acid precursor.

The CRF system consists of various ligands and receptor subtypes. In mammals, the principal ligands are represented by the Urocortin family (UCN1, UCN2, and UCN3) and CRF. Urocortin (UCN) 1 was first discovered in 1995 (Vaughan et al., 1995) followed by the description of UCN2 (or stresscopin-related peptide) and UCN3 (or stresscopin) shortly afterwards (S. Y. Hsu & Hsueh, 2001; Lewis et al., 2001; Reyes et al., 2001). Urocortins share up to 43% amino acid homology with CRF (43% for UCN1, 34% UCN2, 26% UCN3) (Dautzenberg & Hauger, 2002) and bind to the same receptor family, but have different affinities for the different receptor subtypes (Steckler & Holsboer, 1999). The CRF – UCN family of peptides and receptors, are not only structurally and pharmacologically related, but often share a supplementary commonality, such as glucocorticoid control that strengthens the hypothesis that they are likely to act in conjunction as a single functional network (Kuperman and Chen 2008). CRF and the UCNs signal by activating two class B1 membrane-bound G-protein-coupled receptors, CRFR1 and CRFR2, which share 70 % amino acid similarity (Chen, Lewis, Perrin, & Vale, 1993; M. Perrin et al., 1995; M. H. Perrin, Donaldson, Chen, Lewis, & Vale, 1993; Vita et al., 1993). The lowest degree of similarity is the N-terminus (40 % homology) in their extracellular domains. By comparison, CRFR1 and CRFR2 transmembrane domains are highly homologous (80-85 % identity of amino acids) (Dautzenberg & Hauger, 2002) (Fig. 6). In the brain, there is one known functional splice variant of CRFR1 whereas CRFR2 has three functional membrane splice variants in humans (α, β, and γ) and in two in rodents (α and β) (Lovenberg, Chalmers, Liu, & De Souza, 1995). CRF has significantly higher affinity to CRFR1 than to CRFR2, while UCN1 shows equal affinities for both receptors. UCN2 and UCN3 have higher affinity for CRFR2 (Fig. 6). In rodents, CRF and UCN1 expression overlap a little, giving support to the idea that these two neuropeptides serve different functions. For example, it is known that UCN1 plays a limited role in ACTH regulation and release from the pituitary gland (Steckler & Holsboer, 1999) whereas CRF plays a major role. The activity of CRF and UCN1 can be additionally regulated by the CRF binding protein (CRF-BP) (Dautzenberg & Hauger, 2002; Seasholtz, Burrows, Karolyi, & Camper, 2001). Only a few studies have investigated the role of the CRF-BP, which might act as an endogenous buffer, by regulating the availability of active CRF and UCN1 (Behan et al., 1995; Seasholtz et al., 2001; Seasholtz, Valverde, & Denver, 2002).

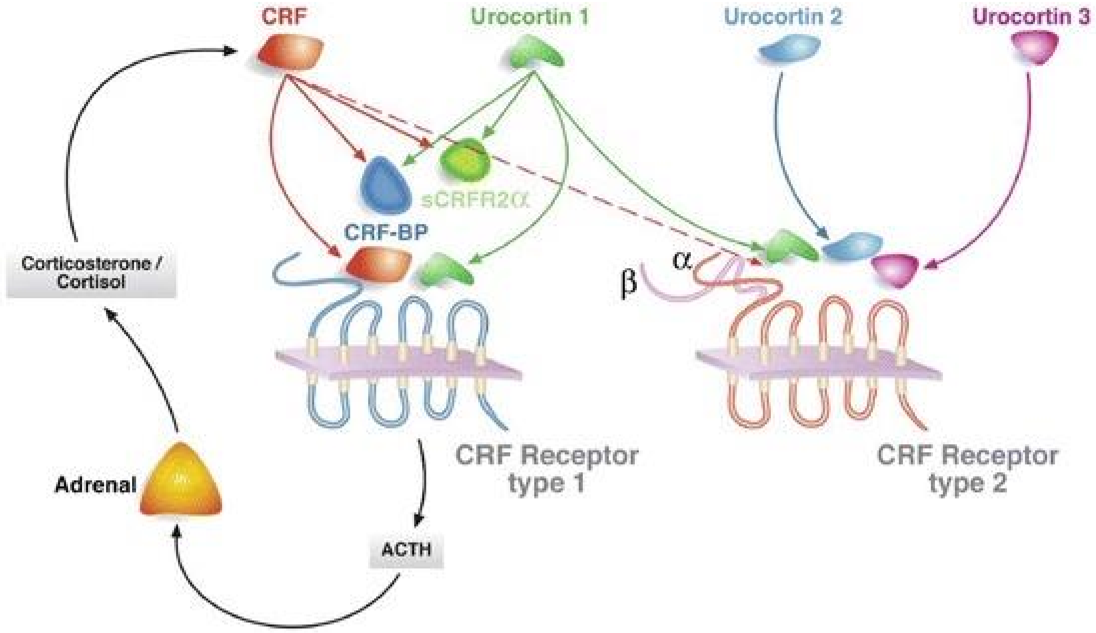

Figure 6: Schematic representation of the peptide, receptor and binding proteins family of CRF – Urocortin (Kuperman and Chen 2008).

The CRF family of neuropeptides and their action on CRFR1 and CRFR2 (Kuperman and Chen 2008, with permission). Colored arrows indicate the receptors with which each ligand preferably interacts; dashed lines indicate relatively lower binding affinity. CRFR2 has two apparent membrane-bound splice variants in rodents, resulting in two receptor proteins, CRFR2α and CRFR2β. CRF has relatively lower affinity for CRFR2 than for CRFR1. Urocortin 1 has approximately equal affinity for both receptors, and Urocortin 2 and Urocortin 3 seem to selectively bind CRFR2.

A recently identified soluble splice variant of CRFR2 (sCRHRα) brings more complexity to the CRF-system. It encodes the ligand-binding extracellular receptor domain but ends before the transmembrane domains (Chen et al., 2005). Initially suggested to serve as a decoy receptor, imitating the ability of CRF-BP to sequester free CRF, Evens and colleagues hypothesized that inefficient splicing of Crhr2 pre-mRNA to sCrhr2, selectively alters cellular amounts of full-length Crhr2 mRNA and thus affects the level of functional CRFR2 receptors (Evans and Seasholtz, 2009).

3.3.2 CRF Expression

CRF is synthesized by the hypophyseotropic neurons in the medial dorsal parvocellular subdivision of the PVN. The axons of these neurons run laterally and caudally and end in the caudal zone of the median eminence, where CRF is released into the portal vein of the anterior lobe of the pituitary gland to initiate the stress response. Additionally, lateral, dorsal, and ventral divisions of the PVN synthesize CRF from cell clusters that project to preganglionic neurons of the medulla and the spinal cord, controlling the stress response (Kovacs, 2013, Fig. 7).

HPA basal- and stress-induced- activity is driven by hypothalamic CRF. Nonetheless, CRF is not only secreted by the PVN but widely distributed across the CNS and the periphery, operating as neurotransmitter and neuromodulator (Merchenthaler, 1984; Palkovits, Brownstein, & Vale, 1985). Multisynaptic tracing of autonomic circuits label cells expressing CRF in the forebrain (extended amygdala comprised of the central nucleus of the amygdala (CeA) and the bed nucleus of the stria terminalis (BNST), dorsal and ventral medial subdivisions of the PVN, lateral hypothalamus) (Buijs et al., 2001, Strack et al., 1989). Most of the cortical regions have been identified as CRF sources such as the prefrontal cortex (PFC), cingulate cortex, hippocampus, Barrington's nucleus, parabrachial complex and nucleus of the solitary tract (Dedic, Chen, & Deussing, 2018, Fig. 7). These pre-autonomic neurons have been involved in providing appropriate sympathetic/parasympathetic outflow under stress.

After perception of a stressor, CRF positive neurons from brainstem, Barrington nucleus, CeA and from the PVN, stimulate the Locus Coeruleus (LC), resulting in elevated norepinephrine into the LC target regions, thereby increasing arousal (Berridge and Waterhouse, 2003, Valentino et al., 1991). The LC also plays a crucial role translating stress challenges into body cardiovascular responses. Moreover, several types of stressors recruit different CRF pathways projecting to the LC, which in turn propagate and integrate different stress-related behaviours (Fig. 7). The role of CRF is not limited to the neuroendocrine HPA axis. Central CRF is also implicated in brain-to-immune signalling via the stimulation of sympathetic/noradrenergic pathways of lymphoid organs such as thymus, spleen and bone marrow (Elenkov et al., 2000, Irwin et al., 1992, Tsagarakis and Grossman, 1994).

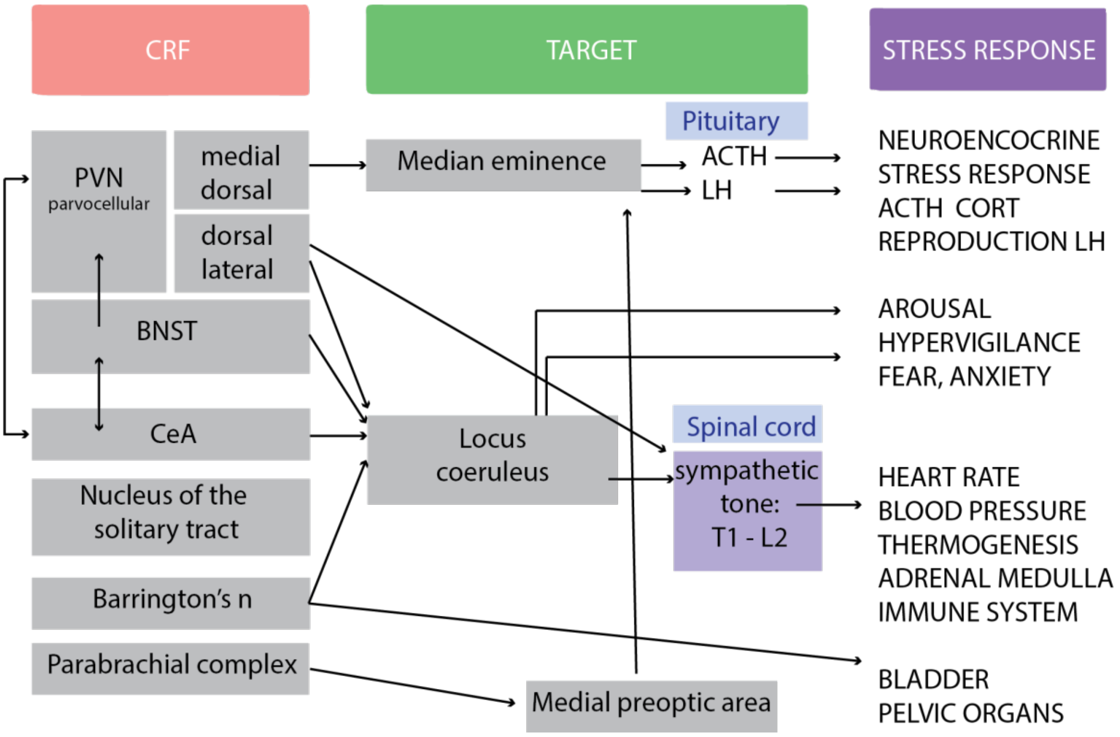
CRF
TARGET
STRESS RESPONSE
PVN
parvocellular
medial
dorsal
dorsal
lateral
BNST
CeA
Nucleus of the
solitary tract
Barrington's n
Parabrachial complex
Median eminence
Pituitary
ACTH
LH
Locus
coeruleus
Spinal cord
sympathetic
tone:
T1 - L2
Medial preoptic area
NEUROENCOCRINE
STRESS RESPONSE
ACTH CORT
REPRODUCTION LH
AROUSAL
HYPERVIGILANCE
FEAR, ANXIETY
HEART RATE
BLOOD PRESSURE
THERMOGENESIS
ADRENAL MEDULLA
IMMUNE SYSTEM
BLADDER
PELVIC ORGANS

Figure 7: The major loci of CRF production, their targets and function in the integrated stress response (adapted from Kovacs, 2013).

CRF acts as a neurotransmitter/neuromodulator in stress-associated limbic areas to propagate and integrate stress-induced behaviours. CRF, produced by parvocellular neurosecretory neurons, functions as a neurohormone to induce the neuroendocrine stress response, whereas CRF produced in extended amygdala, cortex and hippocampus is correlated with multiple vegetative and behavioural dimensions of stress.

The spatial distribution of CRF across the brain suggests two major roles for this peptide: a key neuroendocrine stress mediator and a regulator of neuronal activity in a neuromodulatory fashion. Besides their implication in the stress cascade, these CRF-releasing neuronal populations have also been involved in controlling arousal, executive functions, reward, fear, anxiety, depression, sleep-wake cycles, growth, reproduction, cardiovascular, metabolic and gastrointestinal functions (Bale et al., 2003; Gabr, Gladfelter, Birkle, & Azzaro, 1994). For these reasons, malfunctions in the HPA axis have been linked to anxiety disorders and MDD (Gallagher, Orozco-Cabal, Liu, & Shinnick-Gallagher, 2008).

To summarize, CRF, synthesized by parvocellular neurosecretory neurons, serves as a neurohormone to activate neuroendocrine stress response, whereas CRF produced in extended amygdala, cortex and hippocampus is linked to several vegetative and behavioral dimensions of stress (Fig. 7).

3.3.3 CRF Regulation

Neuroendocrine and physiological responses to stress via the HPA axis are coordinated by CRF. Its transcription is known to be tightly regulated in a site-, stress- and GC-specific manner. An acute stress episode leads to an increase in CRF transcripts and protein levels in hypothalamic and extra-hypothalamic areas (Kovács & Sawchenko, 1996) together with important declines in the olfactory bulb (Imaki, Nahan, Rivier, Sawchenko, & Vale, 1991). In this way, several studies, investigating reaction to acute stress episode, have shown rapid, robust surges in CRF release from the PVN, together with a decrease of neuropeptide stores at the axon terminals (Plotsky, 1985).

After the perception of a stressful situation, stress-related afferents stimulate different signal transduction pathways in the neurosecretory cells of the PVN that gather upon the regulatory region of the CRF gene to initiate the transcription of CRF mRNA. Changes in catecholaminergic (noradrenergic) afferences coming from the brainstem modify the level of CRF transcription in the PVN (Pacak, Palkovits, Makino, Kopin, & Goldstein, 1996). It has been demonstrated that intra-PVN norepinephrine microinjections mimic stress-induced CRF synthesis (Cole & Sawchenko, 2002). The PVN receives a tremendous amount of glutamatergic and GABAergic inputs. While glutamatergic afferences do not seem to play a role in the regulation of CRF transcription, inhibition of the GABAergic neurotransmission leads to an increase of CRF release (Cole & Sawchenko, 2002). Stress additionally causes CRF upregulation in numerous extra-hypothalamic regions, such as limbic regions (CeA, BNST and Barrington's nucleus) (Hsu, Chen, Takahashi, & Kalin, 1998; Makino, Asaba, Nishiyama, & Hashimoto, 1999), which seem to be not related to brainstem ascending catecholaminergic inputs (Pacak et al., 1996). Moreover, it is widely shown that corticosterone plays a role in the regulation of amygdalar CRF release (Watts, 2005), proposing that CeA CRF may act in the regulation of HPA axis activity following stress. In fact, in the CeA, lentiviral-induced CRF overexpression increases expression of CRF and arginine vasopressin (AVP) in the PVN and impairs GC negative feedback on ACTH secretion (Keen-Rhinehart et al., 2009). Additionally, in several limbic and cortical regions such as the hippocampus, PFC and cingulate cortex, distinct stress paradigms, and CRF administration likewise boost CRF expression (Givalois, Arancibia, & Tapia-Arancibia, 2000).

Following stress activation of the HPA axis through the synthesis and release of CRF, a suitable reaction is essential to prevent deleterious impacts of long-term exposure to GCs. The main mechanism that serves this regulatory action is based on the negative feedback of GCs onto CRF expressing neurons within the PVN through a putative adverse GC response element on the CRF gene. It has, therefore, been shown that these CRF-expressing PVN neurons are particularly susceptible to GCs (Bali, Ferenczi, & Kovacs, 2008; Kovács & Sawchenko, 1996). Indeed, targeted disturbance of GR signalling within the PVN has lately been shown to result in the upregulation of CRF mRNA concentrations (Jeanneteau et al., 2012). In addition, GCs influence the CRF transcript half-life. For example, adrenalectomy is known to decrease the degree of degradation of CRF mRNA and corticosterone replacement to decrease the half-life of CRF mRNA in rat PVN (Ma, Camacho, & Aguilera, 2001). By activating the noradrenergic system, which in turn controls parts of the HPA axis, CRF can indirectly control endocrine reactions.

3.4 GR: the finishing actor of the stress response

3.4.1 Nr3c1 gene structure, expression and function

The human GR gene (Nr3c1) (hGR) was initially cloned in 1985 (Fig. 8). It consists of nine exons (Hollenberg et al., 1985). Exons 2–9 form the protein-coding region. Exon 1 forms the 5′- untranslated region. The hGR gene contains two terminal exon 9 (exon 9α and 9 β) alternatively spliced to produce the classic GR (hGRα) and the nonligand-binding GR (hGRβ) isoform. The hGRα and -β isoforms are similar until amino acid 727, but differ in their C-termini. The hGR gene is found on chromosome 5q31– locus 32. The GR is a modular protein consisting of an N-terminal transactivation domain (NTD), a central DNA-binding domain (DBD), a C-terminal ligand-binding domain

(LBD), and a flexible hinge region between the DBD and the LBD. The NTD has a powerful transcription activation role (AF1) by allowing co-regulators to be recruited and activating the transcription machinery. The two zinc-finger motifs patterns in the DBD identify and bind specific DNA sequences on target genes (i.e., GREs) (Fig. 9). The second activation feature (AF2) in the LBD interacts with co-regulators when ligand binding. Both the DBD/hinge and LBD domains contain a nuclear localization signal that enables translocation to the nucleus via an importin-dependent mechanism (Kadmiel & Cidlowski, 2013; Oakley & Cidlowski, 2011) (Fig. 8).

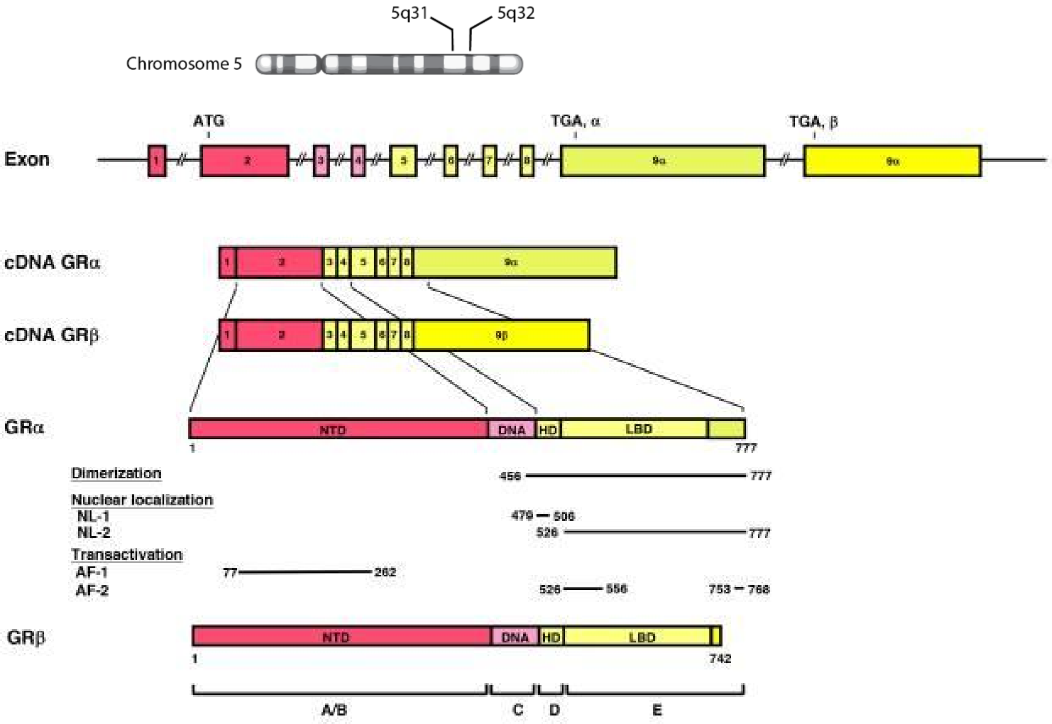
5q31
5q32
Chromosome 5
ATG
TGA, α
TGA, β
Exon
1
2
3
4
5
6
7
8
9α
9β
cDNA GRα
cDNA GRβ
GRα
NTD
DNA
HD
LBD
1
777
Dimerization
456
777
Nuclear localization
NL-1
NL-2
479
506
526
777
Transactivation
AF-1
AF-2
77
262
526
556
753
768
GRβ
NTD
DNA
HD
LBD
1
742
A/B
C
D
E

Figure 8: Genomic and protein structures of the Nr3c1 with its functional distribution, and the isoform formed by alternative splicing (from Kino, Su et al. 2009, updated 2017).

The hGR gene consists of 9 exons. Exon 1 is an untranslated region (UTR), exon 2 codes for NTD (A/B), exon 3 and 4 for DBD (C), and exons 5-9 for the hinge region (D) and LBD (E). The GR (Nr3c1) gene comprises two terminal exons 9 (exon 9α and 9β) alternatively spliced to generate the classic GR and the non-ligand-binding GR isoform. C-terminal domains in GRα and GRβ show their specific portions. AF-1 and -2: activation function-1 and -2; DBD; DNA-binding domain; HD: hinge domain; LBD: Ligand-binding domain; NTD: N-terminal domain, NL-1 and -2: Nuclear translocation signal 1 and 2.

The human GRα DNA-binding domain (DBD) corresponds to amino acid 420-480 and comprises two zinc-finger-type C4, in which GRα binds to the unique GRα sequences, the GREs. The DBD is the most evolutionarily conserved domain of the nuclear receptor family. It consists of two similar zinc finger motifs; each nucleated by a zinc ion coordination center containing four cysteine residues (C) and followed by α-helix (Fig. 9A). The first α-helix of the N-terminal is located in the main groove of the double-stranded DNA, and the C-terminal part of the second α-helix is placed above the minor groove (Fig. 9B).

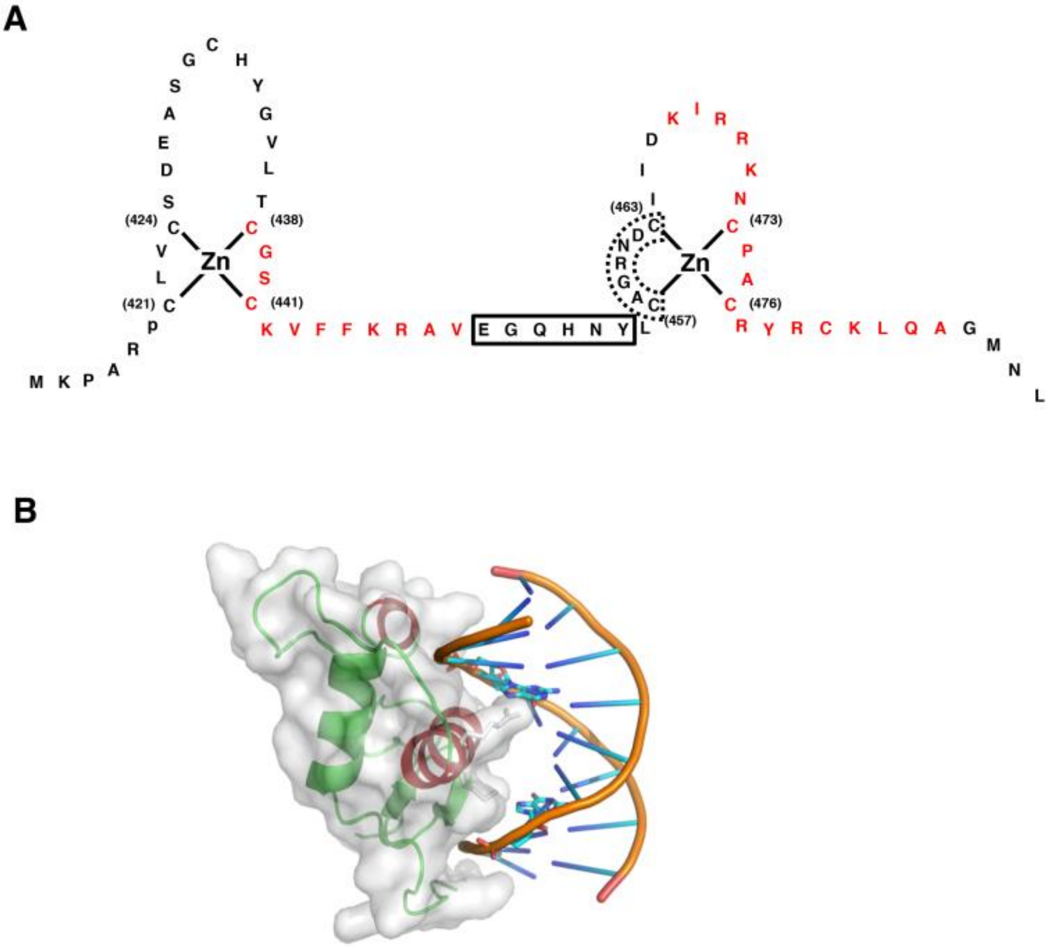
A
M K P A R P C V L C (421) (424) S D E A S G C H Y G V L T C (438) G S C (441)
Zn
K V F F K R A V E G Q H N Y L (457)
C A G R N D C (463) I I D K I R R K N C (473) P A C (476)
Zn
R Y R C K L Q A G M N L
B

Figure 9: Structure of GR DBD and its interaction with DNA GRE (from Kino, Su et al. 2009, updated 2017).

A: Zinc finger structures in hGR DBD. Numbered 8 cysteine (C) residues chelate Zn^{2+} to form two separate finger systems. Red-colored amino acid residues construct the helical structure. B: 3-Dimensional model of the physical interaction between GR DBD and DNA GRE. The image was created and donated by Dr. D.E. Hurt (National Institute of Allergy and Infectious Diseases, NIH, Bethesda, MD)

As reported earlier, the human GR gene displays two mRNAs by alternative use of exon 9α and 9β and generates two splice variants. In exon 2, the GRα isoform also undergoes alternative engagement, creating eight alternative GR isoforms with truncated N-termini. (GRα-A, GRα-B, GRα-C1, GRα-C2, GRα-C3, GRα-D1, GRα-D2, and GRα-D3). GRβ variant mRNA can also produce eight hGRα-like isoforms, across the same initiation sites (Fig. 10).

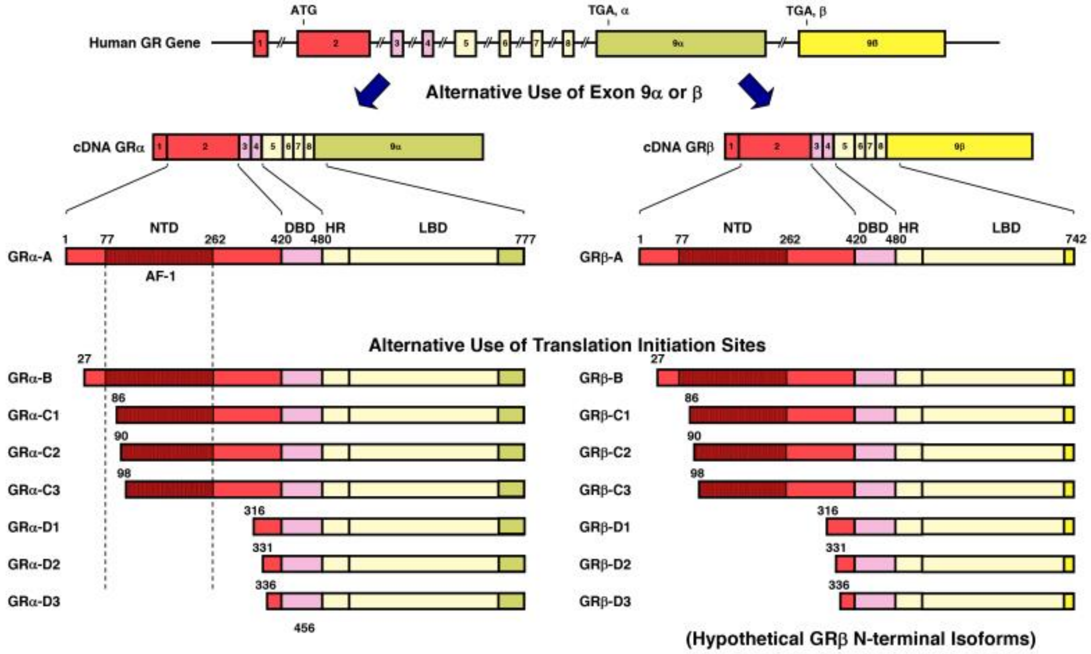
Human GR Gene
ATG
TGA, α
TGA, β
Alternative Use of Exon 9α or β
cDNA GRα
cDNA GRβ
NTD
DBD HR
LBD
AF-1
GRα-A
GRβ-A
Alternative Use of Translation Initiation Sites
GRα-B
GRα-C1
GRα-C2
GRα-C3
GRα-D1
GRα-D2
GRα-D3
GRβ-B
GRβ-C1
GRβ-C2
GRβ-C3
GRβ-D1
GRβ-D2
GRβ-D3
(Hypothetical GRβ N-terminal Isoforms)

Figure 10: Genomic location and organization of the human glucocorticoid receptor (from Kino, Su et al. 2009, updated 2017).

The hGR gene has two terminal exon 9 (exon 9α and 9 β) alternatively spliced to produce the classic GR and the nonligand-binding GR isoform. Using at least 8 different translation initiation sites located in NTD, the hGR gene produces multiple GR isoforms termed A through D (A, B, C1-C3 and D1-D3) with unique transcriptional functions on glucocorticoid-responsive genes.

In the absence of ligand, all human GRα isoforms are randomly distributed in the cytoplasm and/or the nucleus. When the ligand binds, GRα transfer into the nucleus and show distinct transactivation or transrepression motifs on global gene expression analysed by cDNA microarray analyses (Fig. 11). The hGRα, located in the cytoplasm in the absence of ligand, is the classical GR. Upon ligand binding, hGRα translocates to the nucleus, recruits co-regulators to exert transcriptional effects. In opposition, immunohistochemistry studies have shown that hGRβ is constitutively located in the nucleus and does not bind agonists: it acts as a natural dominant-negative inhibitor of the hGRα isoform by altering the ability of hGRα to signal (Bamberger, Bamberger, de Castro, & Chrousos, 1995; Yudt, Jewell, Bienstock, & Cidlowski, 2003).

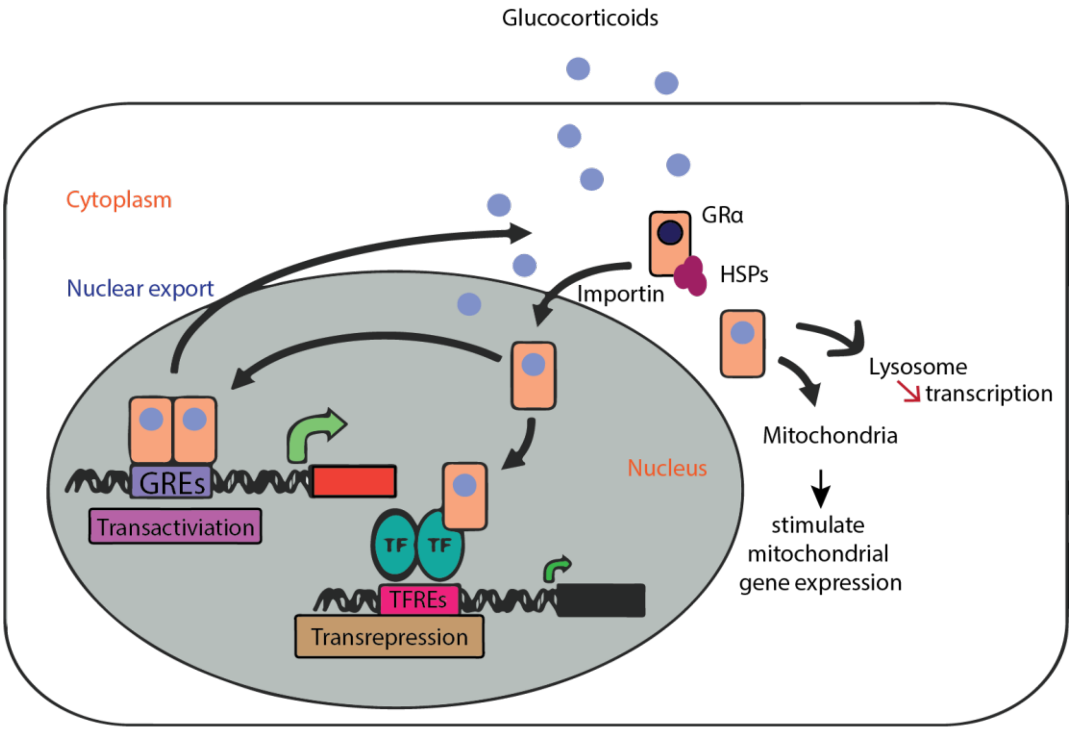
Glucocorticoids
Cytoplasm
Nuclear export
GRα
HSPs
Importin
Lysosome
↘ transcription
Mitochondria
stimulate
mitochondrial
gene expression
Nucleus
GREs
Transactiviation
TF
TF
TFREs
Transrepression

Figure 11: Intracellular circulation of GR (from Kino, Su et al. 2009, updated 2017).
Transit of GR between the cytoplasm and the nucleus, and its transcriptional regulation on the glucocorticoid-responsive genes in the nucleus are shown in the panel. GR translocates into mitochondria or lysosomes as well. GREs: glucocorticoid responsive elements; TFREs: transcription factor responsive elements; HSPs: heat shock proteins; TF: transcription factor

It has been shown that one antagonist, RU486 (mifepristone), binds to hGRβ and regulates its transcription activity (Lewis-Tuffin, Jewell, Bienstock, Collins, & Cidlowski, 2007). These data show that hGRβ negatively regulates the actions of the hGRα isoform as well as exert its individual functions. The β isoform can directly modulate genes that are not regulated by the α isoform. hGRα expression in all cells and tissues is higher than hGRβ expression. Still, the actual amount of hGRβ expression is less clear. hGRβ mRNA was found in a multitude of human tissues (Bamberger et al., 1995), but its protein was detected more limited to cellular distribution. GRβ isoforms are also found in rodents and zebrafish but are produced by an alternative splicing mechanism that differs from the human GRβ (Otto, Reichardt, & Schutz, 1997). All GRα isoforms have comparable binding affinities to GCs and interaction with GREs. GRα -C isoforms are the most biologically active and the most deficient in glucocorticoid-mediated functions are the GRα -D isoforms. Intriguingly, the GRα -D isoform is constitutively located in the nucleus and bound to specific GRE-containing target genes. Wide distribution of both transcriptional and translational GR isoforms enables GR signalling to be fine-tuned based on its relative availability in a given cell or tissue type.

3.4.2 GC-induced negative feedback on CRF neurons of the PVN

GC-induced negative feedback is a significant factor limiting the basal and stress-induced activity of hypophyseotropic CRF neurons. The impacts of GCs on CRF neurons are direct and indirect. In CRF neurons, GR immunoreactivity is co-located (Uht, McKelvy, Harrison, & Bohn, 1988) and GC microinjections in the PVN effectively reduced CRF mRNA and protein levels in adrenalectomized rats (Kovács & Sawchenko, 1996; Sawchenko, 1987). In addition, GC hormones in organotypic PVN cultures that lack extra-hypothalamic connections decrease CRF transcription (Bali et al., 2008). GR knockout mice studies have shown that GCs tonically repress neurosecretory CRF synthesis even under basal (non-stress) conditions (Kretz, Reichardt, Schutz, & Bock, 1999).

To further support the direct inhibitory effect on CRF gene expression, recent research found that targeted disruption of GR signalling within the PVN outcomes in CRF transcription upregulation (Jeanneteau et al., 2012). GR may suppress the transcription of CRF through a putative adverse GRE (nGRE) in neurosecretory neurons. Despite the important inhibitory impact of various GR agonists on CRF transcription, the regulatory region of the CRF gene itself does not appear to include classical GRE. However, a study using the rat GR DNA-binding domain in a DNase I protection assay demonstrated various regions of high-affinity GR binding (Guardiola-Diaz, Boswell, & Seasholtz, 1994).

3.5 Habituation to stress

Habituation, identified as a reduction in reaction to repetitive stimuli, is a type of non-associative learning. It implies that the decrease in response depends only on the self-replying stimulus presentation. Regardless of the paradigm, if the measured reaction shows "decrement as a result of repeated stimuli," it may be an instance of habituation as described in their landmark analysis of the topic by Thompson and Spencer

(Thompson & Spencer, 1966). It can also be seen as a type of sensory filtering as it decreases the reaction of the individual to a repeated non-threatening stimulus. In the field of stress neurobiology, habituation, first described 40 years ago, refers to "the reduction in physiological responses elicited by an exposure to a repeated homotypic stressor in comparison to the large responses elicited by acute exposure to that stressor" (Levine, Smotherman, & Hennessy, 1977; Pfister, 1979). The word habituation came to replace the more general word "adaptation" used in approximately simultaneously published literature. Because of the large quantity of literature on HPA reactions to stress and because of the vital role this axis plays in an individual's reaction to stress, we will concentrate on the HPA axis as the main physiological endpoint of stress reaction. To discuss habituation of HPA activity, the most recent review by Grissom & Bhatnagar (2009) grouped and reorganized the criteria previously defined by Thompson and Spencer (Thompson & Spencer, 1966) as follow:

A) "Habituation occurs to repeated stimuli. This theme encompasses the basic phenomenon of habituation, and habituation of responses to dishabituating stimuli, as the latter can be viewed as a special case of the former (Thompson & Spencer, 1966)."

B) "Habituation is reversible: spontaneous recovery and dishabituation are both examples of the reversibility of habituation under different circumstances (Thompson & Spencer, 1966)."

C) "Habituation can be improved by modifying certain parameters. Habituation is stronger in magnitude and/or more rapid when it is relearned following a period of spontaneous recovery, when stimuli come with increasing frequency and when stimuli are relatively weak (Thompson & Spencer, 1966)."

D) "Habituation can progress beyond experimental expectations. Habituation can progress to responses that are lower than baseline, and can generalize to stimuli other than the original habituating stimulus (Thompson & Spencer, 1966)."

The criteria are used to be able to distinguish habituation from other declines in response and highlight parametric manipulations, which affect whether habituation is observed and to what extent it is observed.

As described previously, stressful stimuli drive the PVN by complex and stress-specific neural circuitry to release CRF and other secretagogues, in particular AVP, in the hypophyseal portal bloodstream. These secretagogues work jointly in initiating the release of ACTH by the anterior pituitary, into the general circulation. ACTH consecutively stimulates the cortex of the adrenal glands to release GCs (de Kloet, 2000). Increased bloodstream release of GC results in negative feedback at the brain and pituitary level to inhibit further activation of HPA (Dallman et al., 1987). Control of GC release is of critical biological significance since a short time exposure is beneficial, but prolonged exposure can be potentially deleterious for the organism. Importantly, HPA activity is stress-induced but also under circadian regulation, with peak levels of ACTH and GC happening shortly before the time when an organism becomes active after a rest period (mornings for diurnal organisms, evenings for nocturnal animals). Stressors vary in how psychologically and/or physically stressful they are. By investigating stressors with a primarily psychological aspect, also referred to as processive stressors (i.e. restraint stress or novel environment) versus those with primarily physical qualities, also referred to as physiological or systemic stressors (i.e. exposure to ether or hypoglycaemia) (Herman & Cullinan, 1997), it became evident that psychological and physiological stressors lead to significant differences. Different pathways activate PVN, whether it is physical or psychological stress. Psychological stress acts via limbic circuitry, whereas physical stress acts directly via brainstem nuclei (Emmert & Herman, 1999). Since HPA activity predominantly habituates to processive stressors, RS has been widely used to study habituation of HPA activity. When exposed to a none familiar stress, animals react by producing a strong and appropriate HPA response, essential for coping with possibly threatening changes in the environment. It is essential from an evolutionary perspective to accustom repeated exposure to the same form of stressors to save energy and resources by dampening non-life-threatening reactions to stressors. On the other side, a lack of habituation from repeated exposure to psychological stressors in humans may be associated with stress-related diseases such as major depression or PTSD, further supporting the relevance of knowing how and under what conditions people are accustomed to repeated stress or not (Golier, Schmeidler, Legge, & Yehuda, 2007; Simeon et al., 2007; Thomson & Craighead, 2008; Yehuda, Teicher, Trestman, Levengood, & Siever, 1996).

Abnormal HPA activity to repeated exposure to various stressors in both animals and humans has been observed. For instance, in animals, such varied stressors as restraint, cold exposure, novel environment, noise-free water immersion, handling, and repeated ethanol injection are regularly noted (for literature, see Grissom & Bhatnagar, 2009). Repeated psychosocial stress and repeated parachute jumps have been shown to lead to habituation phenomenon in humans (see Grissom and Bhatnagar 2009).

It should be observed that most of the research mentioned above has been carried out in male rodents. Habituation of HPA activity in female rodents has also been shown (Lunga & Herbert, 2004) but not consistently reported (Bhatnagar, Lee, & Vining, 2005) due to the particularly rapid oestrous cycle of female rodents, which may have additional effects on HPA activity. Repeated restraint (Marin, Cruz, & Planeta, 2007) or repeated exposures to a novel environment (Hennessy, Levin, & Levine, 1977) were sometimes reported as a failure of HPA habituation. In each particular situation, it is hard to determine the precise cause of these differences, but there are some factors known to favour or reduce a homotypic stressor's HPA habituation. HPA activity habituation may differ on the basis of individual variations (Bhatnagar et al., 2005; Bhatnagar & Meaney, 1995), such as the context in which rodents are subjected to repeated restraint, odour presentation (Grissom, Iyer, Vining & Bhatnagar, 2007), incidental noise and construction (Dallman et al., 1999), repetitive exposure to a novel experimenter during handling (Dobrakovova et al., 1999) or injections (Hodges & Mitchley, 1970).

Overall, the habituation of the HPA axis appears to be faster with weaker rather than stronger stimuli and commonly observed with repeated restraint in which an animal is restrained in a tube, enabling little motion, but is less fast and complete during the more severe pressure of repeated immobilization in which an animal is entirely restricted in motion or individual limbs are restrained (Garcia, Marti, Valles, Dal-Zotto, & Armario, 2000; Vogel & Jensh, 1988).

As it is a metabolically expensive response system, over- or prolonged activation of the HPA axis can be deleterious. Therefore, reducing HPA activity to a non-inherently damaging stressor is adaptive for an organism (Dallman et al., 1987). Due to its involvement in mental disorders such as MDD and PTSD, it is essential to define the neural mechanisms engaged in modifications in HPA activity to repeated stress (Golier et al., 2007; Simeon et al., 2007). Better knowledge of the mechanisms regulating HPA activity may help to understand the etiology and therapy of these and other illnesses. Mechanisms of CORT negative feedback partially regulate the process of habituation to repeated stress. Systemically or centrally blockade of MRs and/or GRs may interfere with HPA activity habituation (M. A. Cole et al., 2000; Jaferi & Bhatnagar, 2006).

Jaferi and colleagues have shown that negative feedback mechanisms cannot wholly account for the occurrence of HPA habituation because adrenalectomized animals (with an absence of stress-induced negative feedback from GCs) are capable of habituation (Jaferi & Bhatnagar, 2006), and so it seems essential to explore the higher part of the axis (i.e., the hypothalamic component of the HPA axis) as a starting point for our study. The diminution of the central stress response is probably the key of habituation; for instance, activation of c-fos expression in medial parvocellular PVN is significantly decreased in PVN after repeated RS (Girotti et al., 2006). The central mechanisms contributing to HPA activity habituation are unclear. Changes in the PVN CRF and AVP may be directly involved.

Repeated RS or immobilization exposure increases CRF mRNA in the PVN (Imaki et al., 1991; Makino et al., 1999). Most of the studies done on HPA habituation involve descriptive results and little is known about the neuronal mechanism, neuronal connectivity, and molecular mechanisms, especially in mice where it is hard to find consistent literature about HPA habituation. That is why using transgenic mouse models to dissect better the negative feedback of the HPA axis will help to understand better the underlying mechanisms. With regards to the points discussed in this chapter, it became apparent that GRs in CRF neurons are privileged targets to start our investigation with.

3.6 Aim of the thesis

It is known that HPA responses are impaired in people suffering from psychopathology, including MDD and PTSD (Golier et al., 2007; Simeon et al., 2007; Thomson & Craighead, 2008). Centrally elevated levels of CRF are found in a subset of depressed patients (Holsboer 1999) and the CSF of untreated depressed subjects (Nemeroff, Widerlov et al. 1984). Lower levels of binding sites for CRF have been reported in suicide victims at the level of the PFC, due to downregulation in CRF secretion (De Bellis, Gold et al. 1993). It becomes evident that more in-depth understanding of the neural mechanisms involved in changes in HPA activity to repeated stress and that influence HPA regulation could likely aid to understand the etiology and treatment of disorders. Current evidence shows that habituation of HPA axis response is more complex than previously thought. The adaptive reduction of repeated stress-induced responses appears to involve complex crosstalk between negative feedback mechanisms induced by the release of GCs under repeated stress, response habituation processes produced by repetitive exposure to the stress stimulus, and likely more complex learning and memory encoding information regarding prior stressful events. A complete understanding of the habituation of repetitive stress is likely to rely on understanding the interaction between both of these processes. In the presented work, we aimed to deepen the current knowledge regarding the regulation of the HPA axis in mice by investigating the role of GRs in CRF expressing neurons of the PVN. The encompassing aim of this thesis is to gain an insight into the neurobiology underlying habituation to repeated homotypic stress. We directed our research towards those two major problems that currently impede advances in modeling HPA habituation in mice and mechanisms leading to it. By doing so, we contribute to a better understanding of normal behavior and mechanisms that could be failing in abnormal responses.

These questions were addressed using a variety of genetic mouse models, stress paradigms, molecular approaches, electrophysiological recordings, imaging methods, and transcriptomic analysis. We hypothesized that the targeted deletion of GRs from CRF PVN neurons would impair stress habituation, which may in part be mediated via differential transcriptional activity in response to the homotypic stressor.

4 Methods

4.1 Animals and animal care.

Mice were maintained in a pathogen-free temperature-controlled (23 ± 1°C) mouse facility on a 12-h light-dark cycle at the Max Planck Institute of Psychiatry, according to institutional guidelines. Food and water were given *ad libitum*. No more than 5 mice were housed per cage if group-housed. Mice were bred in the Max Planck of Biochemistry and housed in sibling-pairs until two weeks before the start of the experiments. Mice were housed in IVC cages under a pathogen-free temperature-controlled (23 ± 1°C) and constant humidity (55 ± 10 %) mouse facility on a 12-h light-dark cycle (lights on at 7 a.m.) at the Max Planck Institute of Psychiatry, according to institutional guidelines. Standard chow and water were given ad libitum. Cages were changed once per week, but never on the day of testing. At weaning mice were numbered by ear-punching, and a small tail biopsy was taken for genotyping. Mice were single housed two weeks prior behavioural testing or hormone assessment. All experimental procedures were carried out in the animal facility of the Max Planck Institute of Psychiatry in Munich, Germany, in accordance with the European Communities Council Directive 2010/63/EU. All efforts were made to minimize animal suffering during the experiments. The protocols were approved by the committee for the Care and Use of Laboratory animals of the Government of Upper Bavaria, Germany.

All experiments were performed during the light cycle. Littermates were divided randomly or according to their genotype if needed: Mice without and with GRs deletions are annotated Ctrl (Control) and cKO (conditional Knock-Out) mice respectively (see 4.2.1.1). The animals were between 12-14 weeks old at the beginning of the experiment if not stated differently.

4.2 Experimental design: Effects of GR KO in CRF expressing neurons in mice

We present here an overview of the *in vivo* experiments, used to answer the main questions of this PhD thesis. For further details concerning the methods, please refer to each corresponding detailed section, listed at the end of the Experimental design chapter (see chapter 4.3).

- Anatomical characterization of GRs in CRF expressing neurons and cKO validation
- Deletion of GRs from CRF neurons towards stress susceptibility
- Effect of GRs deletion on Circadian HPA activity
- Effect of GRs deletion on HPA responsiveness
- Effect of acute and homotypic stress repetition on habituation of HPA axis
- Impact of GR deletion in CRF+ neurons on the stress-induced excitation / inhibition balance needed for the habituation of the HPA axis
    - intrinsic electrical properties of CRF-expressing neurons of the PVN
    - synaptic transmission onto CRF neurons of the PVN and changes of excitation/inhibition balance after stress exposure

4.2.1 Anatomical characterization of GRs neurons expressing CRF and cKO validation

4.2.1.1 Generation of conditional GR knockout mice (GR$^{CRF\text{-}cKO}$)

Colocalization between CRF-expressing neurons and GR was carried out in CRF^{tdTomato} reporter mice resulting from the breeding of *Crf-ires-Cre* line [strain B6(Cg)-Crh$^{tm1(cre)Zjh/J10}$, JAX stock no: 012704] (Taniguchi et al., 2011), and Ai9 (R26$^{CAG::loxP\text{-}STOP\text{-}loxP\text{-}tdTomato}$, JAX stock no: 007905).

Conditional transgenic mice lacking GR in CRF-expressing neurons (GR$^{CRF\text{-}cKO}$) were generated by crossing *Crf-ires-Cre* with GR floxed mice [B6.129P2-Nr3c1^{tm2Gsc}/Ieg11, EMMA strain #02124], as previously described (Tronche et al., 1999).

Crf-ires-Cre and GR floxed mice were a generous gift from Dr. Josh Huang (Cold Spring Harbor, USA) and Dr Günther Schütz (DKFZ, German Cancer Research Center, Heidelberg, Germany) respectively. The Table 1 recapitulates the genotypes used for the experiements.

Control mice are designated: Ctrl or GR$^{CRF-Ctrl}$

- For electrophysiology and IHC analysis, Control mice are: Ctrl or GR$^{CRF-Ai9-Ctrl}$

Conditional knockout mice are designated: cKO or GR$^{CRF-cKO}$

- For electrophysiology and IHC analysis, Conditional knockout mice are designated : : cKO or GR$^{CRF-Ai9-CKO}$

	GR$^{CRF-Ctrl}$			GR$^{CRF-cKO}$		
Experiments (Figure in Results' chapter)	GR	CRF-iCre	TdTomato	GR	CRF-iCre	TdTomato
Colocalization CRF /GR (Fig 1, Fig 6a)	lox/+	+/Cre	+/Ai9	n.a	n.a	n.a
scRNA seq (Fig 2, 3, 4)	lox/lox lox/+	(+/+) +/Cre	n.a n.a	n.a	n.a	n.a
cKO validation (Fig 5, 6b, 12, 13)	lox/lox lox/+	(+/+) +/Cre	n.a	lox/lox	+/cre	n.a
Physiology (Fig 9, 10, 11)	lox/lox lox/+	(+/+) +/Cre	n.a n.a	lox/lox	+/cre	n.a
Dex/CRF test (Fig 14)	lox/lox lox/+	(+/+) +/Cre	n.a n.a	lox/lox	+/cre	n.a
RRS (Fig 15)	lox/lox lox/+	(+/+) +/Cre	n.a n.a	lox/lox	+/cre	n.a
Rescue + RRS (Fig 16, 19, 20, 21)	lox/lox	(+/+)	n.a	lox/lox	+/cre	n.a
CRF and cFos after RRS (Fig 22)	lox/lox lox/+	(+/+) +/Cre	n.a n.a	lox/lox	+/cre	n.a
Electrophysiology (Fig 23-30)	lox/+	+/Cre	+/Ai9	lox/lox	+/cre	+/Ai9
Behavioural experiments (Fig 8)	lox/lox lox/+	(+/+) +/Cre	n.a	lox/lox	+/cre	n.a

Table 1: Summary of the genotypes used for the experiments.

Aiming to visualize the CRF- and GRs-containing neural populations, PVN and CeA tissue of $\text{GR}^{\text{CRF-Ai9-CKO}}$ and $\text{GR}^{\text{CRF-Ai9—Ctrl}}$ mice were submitted to extensive anatomical studies. An average of 6 mice was used per group for staining characterization (ISH, IHC). Sample overview was acquired using an Olympus Confocal microscope. To minimize the number of mice, plasma CORT was measured from tail cuts (50 ul whole blood), once in the morning and in the evening to allow us to define some baseline CORT levels (Fig. 12).

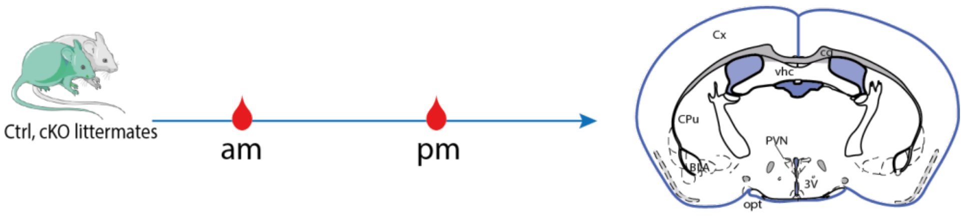

Figure 12: Baseline characterisation for CORT and brain anatomy

4.2.1.2 Single-cell RNA transcriptomics (scRNA-seq)

Mice were anesthetized using isoflurane and transcardially perfused with cold PBS. Brains were quickly dissected, transferred to ice-cold carbogenated aCSF, and kept in the same solution during dissection. Sectioning was performed using a 0.5 mm stainless steel adult mouse brain matrix (Kent Scientific) and a Personna Double Edge Prep Razor Blade. A slice (approximately -0.58 mm bregma to -1.22 mm bregma) was obtained from each brain and the extended PVN was manually dissected under microscope guidance (M205C stereomicroscope Leica, Germany). PVN from five different mice were pooled and dissociated using the Papain dissociation system (Worthington Biochemical Corporation, NJ, USA) following the manufacturer's instructions. All solutions were oxygenated with carbogen (95% O2 / 5% CO2). After this, the cell suspension was filtered (Fig. 13).

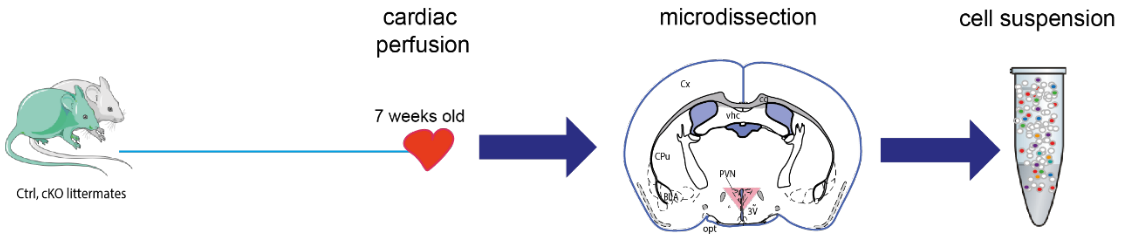

Figure 13: ScRNA sequencing for characterisation

4.2.2 Deletion of GRs from CRF neurons towards stress susceptibility

To further explore the role of the GRs in the CRF neurons Ctrl and cKO mice were submitted to the classical anxiety related tests: Open Field, Elevated Plus Maze, Dark Light box test, Forced Swim Test. 48 h of rest was observed between two tests (Fig. 14). Trunk blood and brains of the animals were collected and stored until further processing (for details see sections 4.3.6, 4.3.7 & 4.3.8). In order to minimize possible carryover effects of the different behavioural tests, the sequence of tests was arranged from least to most stressful (McIlwain et al., 2001; Kalueff and Murphy, 2007).

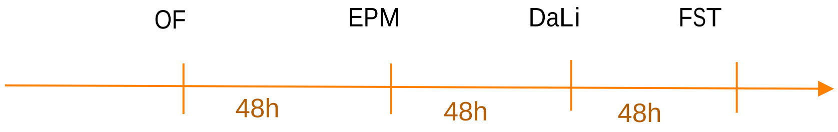

Figure 14: Sequence of behavioural tests

Open field (OF) test: The open field test was originally designed to characterize explorative behavior and general locomotor activity in a novel environment. Open field boxes (30 x 30 cm) were made of grey polyvinyl chloride (PVC) and evenly unaversive illuminated at low conditions (30 Lux) in order to minimize anxiety effects on locomotion. The apparatus was virtually divided into an outer an inner zone (15 cm x 15 cm). All mice were placed into a corner of the apparatus at the beginning of the trial.

Parameters assessed included the total distance travelled, immobility time, number of inner zone entries and inner zone time. The test duration was 30 min. Data were analyzed using the ANYmaze software (Stoelting, Wood Dale, IL).

Elevated plus-maze (EPM) test: The elevated plus-maze is used to assess anxiety-related behavior in mice. It is based on a conflict between the mice's exploratory drive and its innate fear of illuminated, unprotected and heightened areas (Lister, 1987). The EPM consisted of a plus-shaped platform which is elevated 50 cm above the floor, with four intersecting arms. Two opposing open (30 x 5 x 15 cm) and closed arms (30 x 5 x 15 cm) are connected by a central zone (5 x 5 cm). The maze was made of grey PVC. The illumination was 25 lux in the open arms and < 10 lux in the closed arms. Animals were placed in the center of the apparatus facing the closed arm and allowed to freely explore the maze for 10 min. Parameters measured included time spent in the open arms, open arm entries, latency to first open arm entry, immobility time, lit distance and total distance travelled, and were analyzed with the ANYmaze software.

Dark-light box (DaLi) test: The dark-light box test was additionally applied to investigate anxiety-related behavior. It is based on the innate aversion of rodents to brightly illuminated areas and on their spontaneous exploratory behavior, including novel environment and light (Hascoet et al., 2001). The apparatus is made of PVC and consists of a secure black compartment (15 x 28 x 27 cm) and an aversive, illuminated white compartment (48 x 28 x 27 cm), which are connected by an small tunnel (5 x 7 cm). The illumination in the dark compartment was < 5 lux and 500 lux in the lit compartment. Animals were placed into a corner of the dark compartment and allowed to freely explore the test arena for 5 min. Parameters assessed included time spent in the lit compartment, latency to first lit- compartment entry, number of lit compartment entries, lit compartment distance and total distance travelled, and were analysed by means of the ANYmaze software.

Forced swim test (FST): The forced swim test represents a well-established antidepressant-screening paradigm (Porsolt et al., 1977), but is also used to assess active versus passive stress-coping or despair-like behavior in mice (Slattery and Cryan, 2012). On top of that, the FST represents a strong stressor for mice considering that the animals are facing a psychological and physiological challenge. Each animal was placed into a two liter glass beaker (radius: 11 cm, height; 23.5 cm) filled up to a height of 15 cm (1.6 l) with 25-26°C tap water. Three behavioral parameters were assessed for 6 min including time struggling, swimming and floating. A mouse was judged floating once it stopped any movements expect those that were necessary to keep its head above water. Vigorous swimming movements involving all four limbs of the mouse, with the front paws breaking the surface of the water, usually at the walls of the beaker, were regarded as struggling. Behaviour which could not be assigned to either floating or struggling, such as the movement of only two limbs, was termed swimming. The parameters floating (immobility except small movements to keep balance), and struggling (vigorous attempts to escape) were recorded using the ANYmaze software and scored throughout the 5 min test period by a trained observer.

4.2.3 Effect of GRs deletion on Circadian HPA activity

4.2.3.1 Morning and afternoon CORT levels

Morning (am) and afternoon (pm) plasmatic CORT levels were firstly obtained from mice sacrificed for anatomical analysis in order to refine the number of animal used (Fig. 11).

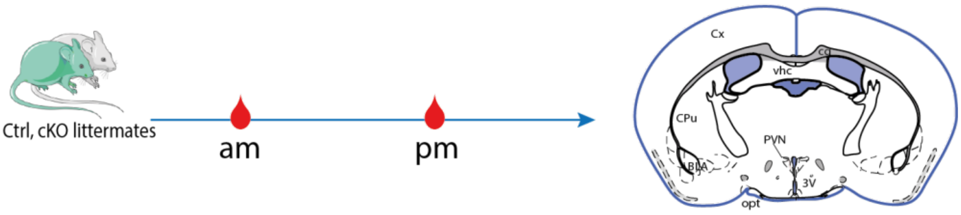

Figure 11: Baseline characterisation for CORT and brain anatomy

4.2.3.2 Microdialysis

Microdialysis was performed as described previously (Anderzhanova et al., 2013).

Surgery for microdialysis

Male mice were anesthetized with isoflurane and placed in a stereotaxic apparatus with adapted components to allow mouse inhalation anaesthesia. After exposure of the skull, a hole was drilled and a guide cannula was implanted into the right PFC of $GR^{CRF\text{-}cKO}$ mice and $GR^{CRF\text{-}Ctrl}$ control littermates (coordinates: anterior +1.9mm, lateral +0.3mm, ventral +0.3mm as referred from the animal's bregma). The guide cannula was fixed to the skull with dental cement. To connect a liquid swivel and counterbalancing arm during the microdialysis experiments, a small peg was additionally mounted to the skull. Mice received analgesic treatment (Metacam, 0.5 mg/kg) during surgery and 3 days afterwards via drinking water at the same dose. Animals were allowed to recover from surgery for 10 days before starting the microdialysis procedures.

***In vivo* microdialysis procedure**

After recovery from surgery, a 2 mm-microdialysis probe (cuprophane membrane with a molecular cut-off of 6 kDa, 0.2 mm OD) was inserted into the PFC through the pre-implanted guide cannula. Probe insertion was performed under a short-lasting isoflurane anaesthesia on the day before the actual experiment. Mice were connected to a liquid swivel mounted on a counterbalancing system. Probes were perfused with sterile artificial cerebrospinal fluid (in mM: NaCl, 145; KCl, 2.7; CaCl2, 1.2; MgCl2, 1.0; Na2HPO4, 2.0; pH 7.4) at a flow rate of 0.3 µl/min, using a microinfusion pump. On the experiment day (over 24h), following a 1h equilibration period, 60-min microdialysis fractions were constantly collected in cooled 300-µl microtubes (Milian AG) containing 2 µl of perchloric acid at a perfusion rate of 1.1 µl/min. The dead volume of the outlet line was compensated by a delay in fraction harvesting (10 min) (Fig. 15).

All microdialysate samples were kept refrigerated or frozen at -80°C until the measurement of CORT using radioimmunoassay, according to the manufacturer's protocol (MP Biomedicals, Eschwege, Germany). All samples were measured in duplicates and the intra- and inter-assay coefficients of variation were both below 10%.

Corticosterone measurements

Corticosterone measurements were performed in collaboration with Pr Stalla's laboratory at the Max Planck Institute of Psychiatry.

Histology

After completion of the microdialysis experiments, animals were decapitated under isoflurane anaesthesia, and brains were extracted and stored at -80°C. Brains were further sectioned with a cryostat, and sections were stained with cresyl violet for histological verification of the probe's localization. In case of non-correctly placed microdialysis probes, mice were excluded from the experiment.

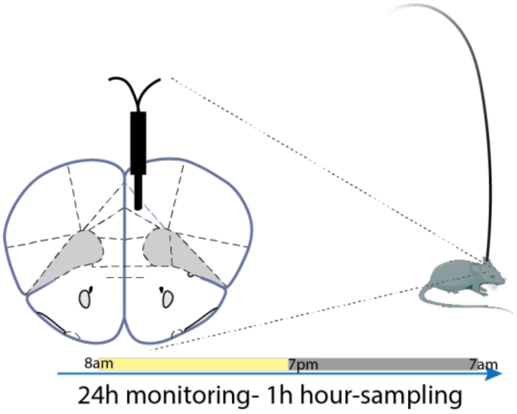

Figure 15: Microdialysis experiment design

4.2.4 Effect of GRs deletion on HPA responsiveness

In the combined Dex/CRF test, CORT secretion in $GR_{CRF\text{-}Ctrl}$ and $GR_{CRF\text{-}cKO}$ mice was monitored in response to a pharmacological suppression of adrenocortical activity with the GR agonist Dex and a subsequent stimulation with CRF (Touma et al., 2011). Seven days before the actual test, a blood sample was taken from the tail vessel of the animals at 3 p.m. in order to get a basal reference value ("Untreated"). On the day of testing, the mice received an intraperitoneal injection of Dex at 9 a.m. (Dexaratiopharm, Ratiopharm GmbH, Ulm, Germany), followed by an injection of CRF at 3 p.m. (Ferring Arzneimittel GmbH, Kiel, Germany; dose: 0.15 mg/kg body weight, solution freshly prepared shortly before the injection, injection volume: 0.3 ml, solvent: sterile Ringer's solution). Immediately before CRF injection, a tail blood sample was collected ("After Dex" value) and a second one 30 min later ("After CRF" value). Two independent Dex/CRF tests were performed using either a relatively high dose (2 mg/kg body weight) or a relatively low dose of Dex (0.05 mg/kg body weight) (Touma *et al.*, 2011).

Samples were stored at -20°C and plasma CORT concentrations were measured as described further (see 4.3.8) (Fig. 16).

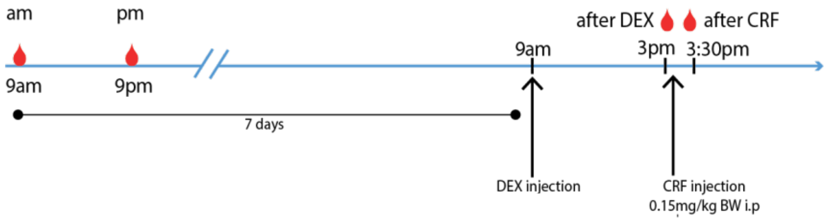

Figure 16: Dex/CRF reactivity test

4.2.5 Effect of acute and repeated homotypic stress in GR$^{\text{CRF-CKO}}$ mice

4.2.5.1 Restraint Stress

In a next step, we investigated the effects of an acute Restraint Stress and Repeated Restraint Stress. Therefore, male GR$^{\text{CRF-cKO}}$ and GR$^{\text{CRF-Ctrl}}$ were used.

Two weeks before the experiments, male mice were separated and single housed with a 12:12 h light:dark schedule (lights on at 7:00 a.m.). To determine the basal hormone plasma levels, mice were left undisturbed throughout the night before the experiment. Blood sampling was performed in the early morning (~ 9 a.m.) and evening (~ 9 p.m.) by collecting blood from tail cut, with the time from first handling of the animal to completion of bleeding not exceeding 45 sec. For evaluation of the endocrine response to stress, blood samples were collected immediately after 15 min of restraint stress, for which animals were placed in a 50 ml conical tube. A last blood sample was collected 90 min after the end of the restraint to assess the recovery period (Fig. 17). All plasma samples were stored at -20°C until the CORT measurement. Stress experiments were performed in the morning (~ 9 a.m.). To study the habituation of the HPA axis to a repeated homotypic stressor, this restraint stress protocol (except for the recovery sample, which was omitted) was repeated 3 times with one-week interval between each stress session (RRS), where the animals were left undisturbed (Fig. 18). All blood samples were kept on ice until centrifuged (4°C) and plasma was removed for measurement of CORT using radioimmunoassay, according to the manufacturer's protocol (MP Biomedicals, Eschwege, Germany). All samples were measured in duplicates and the intra- and inter-assay coefficients of variation were both below 10%.

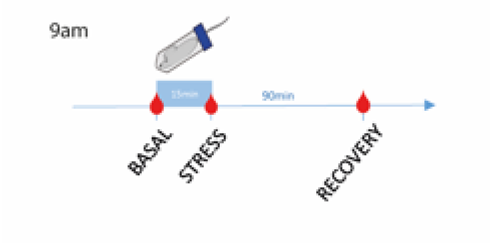

Figure 17: Single Restraint Stress

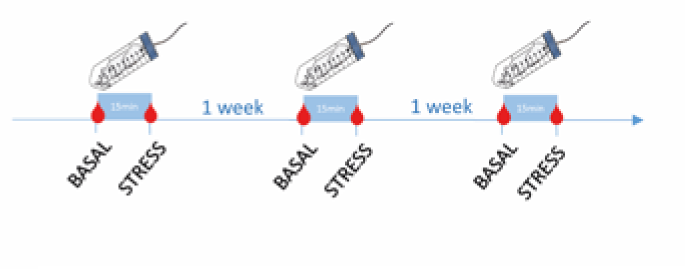

Figure 18: Repeated Restraint Stress

4.2.5.2 Rescue Experiment

Mice were anesthetized with isoflurane (Floren, Abbott), 2% v/v in O_2 and placed in a stereotactic apparatus (TSE Systems Inc., Bad Homburg, Germany) with adapted components to allow mouse inhalation anesthesia. $GR^{CRF\text{-}cKO}$ and $GR^{CRF\text{-}Ctrl}$ mice were bilaterally injected with either AAV EF1α-DIO-mGR or AAV-EF1α-DIO-mCherry into the dorso-lateral part of the PVN (300 nl) using a 33-gauge microinjection needle with a 10 µl syringe (Hamilton) coupled to an automated microinjection pump (World Precision Instruments Inc.) at 50 nl/min. Coordinates from bregma were as follows: AP: -0.75 mm, ML: +/- 0.25 mm, and DV: - 4.6 mm from the cortical surface. At the end of the infusion, needles were kept at the site for 10 min and then slowly withdrawn. Post-surgery recovery included Metacam supplementation (sub-cutaneous injection of 0.5 mg/kg body weight of a 0.1 mg/mL solution) for 3 days after surgery. Four weeks after virus injection, mice were subjected to RRS and CORT levels measured as described above (Fig. 19). After completion of the experiments, mice were killed with an overdose of isoflurane and transcardially perfused with PBS followed by 4% PFA, and brains removed for subsequent analysis. Brains were sectioned (40 µm) using a vibratome (HM 650 V, Thermo Scientific) and accurate microinjection and mGR re-expression verified by GR immunostaining (or mCherry expression for the control virus).

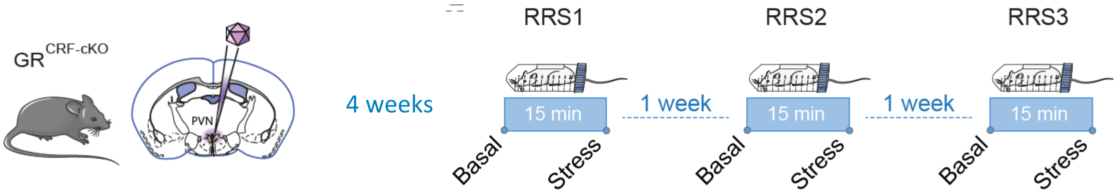
GR$^{CRF\text{-}cKO}$
PVN
4 weeks
RRS1
RRS2
RRS3
15 min
15 min
15 min
1 week
1 week
Basal
Stress
Basal
Stress
Basal
Stress

Figure 19: Rescue experiment

4.2.6 Impact of GR deletion in CRF+ neurons on the stress-induced excitation / inhibition balance needed for the habituation of the HPA axis

Animals

All mice used were generated from the CRF^{tdTomato} background to visually identify the CRF^{+} neurons. GR$^{CRF\text{-}Ctrl}$ and GR$^{CRF\text{-}cKO}$ mice were assigned randomly to Basal (No stress) and RRS groups. Mice from the RRS groups were used for electrophysiological recordings one day after the third session of restraint stress (Fig. 20).

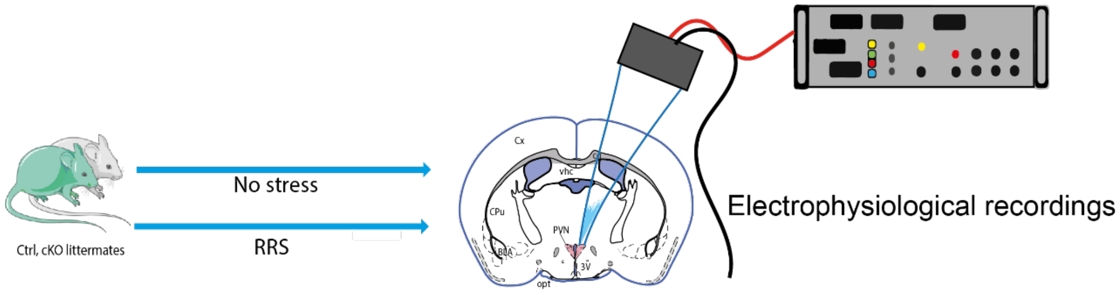
Ctrl, cKO littermates
No stress
RRS
Cx
vhc
CPu
PVN
3V
opt
Electrophysiological recordings

Figure 10: Electrophysiology experiments

Brain slices preparation

Mice were anesthetized with isoflurane and decapitated. All following steps were done in ice-cold cutting solution saturated with carbogen gas (95% O_2/5% CO_2). The cutting solution (pH 7.4, 340 mOsm) consisted of (in mM): 120 choline chloride, 3 KCl, 27 $NaHCO_3$, 8 $MgCl_2$, and 17 D-glucose. After decapitation, the brain was rapidly removed from the cranial cavity and 300 µm thick coronal slices containing the hypothalamus were cut using a vibratome (HM650 V, Thermo Scientific). Subsequently, slices were incubated for 30 min in carbogenated physiological saline at 34 °C. The physiological saline (pH 7.4; 310 mOsm) consisted of (in mM): 125 NaCl, 2.5 KCl, 25 $NaHCO_3$, 1.25 NaH_2PO_4, 2 $CaCl_2$, 1 $MgCl_2$, and 10 D-glucose. Afterward, slices were stored at room temperature (23−25 °C) for at least 30 min in carbogenated physiological saline before patch-clamp recordings.

Patch-clamp recordings

All experiments were conducted at room temperature. In the recording chamber, slices were superfused with carbogenated physiological saline (4−5 mL/min flow rate). CRF neurons of the PVN expressing tdTomato were visually identified by epifluorescence microscopy. After identification, the cell bodies of these neurons were visualized by infrared videomicroscopy and the gradient contrast system. Somatic whole-cell voltage-clamp recordings (>1 GΩ seal resistance, −70 mV holding potential) were performed using a SEC-10L amplifier (NPI Electronic, Tamm, Germany). The current was low-pass filtered at 1.3 kHz, digitized at 6.5 kHz, and stored with the standard software Pulse 8.31 (HEKA Elektronik, Lambrecht/Pfalz, Germany). Recordings were excluded from analysis if the series resistance changed more than 10%.

Current-clamp recordings

These recordings were performed to compare the intrinsic electrical properties of CRF^+ neurons in the different experimental conditions. The patch-clamp electrodes (open-tip resistance 5-7 MΩ) were pulled from borosilicate glass capillaries (Harvard Apparatus, Kent, UK) on a DMZ-Universal puller (Zeitz-Instruments, Munich, Germany) and filled with a solution consisting of (in mM): 130 K-gluconate, 5 NaCl, 2 $MgCl_2$, 5 D-Glucose, 10 HEPES, 0.5 EGTA, 2 Mg-ATP, 0.3 Na-GTP, 20 phosphocreatine, pH 7.3 with KOH, 305 mOsm (all substances were from Sigma-Aldrich, St. Louis, MO). All potentials were corrected for a liquid junction potential of 10 mV. The input resistance was calculated from steady-state voltage responses upon negative current injections (1,500 ms). Firing frequency was evaluated by positive current injections that induced mild firing (4 - 10 action potentials) of the neurons.

mEPSCs recordings

Slices were superfused with carbogenated physiological saline containing TTX (1 µM), bicuculline methiodide (BIM, 10 µM), CGP 55845 (5 µM), and APV (50 µM) to block voltage-gated sodium channels, $GABA_A$, $GABA_B$ and NMDA receptors respectively and isolate miniature excitatory post-synaptic currents (mEPSCs). The patch-clamp electrodes (5−7 MΩ open-tip resistance) were filled with a solution consisting of (in mM): 125 Cesium MethaneSulfonate, 8 NaCl, 4 Mg-ATP, 20 phosphocreatine, 0.3 Na-GTP, 10 HEPES, 0.5 EGTA, and 5 QX-314 chloride (pH 7.2 adjusted with CsOH, 285 mOsm).

mIPSCs recordings

Slices were superfused with carbogenated physiological saline containing TTX (1 µM), CGP 55845 (5 µM), NBQX (5 µM) and APV (50 µM) to block voltage-gated sodium channels, $GABA_B$, AMPA and NMDA receptors respectively and isolate miniature inhibitory post-synaptic currents (mIPSCs). The patch-clamp electrodes (5−7 MΩ open-tip resistance) were filled with a solution consisting of (in mM): 140 KCl, 5 NaCl, 2 Mg-ATP, 20 phosphocreatine, 0.3 Na-GTP, 10 HEPES, 0.1 EGTA, and 2 QX-314 chloride (pH 7.2 adjusted with KOH, 285 mOsm). In a subset of experiments, slices were pre-incubated in the nitric oxide synthase 1 (NOS 1) inhibitor L-NAME (100 µM) for at least 15 min prior to and during the recordings.

Analysis

Offline analysis was performed using the Pulse Software for the intrinsic electrical properties and Mini Analysis Program (Synaptosoft Inc.) for mEPSCs and mIPSCs recordings. Miniature currents were automatically detected using templates from the software with a threshold for event detection set to 3 times the RMS.

4.3 Microbiological methods

4.3.1 Genotyping

For genotyping PCRs of transgenic mice, tail tissue was digested in 100 µl 50 mM NaOH for 30 min at 95°C followed by a neutralization step using 30 µl 1 M Tris-HCl (pH 7.0) and stored at 4°C. 1-2 µl of the tail lysates were used as template for PCRs. For genotyping, 1 µl of the lysed genomic DNA was used in a 25 µl-PCR reaction, containing 2.5 µl 10x PCR buffer (Abgene), 1.5 µl 25 mM MgCl2, 0.5 µl dNTPs (10 mM each, Roche), 0.5 µl of each primer and 0.5 µl Taq DNA polymerase (5 U/µl, Abgene). A standard PCR program was carried out: 95°C 5 min, 35 cycles of 95°C for 30 sec, 58-60°C for 30 sec, 72°C for 1 min per 1 kb of DNA, followed by 72°C for 10 min and subsequent hold at 4°C.

Genotyping was performed by PCR using the following primers to identify GRflox/flox mutants: GR-flox1, 5´GGC ATG CAC ATT ACG GCC TTC T3´; GR-flox8, 5´CCT TCT CAT TCC ATG TCA GCA TGT3´ and GR-flox4, 5´GTG TAG CAG CCA GCT TAC AGG A3´. Standard PCR conditions resulted in a 225-bp wild-type and a 275-bp floxed PCR product. A premature deletion of the floxed allele would have been identified by the occurrence of a 390-bp PCR product. The following primers were used to identify Crf-IRES-Cre mutants: 5′CTT ACA CAT TTC GTC CTA GCC3’ and 5′CAA TGT ATC TTA TCA TGT CTG GAT CC3′ (468 base pair resultant PCR band, Fig. 21).

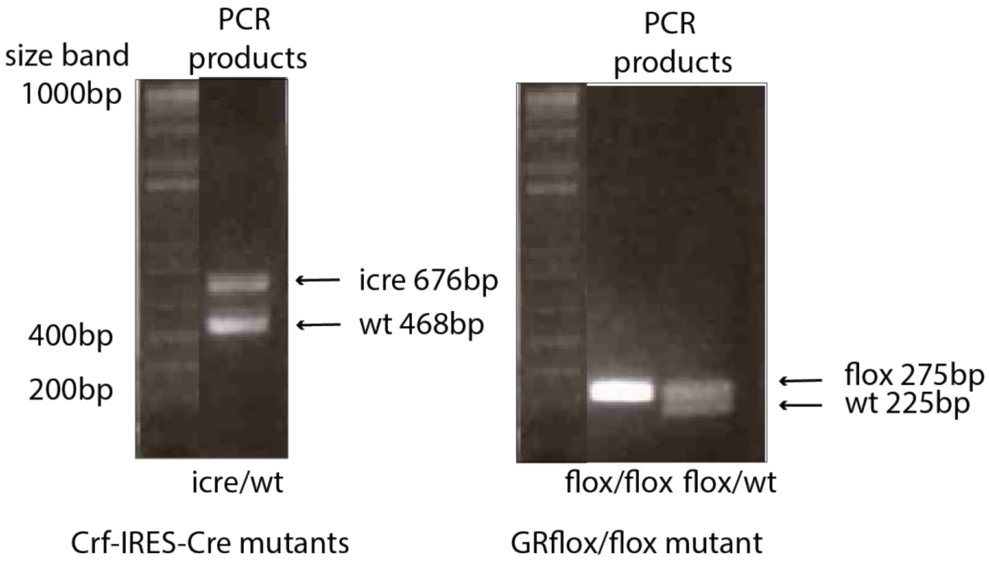
size band
PCR products
1000bp
400bp
200bp
icre 676bp
wt 468bp
icre/wt
Crf-IRES-Cre mutants
PCR products
flox 275bp
wt 225bp
flox/flox flox/wt
GRflox/flox mutant

Figure 21: Genotyping

4.3.2 Polymerase Chain Reaction (PCR)

In order to amplify desired DNA sequences for further cloning procedures, PCRs were carried out using genomic DNA, cDNA or plasmid DNA as templates. For a regular 50 µl PCR reaction 0.5-5 µg genomic DNA, 0.1-1 µg cDNA or 20-200 ng plasmid DNA were used. The reaction was prepared as follows (Table 2):

Table 2: PCR protocol

x template (as stated above)
5 µl 10 x reaction buffer IV (ABgene)
3 µl 25 mM $MgCl_2$ (ABgene)
1 µl 10 mM dNTPs (Roche)
3 µl 10 µM primer forward
3 µl 10 µM primer reverse
0.5 µl Thermoprime Plus DNA polymerase (5 U/µl, ABgene)
adjust to 50 µl with H_2O_{bidest}

In general, the following standard PCR reaction was carried out: 95°C 5 min, 35 cycles of 95°C for 30 sec, 58-60°C for 30 sec, 72°C for 1 min per 1 kb of DNA, followed by 72°C for 10 min and subsequent hold at 4°C. If required, the annealing and elongation temperatures were adjusted for a specific DNA product. PCR products were analyzed via gel electrophoresis in a 1-2% agarose gel (1 x TAE), containing ethidium bromide. For this, a small aliquot of the PCR (1-5µl) was mixed with 6x Orange loading dye and loaded onto the gel, which was subsequently analysed with a UV-transilluminator and a BioDoc II gel documentation system from Biometra or the Quantum gel documentation system 1100 from Vilber Lourmat.

4.3.3 Assessment of DNA/RNA concentrations

DNA or RNA concentrations were measured in a UV photometer (Gene Quant II, Pharmacia Biotech). An optical density (OD) of 1 at a wavelength of 260 nm and a cuvette thickness of 1 cm corresponded the following concentrations: 50 µg/ml double stranded DNA, 33 µg/ml single stranded DNA and 40 µg/ml RNA. Consequently, concentrations can be determined by the following equation: X µg/ml = OD260 x n x f, with f being the dilution factor and n the default 50 µg/ml double stranded DNA, 33 µg/ml single stranded DNA and 40 µg/ml RNA.

4.3.4 Preparation, analysis of plasmid DNA and cloning steps

Plasmid construction

The guide plasmid pRK5-mGR-Flag was a generous gift from T. Rein (MPI of Psychiatry, Munich, Germany), and the backbone plasmid pAAV212 Ef1α-DIO-mCherry-WPRE-pA was purchased from Addgene (plasmid # 37093). The mGR-Flag sequence was subcloned in the backbone plasmid using the restriction enzyme AscI and NheI. The primer for PCR were: mGR-Flag NheI forward GCTAGCATGGACTACAAGGACGACGA and mGR-Flag AscI reverse GGCGCGCCTCATTTCTGATGAAACAGAA.

Preparation of plasmid DNA

Plasmid DNA was prepared using DNA isolation Kits from Qiagen (Mini-, Midi- and Plasmid Maxi-Kit) according to the manufacturer's instructions. For MiniPreps, a single colony was inoculated in 3-5 ml LB medium with a selective antibiotic o.n. on a shaker at 37°C. For MidiPreps, a single colony was inoculated in 100 ml LB medium with a selective antibiotic o.n. on a shaker at 37°C. For MaxiPreps, 500 µl of an o.n. MiniPrep, or the appropriate glycerol-stock of bacteria was added to 250 ml LB medium with the appropriate antibiotic and incubated overnight on a shaker at 37°C.

DNA restriction digests

For analytical purposes only, restriction digestion of DNA samples was performed using restriction enzymes and working buffers from Fermentas Life Science or New England Biolabs (NEB). Plasmid-DNA was digested for 1-2 h at 37°C with 10 units/µg of the restriction enzyme in corresponding buffers. Fragment sizes were analyzed by agarose gel electrophoresis.

DNA gel extraction

The QIAquick Gel Extraction Kit (Qiagen) was used according to manufacturer´s instructions to purify DNA fragments out of an agarose gel. DNA was eluted in 30-50 µl of H2O bidest. The DNA concentration was determined by spectrophotometry and the DNA quality was assessed by gel electrophoresis.

Ligation of DNA fragments

For ligations of linearized vectors and the insert the Rapid DNA Ligation Kit (Fermentas) was used. 50 ng of vector backbone was ligated to 3x molar excess of insert. The appropriate amount of insert was calculated as following: m insert (ng) = 3 x 50 ng x (bp of insert / bp of backbone vector). T4 DNA ligase buffer and 5 U of T4 DNA ligase (Fermentas) were added in a total volume of 10-15 µl, and incubated overnight at 16°C. On the next day, a heat shock transformation using 1-2 µl of the ligation product was performed in chemocompetent bacteria.

TOPO TA Cloning

For ligation of products obtained from PCR reactions, inserts were cloned into the pCRII-TOPO vector (TOPO TA cloning Dual promoter Kit, Invitrogen), containing Sp6 and T7 promoters for efficient *in vitro* transcription. PCR products with 3'-Aoverhangs were inserted into linearized pCRII-TOPO vector with single 3’-T-overhangs. The reaction was set up as follows: 4 µl PCR product, 1 µl salt solution and 1 µl pCR®II-TOPO® vector. After 10 min of incubation at room temperature 1-4 µl of the mixture was transformed into chemically competent bacteria as described above. For blue-white selection of the colonies, 40 µl of 40 mg/ml X-Gal in dimethylformamide (DMF) solution were added to the LB-agar plates.

Sequencing

All sequencing reactions were carried out by Sequiserve (www.sequiserve.de).

Preparation of chemically competent bacteria

Initially, 5 ml of DH5α or XL1-Blue *E. coli* culture was grown overnight in LB medium. On the following day, 100 ml LB medium was inoculated with the overnight culture and grown on a shaker at 37°C until an optical density (OD) of OD 550nm < 500 was obtained. Subsequently, the bacteria were centrifuged for 15 min at 5000 rpm at 4°C. The supernatant was decanted and the pellet was gently resuspended on ice in 30 ml cold TBFI. After incubation on ice for 20 min bacteria were centrifuged for 5 min at 4000 rpm at 4°C. The pellet was gently resuspended in 3.6 ml TBFII and 100 µl aliquots were prepared. Competent bacteria were frozen and stored at -80°C.

Transformation

Chemically competent DH5α or XL1-Blue *E. coli* bacteria were shortly thawed on ice. The DNA was added to the bacteria and mixed by gently tapping the tube. Bacteria were incubated for 20-30 min on ice. Competent cells were then heat-shocked at 42°C for 30-90 sec and subsequently put on ice. This enabled the uptake of the plasmid DNA. 1 ml SOC or LB medium was added, and the cells were incubated on a shaker at 37°C for 1-2 h. Subsequently, cells were plated on LB plates containing the appropriate antibiotic for selection (100 µg/ml ampicillin or 50 µg/ml kanamycin) and incubated overnight at 37°C. Single colonies were picked and inoculated in 5 ml LB medium containing the appropriate selection marker (100 µg/ml ampicillin or 50 µg/ml kanamycin) and grown overnight at 37°C on a shaker at 250 rpm for subsequent DNA preparation.

Glycerol stocks

For long-term storage, 750 µl of an overnight bacteria culture was mixed with 250 µl 80% glycerol and frozen at -80°C.

Production and purification of adeno-associated viruses (AAVs)

Packaging and purification of recombinant (r) AAVs (serotype 1/2) was conducted as previously described (Pilpel et al., 2009), with the following modifications. A variant of the human embryonic kidney cells (HEK293T), containing the SV40 large T-antigen, was transfected with the AAV transfer plasmid and the helper plasmids at a molar ratio of 1:1:1 using 1 mg/ml linearized Polyethylenimine (PEI). Three days after transfection, the cells were harvested and lysed by undergoing 3 repetitive freeze-and-thaw cycles using a dry ice/ethanol bath and a 37°C water bath. The crude lysate was obtained after a centrifugation step. The rAAV particles were then purified using a Heparin Agarose Type I chromatography column22. After elution, the viral particles were washed with PBS using a 100000 MWCO Amicon Ultra Filter (Millipore; Cat.: UFC910024) and concentrated to a final volume of ~100 µl. The rAAV titers were determined by qPCR and resulted in 3x1011 genomic particles per microliter for the AAV1/2-Ef1α-DIO-Flag-mGR. The AAV1/2-Ef1α-DIO-mCherry (titer of 1,4x1012 genomic particles per microliter) was used as a control (plasmid purchased from Addgene; plasmid 50462, donated by Bryan Roth).

4.3.5 RNA isolation and quantitative real-time PCR (qRT-PCR)

RNA was isolated either from mammalian cells or from murine tissue using the TRIzol protocol (Invitrogen). cDNA was generated from the RNA using Reverse Trancriptase Superscript II from Invitrogen and oligo-dT primers according to the manufacture's protocol. Aliquots of the prepared cDNA were utilized as templates for quantitative real time PCR, which was carried out in the Lightcycler 2.0 System (Roche) using the QuantiFast SYBR Kit (Quiagen). The mastermix was prepared as follows (volume/sample): 5 µl 5x PCR mix (QuantiFast SYBR Green PCR Mix), 1 µl 10 µM primer fwd , 1 µl 10 µM primer rev and 1 µl H2O (Quiagen, Hilden). 8 µl of the mastermix were pipetted into each capillary, which was fixed in the Lightcycler carousel (Roche). Subsequently, 2 µl of diluted cDNA (1/10) were added and the capillaries were closed. Samples were centrifuged before they were placed into the LightCycler. The same PCR settings were chosen for all runs. At the end of every run a melting curve was measured to ensure the quality of the PCR product. Crossing points (Cp) were determined using the absolute quantification fit points′ method. The calculations were conducted by the LightCycler®Software 4.05 (Roche). Threshold and noise band values were set to the same level in all compared runs. Relative gene expression was determined with the 2-ΔΔCT method (Livak and Schmittgen, 2001), using the real PCR efficiency calculated from an external standard curve, normalized to the housekeeping genes Hprt and Gapdh and related to the data of control experiments.

4.3.6 Preparation of brain slices and immunohistochemistry

Mice were killed with an overdose of isoflurane (Floren®, Abbott) and transcardially perfused with a peristaltic pump for 1 min with PBS, 5 min with 4% PFA (w/v) in PBS, pH 7.4, and 1 min with PBS at a flow rate of 10 ml/min. The brains were removed and post-fixed overnight. in 4% PFA at 4°C and subsequently cryoprotected in 15% (w/v) saccharose in PBS, pH 7.6 overnight. at 4°C. Brains were washed with PBS and embedded in warm 4% (w/v) agarose (Invitrogen) in PBS for vibratome-sectioning (MICROM HM 650V, ThermoScientific). 40-50 µm thick sections were prepared and stored in cryopreservation solution (25 % (v/v) glycerol, 25% (v/v) ethylenglycol, 50% (v/v) PBS, pH 7.4) until further use. Slices were washed 3 x with PBS and permeabilized with PBS-TritonX-100 0.1% 3 x 5 min. Blocking was performed at room temperature for 1 h in 5% BSA (w/v) in PBS-TritonX-100 0.1%. Brain slices were then incubated overnight. at 4°C with the primary antibody, which was previously diluted in 5% BSA (w/v) in PBS-TritonX-100 0.1%. After a 3 x 10 min washing step with PBS, an Alexa Fluor secondary antibody (Invitrogen), diluted in PBS-Triton 0.01%, was added and incubated for 2 h at room temperature. Brain sections were washed 3 x with PBS, stained with DAPI and mounted with anti-fading fluorescence VectaShield medium (Vector Labs).

4.3.7 *In situ* hybridization (*ISH*)

ISH was performed as previously described (Lu et al., 2008; Refojo et al., 2011). Male mice (age 2-4 months) were anaesthetized with isoflurane and sacrificed by decapitation. Brains were immediately dissected, and shock frozen on dry ice. Frozen brains were cut on a cryostat in 20-µm thick sections and mounted on SuperFrost Plus slides and shortly dried on a 37°C warming plate. Slides were stored at -20°C until further processing. Before pretreatment, slides were thawn approximately for 30 min at 37°C. Fixation and pretreatment of slides were performed at room temperature according to Table 3.

Table 3: Pretreatment of slides during *ISH*

Steps	Minute	Product	Comment
1. Fix	10	4% PFA in 1x PBS / DEPC	On ice
2. Wash	2 x 5	1x PBS / DEPC	
3. Acetylate	10	0,1M triethanolamine-HCl in 1 TEA, pH 8,0	Add freshly 600 µl acetic anhydride per 200 ml TEA and stir
4. Wash	2 x 5	2x SSC / DEPC	
9. Dehydrate			
	1	60% Ethanol/DEPC	
	1	70% Ethanol/DEPC	
	1	96% Ethanol/DEPC	
	1	100% Ethanol	
	1	CHCl3	
	1	100 % Ethanol	
Air dry slides in a dust free, RNase-free area			

Specific riboprobes were generated by PCR applying T7 and SP6 primers using plasmids containing the required template cDNA (Table 9). Radiolabeled sense and antisense cRNA probes were generated from the respective PCR products by in vitro transcription with 35S-UTP (PerkinElmer) using T7 and SP6 RNA polymerase. After 20 min of DNase I (Roche) treatment, the probes were purified using the RNeasy-Mini Kit protocol (Qiagen) and measured in a scintillation counter. The sections were hybridized overnight at 57°C with a probe concentration of $7x10^6$ counts per minute (cpm)/µl. Subsequently, they were washed at 64°C in 0.1 x saline sodium citrate (SSC) and 0.1 mM dithiothreitol. The stringency washing steps are described in Table 4.

Table 4: Stringency washing procedure during *ISH*

1. Wash	RT	4 x 5	4x SSC	
2. RNase	37	20	1x NTE / 500 µl RNaseA (20 µg / ml)	Add RNase freshly
3. Wash	RT	2 x 5	2x SSC / 1mM DTT	Add DTT freshly

4. Wash	RT	10	1x SSC / 1mM DTT	Add DTT freshly
5. Wash	RT	10	0.5x SSC / 1mM DTT	Add DTT freshly
6. Wash	64	2 x 30	0.1x SSC / 1mM DTT	Add DTT freshly
7. Wash	RT	2 x 10	0.1x SSC	
8. Dehydrate	RT	2 x 1 1 1 1 1	30% Ethanol / 300mM NH4OAc 50% Ethanol / 300mM NH4OAc 70% Ethanol / 300mM NH4OAc 95% Ethanol 100% Ethanol	
Air dry slides in a dust free area				

In order to visualize hybridization signals, dried slides were exposed to a special high performance X-ray film (Kodak, BioMax) for different time intervals. For quantification, autoradiographs were digitized and relative levels of mRNA were determined by computer-assisted optical densitometry (ImageJ). To obtain cellular signal-resolution hybridized slides were dipped in autoradiographic emulsion (type NTB2), developed after 3-6 weeks and counterstained with cresyl violet. Dark-field photomicrographs were captured with digital cameras adapted to an imaging microscope and a stereomicroscope (Leica, Wetzlar, Germany). Images were digitalized using Axio Vision 4.5, and afterwards photomicrographs were integrated into plates using image-editing software. Only sharpness, brightness and contrast were adjusted. For an adequate comparative analysis in corresponding mutant and control sections the same adjustments were performed. Brain slices were digitally cut out and set onto an artificial black or white background using Adobe Photoshop CS2.

4.3.8 Stress reactivity and CORT measurement

As a measure of HPA axis responsiveness we used a single restraint stress, as previously described (Touma et al., 2008). Briefly, each mouse was removed from its home cage and an “basal” blood sample was obtained through a small incision from the ventral tail vessel (to ensure the reference sample was very close to baseline levels, the time between initial handling of the cage until completing the blood sampling was less than 1 min). The mouse was then placed into a small restrainer (50 ml falcon tube, with holes for ventilation and an aperture in the cap for the tail) for 15 min. The same blood sampling technique was applied to collect the “reaction sample” and the “recovery sample” 90 min after the beginning of the restraint stress. In some cases, the “recovery sample” was collected from the trunk blood according to experimental further needs. The animal was shortly anesthetized with isoflurane and decapitated carefully to allow the collection of the trunk blood. All blood samples were collected in EDTA tubes and kept on ice until they were centrifuged (4°C, 15000g, 15min) and plasma was removed for measurement of CORT using radioimmunoassay, according to the manufacturer’s protocol (DRG Instruments GmbH, Marburg, Germany). All samples were measured in duplicates and the intra- and inter-assay coefficients of variation were both below 10 %. All stress experiments were performed in the morning (08:00–10:00 a.m.).

5 Results

5.1 Anatomical characterization of GRs neurons expressing CRF and cKO validation

In order to quantify the colocalization between CRF and GR in neurons of the PVN, we used immunohistochemistry (IHC) on coronal brain sections obtained from $CRF^{tdTomato}$ (Crf-ires-Cre crossed with Ai9) mice, a well-established CRF reporter mouse line (Fig. 1). We found that 98 ± 0.4 % of CRF+ neurons in the PVN co-express GR and conversely 72 ± 1.5 % of GR+ cells in the PVN co-express CRF (n = 5 mice) (Fig. 22).

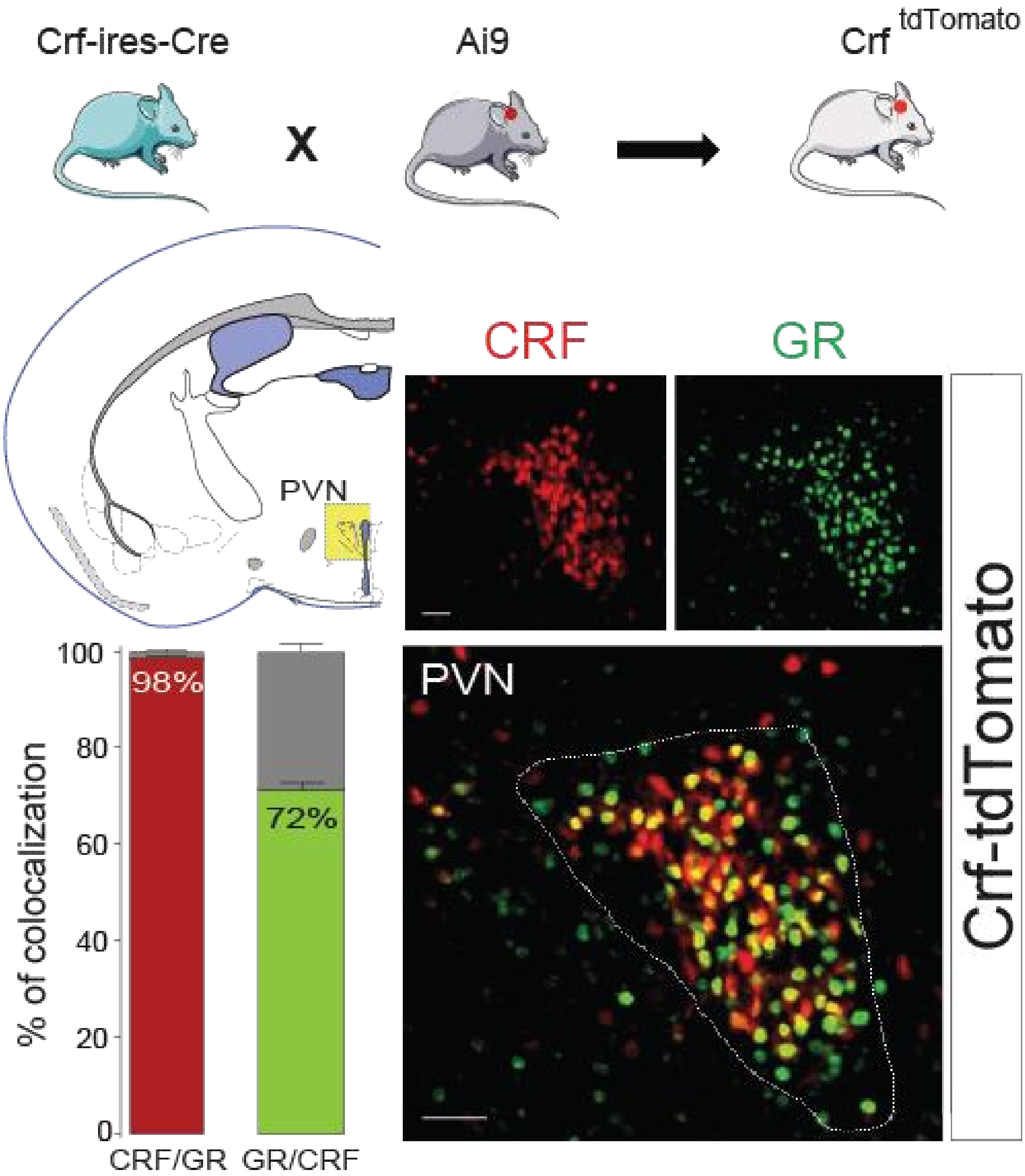
Crf-ires-Cre
X
Ai9
Crf tdTomato
PVN
CRF
GR
PVN
Crf-tdTomato
100
80
60
40
20
0
% of colocalization
98%
72%
CRF/GR
GR/CRF

Figure 22: GR expression in CRF+ neurons of the PVN .

Breeding scheme to obtain CRF^{tdTomato} mice. CRF expression is mapped by tdTomato expression (red) that mirrors the endogenous CRF pattern. Sections are immunostained for the glucocorticoid receptor (GR, green channel). 98 ± 0.4% of CRF+ neurons of the PVN co-express GR and 72 ± 1.5% of GR+ cells co-express CRF (n = 5 mice). Scale bars, 100 µm.

Using single-cell RNA (scRNA) sequencing, we profiled the transcriptome of 5,179 cells from the extended PVN (Uniform Manifold Approximation and Projection

(UMAP) plot of 5,179 cells coloured per density clustering and annotated according to known cell types). We systematically catalogued their cell type under baseline (unstressed) conditions. Our clustering analysis revealed 21 distinct cell populations (10 neuronal (and 11 non-neuronal) (Fig. 23a, b, and 24). While *Crh* mRNA is weakly expressed in non-neuronal cell populations (except for a few astrocytes), its expression is higher in neuronal cells and especially highly enriched in cluster 3 (*Crh* cluster).

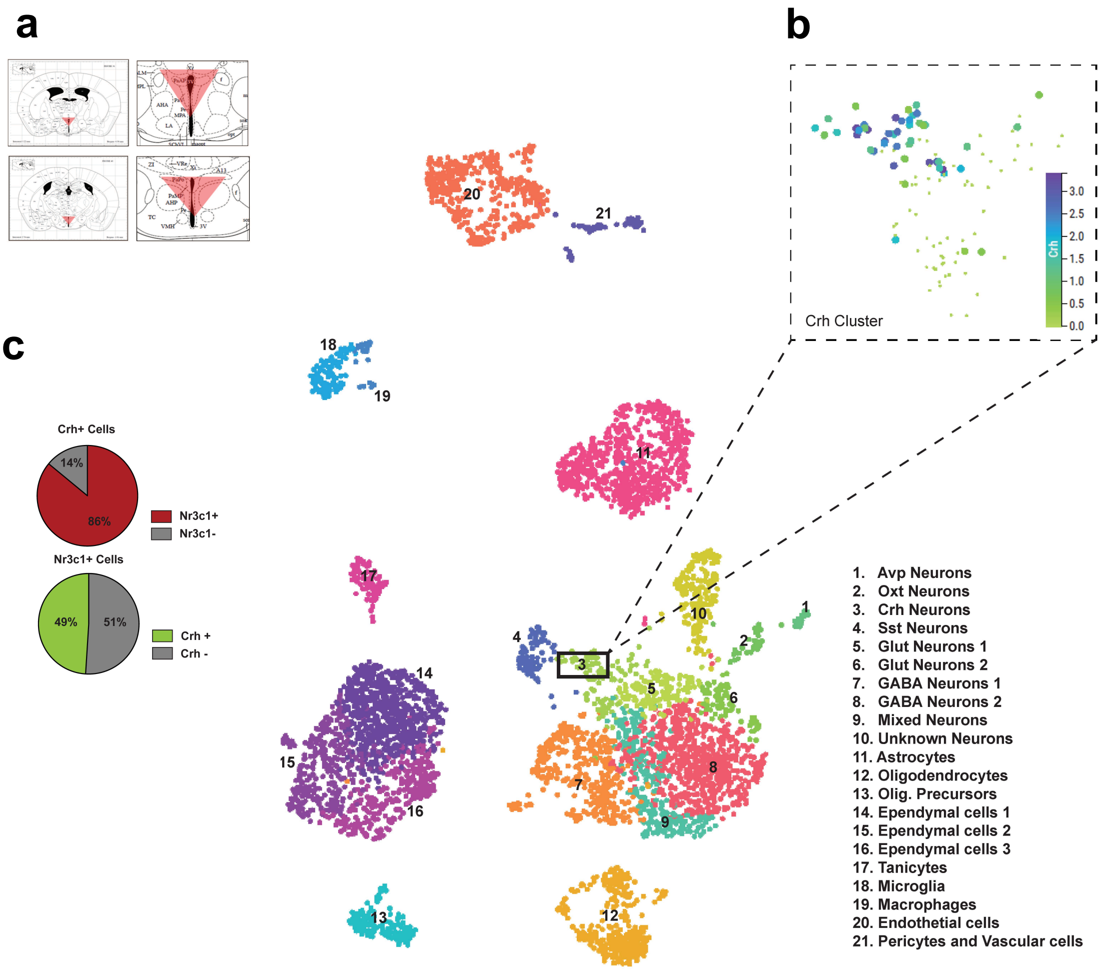

Figure 23: Transcriptomic profile of the mouse hypothalamic paraventricular nucleus (PVN) and Crh expression.

(a) Scheme depicting the dissection of the PVN for single-cell RNA (scRNA) sequencing experiment (adapted from the Paxinos mouse brain atlas). (b) Uniform Manifold Approximation and Projection (UMAP) plot of 5,179 cells coloured per density clustering and annotated according to known cell types. From the neuronal clusters, cluster 3 showed higher expression levels of Crh mRNA. (c) 86% of Crh+ neurons also express Nr3c1 (red pie chart), while 49% of Nr3c1+ cells coexpress Crh (green pie chart)

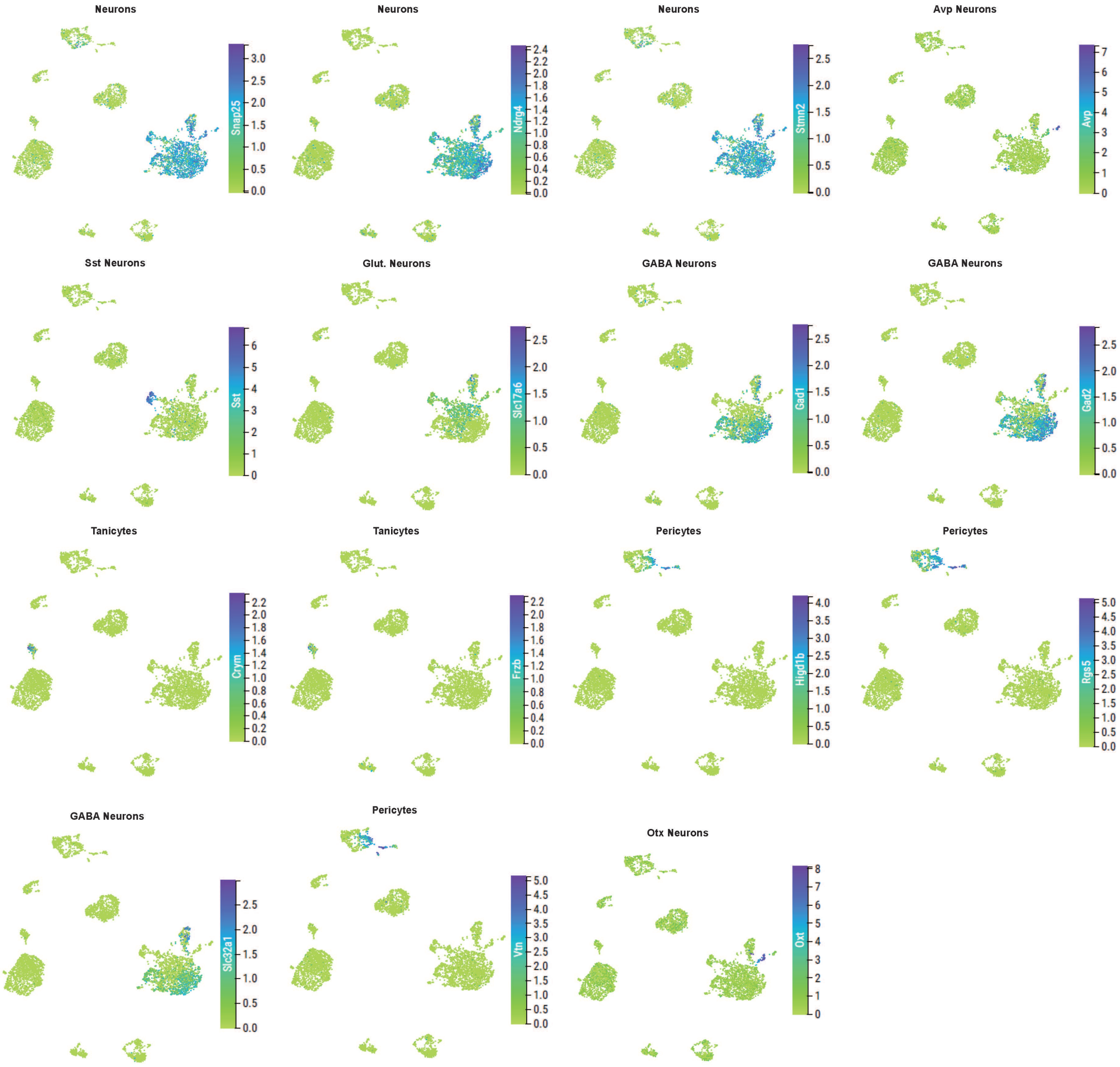

Figure 24: Transcriptomic profile of the mouse hypothalamic paraventricular nucleus (PVN)

UMAP plots showing expression levels of the marker genes for neuronal clusters identified.

Consistent with our immunostaining results, we found that 86% of Crh+ neurons in cluster 3 also express the Nr3c1 gene (GR). On the other hand, 49% of Nr3c1+ neurons coexpress Crh (Fig. 24).This value is slightly lower than the 72% co-expression observed with IHC (Fig. 22). This is likely due to the dissection method used for the scRNA sequencing.

To elucidate the physiological role of GR in CRF+ neurons of the PVN, we generated a conditional deletion of GRs specifically in CRF+ neurons ($GR^{CRF\text{-}cKO}$; Fig. 25) by breeding Crf-ires-Cre to GR floxed mice. In $GR^{CRF\text{-}cKO}$ animals, GRs were deleted from all CRF+ neurons of the brain, while they were still present in respective control littermates ($GR^{CRF\text{-}Ctrl}$) (Fig. 25). The deletion was validated by assessing GR protein and Nr3c1 mRNA expression levels using immunohistochemistry (IHC) and *in situ* hybridization (ISH), respectively. $GR^{CRF\text{-}cKO}$ mice express 66 ± 4.8% less Nr3c1 mRNA in the PVN than $GR^{CRF\text{-}Ctrl}$ mice (unpaired t-test, t25 = 6.21, *** $p < 0.001$, n = 4 control and 4 $GR^{CRF\text{-}cKO}$ mice). Those findings are in line with our colocalization studies (Fig. 22). The previous IHC stainings showed that 72% of GR neurons are also CRF positive in the PVN (Fig. 22). Therefore, it is not surprising that ISH reveals that the deletion of those neurons leads to ~60% less Nr3c1 mRNA expression in the cKO mice compare to the Ctrl.

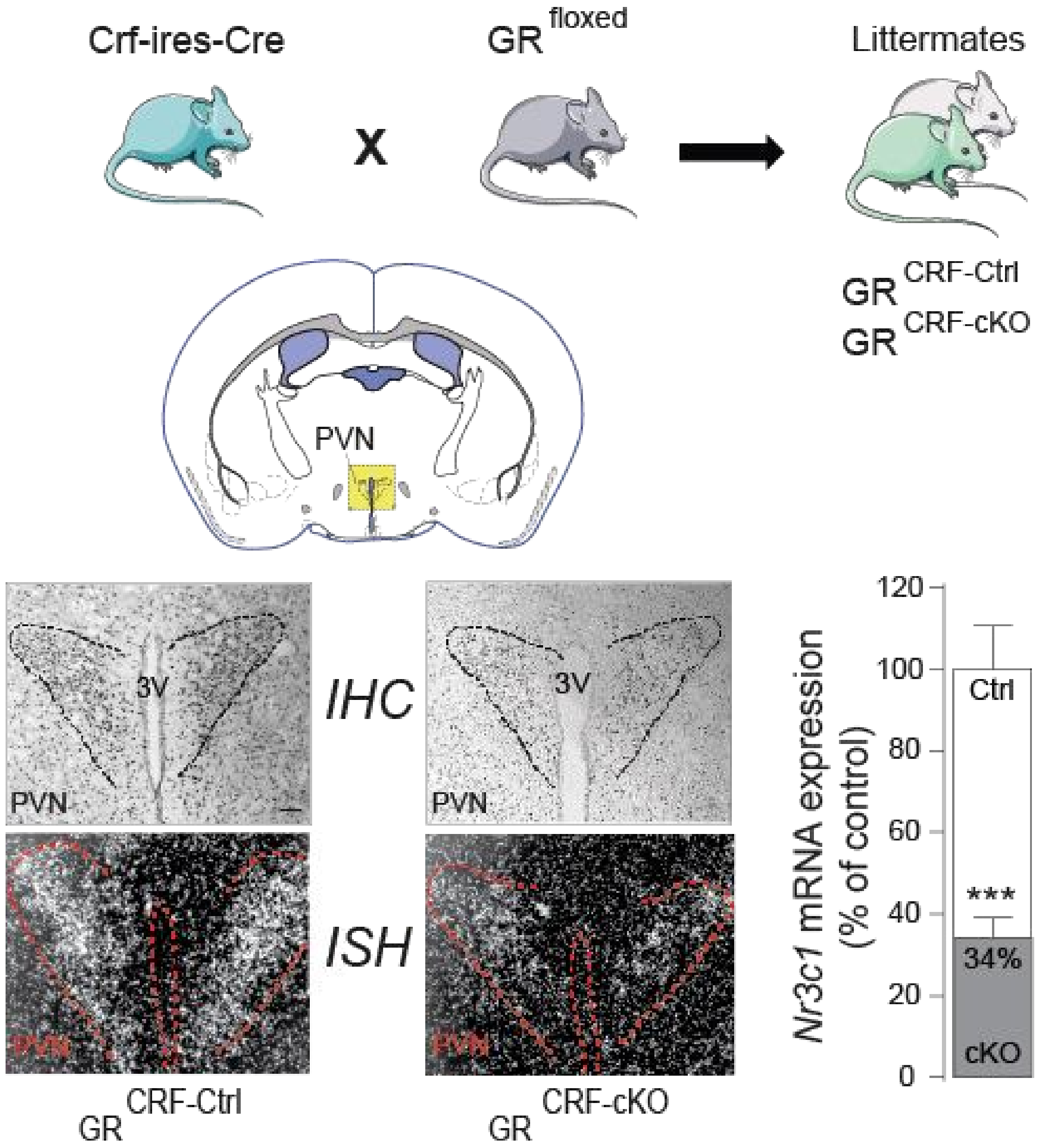
Crf-ires-Cre
X
GR floxed
Littermates
GR CRF-Ctrl
GR CRF-cKO
PVN
3V
PVN
IHC
3V
PVN
PVN
ISH
PVN
GR CRF-Ctrl
GR CRF-cKO
Nr3c1 mRNA expression (% of control)
120
100
80
60
40
20
0
Ctrl
***
34%
cKO

Figure 25:.GR expression in CRF+ neurons of the PVN and generation of conditional GR deletion in CRF-expressing neurons of the brain.

Breeding scheme to generate conditional GR knockout mice, GR$^{\text{CRF-cKO}}$, and their control littermates GR$^{\text{CRF-Ctrl}}$. The deletion was validated by assessing GR protein and Nr3c1 mRNA expression levels using immunohistochemistry (IHC) and in situ hybridization (ISH), respectively. GR$^{\text{CRF-cKO}}$ mice express 66 ± 4.8% less Nr3c1 mRNA in the PVN than GRCRF-Ctrl mice (unpaired t-test, t25 = 6.21, *** $p < 0.001$, n = 4 control and 4 GR$^{\text{CRF-cKO}}$ mice). PVN, hypothalamic paraventricular nucleus, 3V, third ventricle. Magnification, 20x; scale bar, 100 µm. Data are shown as mean ± SEM .

CRF/GR colocalization and GR deletion was also observed in the central nucleus of the amygdala (CeA) where CRF+ neurons are present. We found that 99 ± 0.4% of CRF+

neurons express GR but only 28 ± 1.5% of GR+ neurons co-express CRF (n = 5 mice, Fig. 26a). Accordingly, $GR^{CRF\text{-}cKO}$ mice showed a 31 ± 2.6 % decrease in Nr3c1 mRNA expression in the CeA compared to $GR^{CRF\text{-}Ctrl}$ mice (unpaired t-test, t10 = 11.95, *** $p < 0.001$, n = 4 $GR^{CRF\text{-}Ctrl}$ and 4 $GR^{CRF\text{-}cKO}$ mice (Fig. 6b).

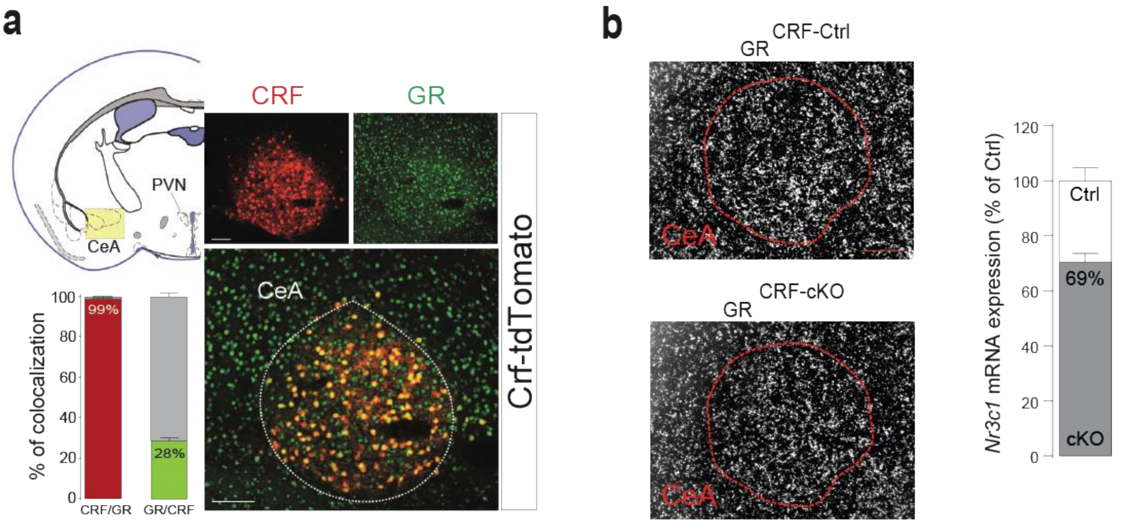
a
CRF
GR
PVN
CeA
CeA
Crf-tdTomato
% of colocalization
100
80
60
40
20
0
99%
28%
CRF/GR
GR/CRF
b
GR CRF-Ctrl
CeA
GR CRF-cKO
CeA
Nr3c1 mRNA expression (% of Ctrl)
120
100
80
60
40
20
0
Ctrl
69%
cKO

Figure 26: Characterization of GR deletion in CRF expressing neurons in the CeA.
(**a**) CRF / GR colocalization was also observed in the central nucleus of the amygdala (CeA). We found that 99 ± 0.4% of CRF+ neurons express GR but only 28 ± 1.5% of GR+ neurons co-express CRF (n = 5 mice). Scale bars, 50 µm. (**b**) $GR^{CRF\text{-}cKO}$ mice showed a 31 ± 2.6% decrease in *Nr3c1* mRNA expression in the CeA compared to $GR^{CRF\text{-}Ctrl}$ mice (unpaired t-test, t10 = 11.95, *** $p < 0.001$, n = 4 $GR^{CRF\text{-}Ctrl}$ and 4 $GR^{CRF\text{-}cKO}$ mice). Magnification 20x. Scale bar, 50 µm.

5.2 Impact of GRs from CRF neurons on stress susceptibility

Juvenile and adult $GR^{CRF\text{-}cKO}$ mice did not differ in body weight and did not show any gross abnormalities compared to their control littermates: $GR^{CRF\text{-}Ctrl}$ = 21.70 ± 0.28 g vs. $GR^{CRF\text{-}cKO}$ = 21.78 ± 0.47 g, unpaired t-test t14 = 0.0977, p = 0.924; 12 weeks old: $GR^{CRF\text{-}Ctrl}$ = 24.40 ± 0.4 g vs. $GR^{CRF\text{-}cKO}$ = 23.4 ± 0.42 g, unpaired t-test, t21 = 1.654, p = 0.11) n = 4 control and 12 $GR^{CRF\text{-}cKO}$ mice of 7 weeks old and 11 $GR^{CRF\text{-}Ctrl}$ and 15 $GR^{CRF\text{-}cKO}$ mice of 12 weeks old (Fig. 27).

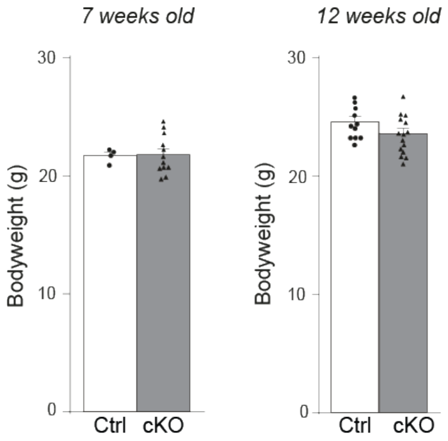

Figure 27: Body weight in juvenile and adult mice

Juvenile and adult GR$^{\text{CRF-Ctrl}}$ and GR$^{\text{CRF-cKO}}$ mice showed similar body weight (7 weeks old: GR$^{\text{CRF-Ctrl}}$ = 21.70 ± 0.28 g vs. GR$^{\text{CRF-cKO}}$ = 21.78 ± 0.47 g, unpaired t-test t_{14} = 0.0977, p = 0.924; 12 weeks old: GR$^{\text{CRF-Ctrl}}$ = 24.40 ± 0.4 g vs. GR$^{\text{CRF-cKO}}$ = 23.4 ± 0.42 g, unpaired t-test, t_{21} = 1.654, p = 0.11). n = 4 control and 12 GR$^{\text{CRF-cKO}}$ mice of 7 weeks old and 11 GR$^{\text{CRF-Ctrl}}$ and 15 GR$^{\text{CRF-cKO}}$ mice of 12 weeks old.

To functionally assess the role of GR in CRF-expressing neurons on emotional behaviour, GR$^{\text{CRF-CKO}}$ mice were subjected to a series of behavioural tests. GR deletion in CRF expressing neurons did not affect locomotor activity measured in the open field (OF: Distance travelled: unpaired t-test, t24 = 0.874, p = 0.39; % Time in inner zone: unpaired t-test, t24 = 0.03, p = 0.97) (Fig. 28a). GR deletion in CRF expressing neurons does not affect anxiety-related behaviour in the dark - light box (DaLi: % Time in lit zone: unpaired t-test, t24 = 0.91, p = 0.37; Latency to 1st entry in lit zone: unpaired t-test, t24 = 0.51, p = 0.61; Distance travelled in lit zone, t24 = 0.23, p = 0.81) (Fig. 28b). GR deletion in CRF expressing neurons does not affect anxiety-related behaviour in the elevated plus maze (EPM: % Time on the open arm: unpaired t-test, t24 = 0.06, p = 0.95; % Entries on the open arm: unpaired t-test, t24 = 0.51, p = 0.61; Latency to 1st entry on open arm: unpaired t-test, t20 = 1.19, p = 0.24) (Fig. 28c). GR deletion in CRF expressing neurons does not affect stress-coping behaviour in the forced-swim test (FST: Struggling time: unpaired t-test, t16 = 0.71, p = 0.48; Floating time: unpaired t-test, t16 = 1.08, p = 0.29) (Fig. 28d).

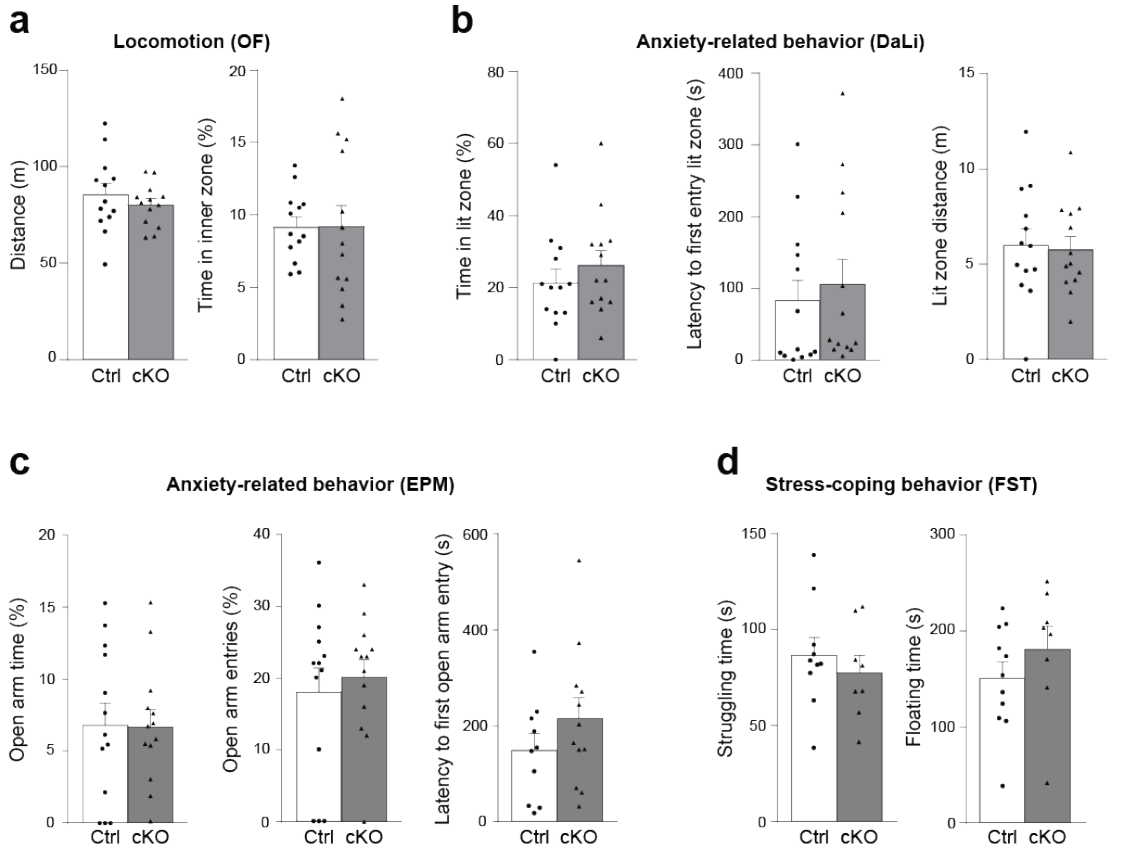

Figure 28: Behavioural characterization of GR$^{CRF\text{-}cKO}$ mice.

(**a**) GR deletion in CRF expressing neurons does not affect locomotor activity measured in the open field (OF: Distance travelled: unpaired t-test, t24 = 0.874, p = 0.39; % Time in inner zone: unpaired t-test, t24 = 0.03, p = 0.97). (**b**) GR deletion in CRF expressing neurons does not affect anxiety-related behaviour in the dark - light box (DaLi: % Time in lit zone: unpaired t-test, t24 = 0.91, p = 0.37; Latency to 1st entry in lit zone: unpaired t-test, t24 = 0.51, p = 0.61; Distance travelled in lit zone, t24 = 0.23, p = 0.81). (**c**) GR deletion in CRF expressing neurons does not affect anxiety-related behaviour in the elevated plus maze (EPM: % Time on the open arm: unpaired t-test, t24 = 0.06, p = 0.95; % Entries on the open arm: unpaired t-test, t24 = 0.51, p = 0.61; Latency to 1st entry on open arm: unpaired t-test, t20 = 1.19, p = 0.24). (**d**) GR deletion in CRF expressing neurons does not affect stress-coping behavior in the forced-swim test (FST: Struggling time: unpaired t-test, t16 = 0.71, p = 0.48; Floating time: unpaired t-test, t16 = 1.08, p = 0.29). Data are shown as mean ± SEM.

GR$^{CRF\text{-}CKO}$ mice displayed no alterations in locomotion, anxiety and stress-coping behaviour (Fig. 28), since GR-deletion was mainly restricted to the PVN region; brain structure which is rarely implicated in emotional behaviour. One could have also expected changes in emotional behaviour since the deletion affect also the CeA (30% less GR in cKO mice), but we see our results indicate that it is not the case.

To summarize, body weight, emotional and anxiety-related behaviour were not altered in $GR^{CRF\text{-}CKO}$ mice. The lack of behavioural effects in $GR^{CRF\text{-}CKO}$ mice might be explained by one, or a combination of the following. 1st) Recombination of the CRF-Cre during development might have induced early compensatory mechanisms. 2nd) Constitutive activity of the remaining GRs (30% in the PVN) is probably the more likely explanation. GRs might exhibit constant tonic activity, even if the total number of receptors is decreased, resulting in the initiation of downstream signalling events involving a cascade of cellular, immunological and physical changes via genomic transcriptional regulation (Joëls et al., 2009). 3rd) Mineralocorticoid receptors (MRs) take over the role of GRs by binding with glucocorticoids. However, while GR is expressed across the brain, MR is primarily found in limbic areas like hippocampus and amygdala. (Patel et al., 2001; Reul and de Kloet, 1985; Seckl et al., 1991). 4th) GRs feedback impact is not in charge of emotional and anxiety-related behaviour in basal condition but rather under stress paradigm.

5.3 Effect of GRs deletion on circadian HPA activity

In this chapter, we investigated the impact of GRs deletion from CRF neurons on corticosterone secretion in plasma and free corticosterone in the brain by tail cut and microdialysis sampling respectively. GRs are indispensable for negative feedback after corticosterone increase (circadian rhythm and stress-induced) to return to a homeostatic state. To evaluate the consequences of GR deletion from CRF+ neurons on circadian rhythmicity of the HPA axis, we measured circulating plasma CORT levels. $GR^{CRF\text{-}Ctrl}$ mice displayed normal circadian fluctuations in CORT levels with a typical morning trough and afternoon peak. $GR^{CRF\text{-}CKO}$ mice also displayed normal circadian fluctuations of corticosterone levels, evident by higher afternoon (p.m.) compared to morning (a.m.) values (Fig. 29a). However, interestingly, GR deletion in CRF-expressing neurons of the PVN, resulted in significantly higher evening plasma CORT levels compared to those of $GR^{CRF\text{-}Ctrl}$ (Fig 29a: 2-way RM-ANOVA Genotype * Time of the day F(1,23) = 7.342, p = 0.0125; Bonferroni post-hoc test [afternoon plasma CORT] in $GR^{CRF\text{-}cKO}$ = 111.6 ± 18.29 ng/ml vs. [afternoon plasma CORT] in $GR^{CRF\text{-}Ctrl}$ = 51.65 ± 10.8 ng/ml, ** p = 0.0013, n = 12 control and 13 $GR^{CRF\text{-}cKO}$ mice). To further substantiate the HPA axis rhythmicity of $GR^{CRF\text{-}Ctrl}$ and $GR^{CRF\text{-}cKO}$ animals, we performed *in vivo* microdialysis. This allowed us to measure free CORT levels in the brain continuously during 24 h. Microdialysis enables the measurement of neurotransmitter concentrations in the extracellular space within the targeted brain region of a living, freely moving animal (Anderzhanova and Wotjak, 2013). It was previously shown that free levels of CORT are comparable all over the brain (Anderzhanova and Wotjak, 2013). Therefore, the probe was implanted in a less invasive area, routinely executed in our lab, the prefrontal cortex (including the cingulate, prelimbic and infralimbic cortex). After probe implantation, mice were left undisturbed for one day in order to recover and get accustomed to the wiring. Dialysates samples were collected every 60 min. As for plasma levels, free CORT in the mPFC follows circadian fluctuations with an afternoon peak (Fig. 29b). Moreover, $GR^{CRF\text{-}cKO}$ mice again showed higher levels of free CORT in the afternoon compared to $GR^{CRF\text{-}Ctrl}$ mice. A two-way repeated measures ANOVA showed a statistically significant interaction between the effect of genotypes and time on CORT levels, Time * Genotype F(2,23) = 2.26, p = 0.001; Bonferroni post-hoc test *** $p < 0.001$, ** $p < 0.01$, * $p < 0.05$, ~ $p = 0.1$). n = 12 control and 13 $GR^{CRF\text{-}cKO}$ mice (Fig. 29b).

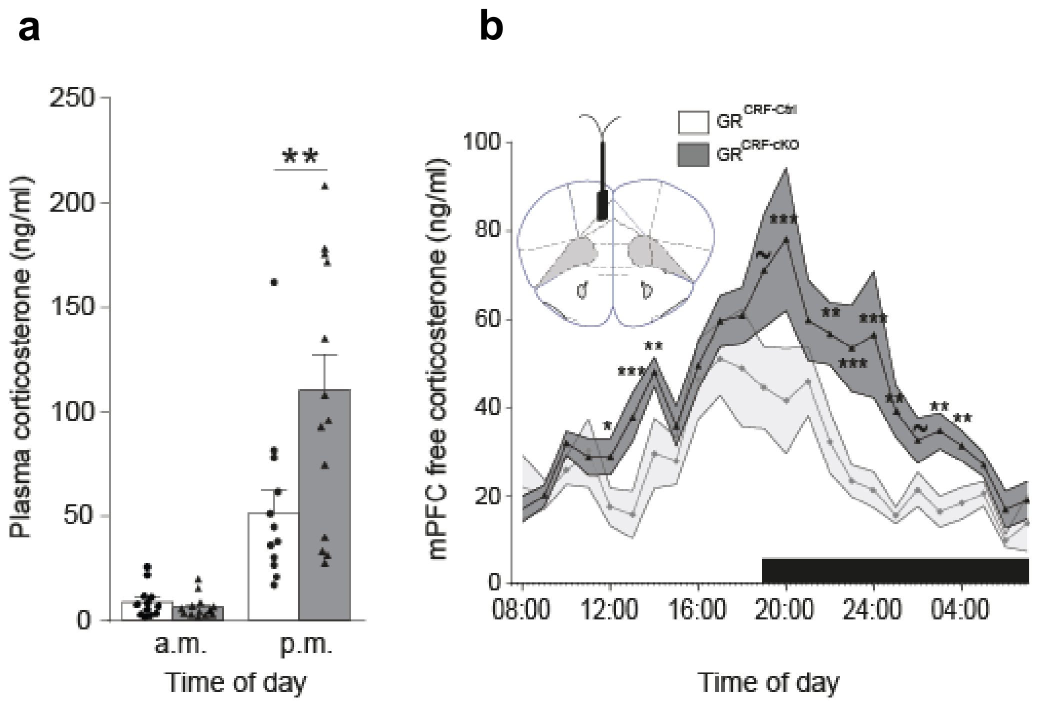

Figure 9: GR deletion in CRF+ neurons affects HPA axis rhythmicity of plasma CORT.
(a) $GR^{CRF\text{-}cKO}$ mice exhibited a higher peak of plasma CORT in the afternoon (p.m.) compared to $GR^{CRF\text{-}Ctrl}$ (2-way RM-ANOVA Genotype * Time of the day F(1,23) = 7.342, p = 0.0125; Bonferroni post-hoc test [afternoon plasma CORT] in $GR^{CRF\text{-}cKO} = 111.6 \pm 18.29$ ng/ml vs. [afternoon plasma CORT] in $GR^{CRF\text{-}Ctrl} = 51.65 \pm 10.8$ ng/ml, ** p = 0.0013). n = 12 control and 13 $GR^{CRF\text{-}cKO}$ mice. (b) Microdialysis probes were implanted in the mPFC to measure free CORT

levels. As for plasma levels, free CORT levels in the mPFC were significantly higher in GR$^{CRF\text{-}cKO}$ mice in the afternoon (2-way RM-ANOVA Time * Genotype F(2,23) = 2.26, p = 0.001; Bonferroni post-hoc test *** $p < 0.001$, ** $p < 0.01$, * $p < 0.05$, ~ p = 0.1). n = 12 control and 13 GR$^{CRF\text{-}cKO}$ mice.

In order to compare circulating and free CORT levels, we extracted from the microdialysis data the same time points (8am trough and 8 pm peak) used for the plasma CORT. While morning CORT levels were similar in both groups, GR$^{CRF\text{-}cKO}$ mice exhibited an increased mPFC free CORT peak in the afternoon compared to GR$^{CRF\text{-}Ctrl}$ mice (Fig. 30). [afternoon mPFC free CORT] in GR$^{CRF\text{-}cKO}$ = 79.56 ± 5.38 ng/ml *vs.*[afternoon mPFC free CORT] in GR$^{CRF\text{-}Ctrl}$ = 41.95 ± 2.72 ng/ml).

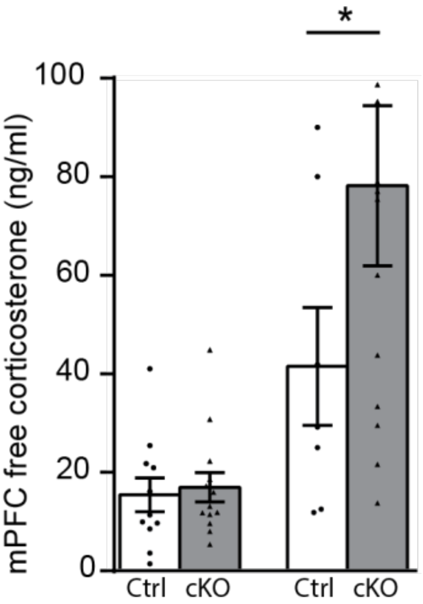

Figure 30: GR deletion in CRF+ neurons affects HPA axis rhythmicity of free CORT in the brain. Microdialysis extract at 8 am (Through") and 8 pm ("Peak"). GR$^{CRF\text{-}cKO}$ mice exhibited a higher "peak" of plasma CORT compared to GR$^{CRF\text{-}Ctrl}$ (2-way RM-ANOVA Genotype * Time of the day F(1,20) = 4.41, p = 0.0485; Bonferroni post-hoc test [afternoon plasma CORT] in GR$^{CRF\text{-}cKO}$ 83.56 ± 5.38 ng/ml vs.[afternoon plasma CORT] in GR$^{CRF\text{-}Ctrl}$ = = 46.95 ± 2.72 ng/ml, * p = 0.0227). n = 10 control and 11 GR$^{CRF\text{-}cKO}$ mice.

Taken together, these results suggest that both mouse lines show typical circadian CORT fluctuations but $GR^{CRF\text{-}CKO}$ mice exhibit higher CORT levels (both plasma and free CORT) during the diurnal phase than $GR^{CRF\text{-}Ctrl}$ mice (Fig. 29 and 30).

In our model, the removal of GR in CRF neurons mimics a physiological situation of chronic stress since the negative feedback is disrupted. Daily higher CORT levels exposure commonly increases adrenal weight, in Human and in rodents (Carroll *et al.*, 1976; Ulrich-Lai *et al.*, 2006). Therefore, it is not surprising that the adrenal weight (Fig. 31, left graph) was significantly higher in $GR^{CRF\text{-}cKO}$ compared to $GR^{CRF\text{-}Ctrl}$ mice (% Bodyweight: 0.020 ± 0.0006 % vs. 0.026 ± 0.001 %, unpaired t test, t24 = -3.718, ** p = 0.0011). On the other hand, the thymus weight (Fig. 31, right graph) was significantly lower in $GR^{CRF\text{-}cKO}$ compared to $GR^{CRF\text{-}Ctrl}$ mice (% Bodyweight: 0.256 ± 0.007 % vs. 0.219 ± 0.011, unpaired t-test, t24 = 2.64, ** p = 0.014; n = 11 control and 15 $GR^{CRF\text{-}cKO}$ mice).

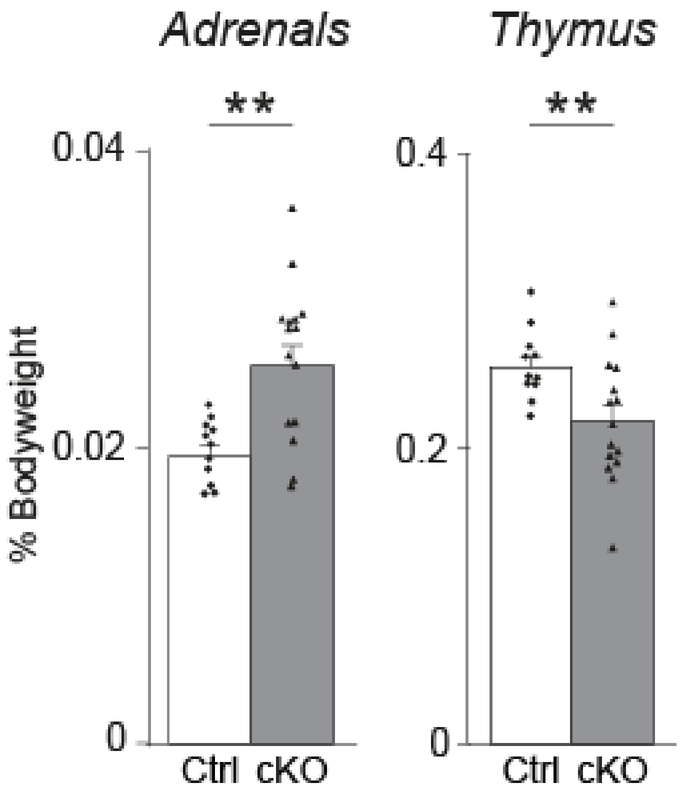

Figure 31: GR deletion in CRF+ neurons affects Adrenals and Thymus size

The adrenal weight (left graph) was significantly higher in $GR^{CRF\text{-}cKO}$ compared to $GR^{CRF\text{-}Ctrl}$ mice (% Bodyweight: 0.020 ± 0.0006 % *vs.* 0.026 ± 0.001 %, unpaired t test, $t_{24} = -3.718$, ** $p = 0.0011$). The thymus weight (right graph) was significantly lower in $GR^{CRF\text{-}cKO}$ compared to $GR^{CRF\text{-}Ctrl}$ mice (% Bodyweight: 0.256 ± 0.007 % *vs.* 0.219 ± 0.011, unpaired t-test, $t_{24} = 2.64$, ** $p = 0.014$). n = 11 control and 15 $GR^{CRF\text{-}cKO}$ mice.

Thus, partly preserved GR expression in the PVN is sufficient for normal HPA axis rhythmicity but has an impact on pulse amplitude. As expected, by deleting GR from CRF+ neurons, the GC-mediated negative feedback on the HPA axis is affected, and thus Crh mRNA levels were increased in $GR^{CRF\text{-}cKO}$ animals compared to $GR^{CRF\text{-}Ctrl}$ mice in the PVN but not in the CeA (Fig. 32, left graph: 115.7 ± 4.1% of control in $GR^{CRF\text{-}cKO}$ mice, unpaired t-test, $t50 = 2.758$, ** $p = 0.008$; n = 25 control and 27 $GR^{CRF\text{-}cKO}$ mice), but not in the CeA (Fig. 32, right graph: 86.7 ± 9.3% of control in $GR^{CRF\text{-}cKO}$ mice, unpaired t-test, $t32 = 1.105$, $p = 0.277$; n = 19 control and 15 $GR^{CRF\text{-}cKO}$ mice).

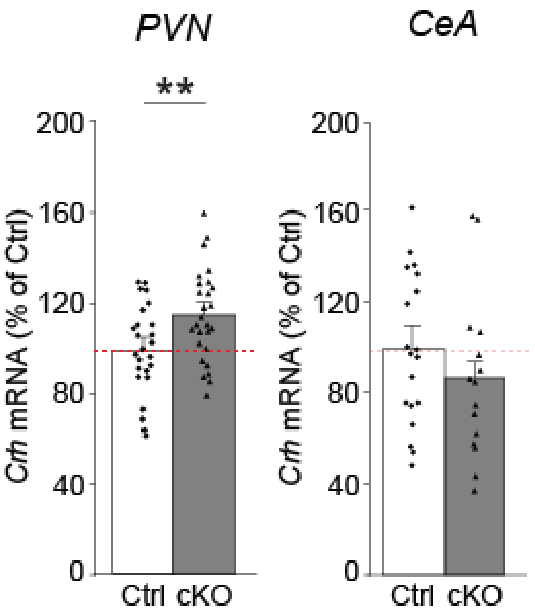

Figure 32: *Crh* mRNA levels in the brain

GR deletion in CRF expressing neurons led to increased *Crh* mRNA expression levels under basal conditions in the PVN of $GR^{CRF\text{-}cKO}$ mice (left graph; 115.7 ± 4.1% of control, unpaired t-test, $t_{50} = 2.758$, ** p = 0.008; n = 25 control and 27 $GR^{CRF\text{-}cKO}$ mice), but not in the CeA (right graph, 86.7 ± 9.3% of control, unpaired t-test, $t_{32} = 1.105$, p = 0.277; n = 19 control and 15 $GR^{CRF\text{-}cKO}$ mice).

Since the deletion is specific to CRF+ neurons, GR expression levels in the pituitary and the hippocampus of Ctrl and $GR^{CRF\text{-}cKO}$ mice should be similar, due to the fact that very few CRF+ neurons are found in those regions. qPCR analysis revealed no differences in Nr3c1 expression levels in the hippocampus (Fig. 33 left bar graph: 93 ± 5.3 % of control, unpaired t-test, t18 = 0.94, p = 0.358) and surprisingly a slight but significant increase in the pituitary (Fig. 33 right bar graph: 24.7 ± 7.73 % increase, unpaired t-test, t17 = 2.156, p = 0.045), most likely compensating for the daily higher levels of plasma CORT.

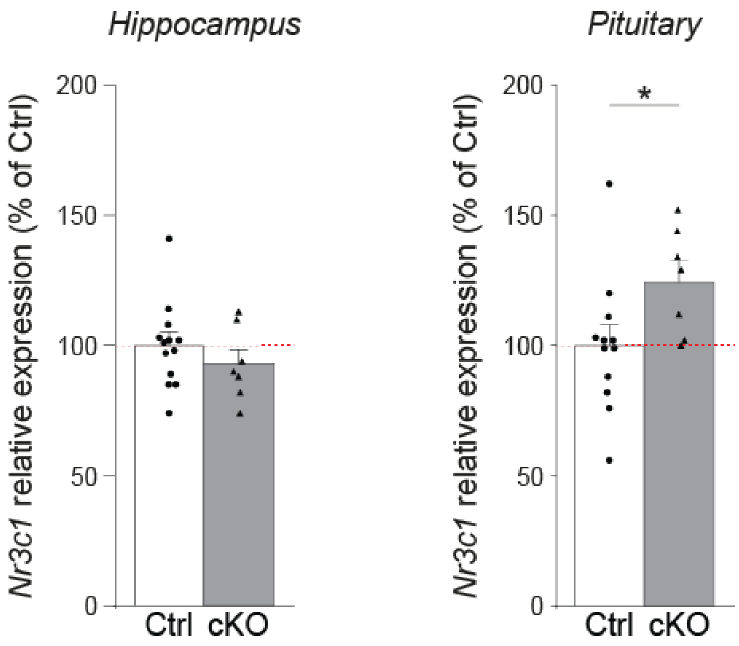

Figure 33: Nr3c1 expression is slightly increased in the pituitary of GR$^{CRF\text{-}cKO}$ mice but not in the hippocampus.

GR$^{CRF\text{-}cKO}$ mice showed a slight but significant increase in *Nr3c1* expression level in the pituitary compared to GR$^{CRF\text{-}Ctrl}$ mice (right bar graph: 24.7 ± 7.73 % increase, unpaired t-test, $t_{17} = 2.156$, $p = 0.045$), while no difference was observed in the hippocampus (left bar graph: 93 ± 5.3 % of control, unpaired t-test, $t_{18} = 0.94$, $p = 0.358$). Data are shown as mean ± SEM.

5.4 HPA responsiveness

5.4.1 Dex/CRF test

Next, HPA axis responsiveness was assessed in GR$^{CRF\text{-}Ctrl}$ and GR$^{CRF\text{-}cKO}$ mice. Plasma CORT levels were measured in response to a pharmacological suppression of adrenocortical activity by means of the dexamethasone (Dex)/CRF test (see Methods for details).Two independent tests were performed using either a low (0.05 mg/kg, Fig. 34a) or a relatively high dose of Dex (2 mg/kg, Fig. 34 b), to assess GR negative feedback at the level of the pituitary alone or at the level of pituitary and brain respectively. Plasma CORT levels were measured in GR$^{CRF\text{-}Ctrl}$ and GR$^{CRF\text{-}cKO}$ mice 1 week before (Untreated, measure in the afternoon), 6 hours after Dex treatment (After Dex, Dex injection at 9 a.m.) and 30 min after CRF injection (After CRF, CRF injection

0.15 mg/kg at 3 p.m.). In both tests, $GR^{CRF\text{-}cKO}$ mice showed significantly higher afternoon CORT levels under basal conditions (Fig. 34a and b, “Untreated”) compared to $GR^{CRF\text{-}Ctrl}$ mice. This difference is similar to what we previously observed (Fig. 9a). As expected, the low dose of Dex strongly suppressed adrenocortical activity in $GR^{CRF\text{-}Ctrl}$ mice, but was ineffective in $GR^{CRF\text{-}cKO}$ (Fig. 34a “After Dex”). Both genotypes responded to stimulation with CRF with a similar increase in CORT levels (Fig. 34a, “After CRF”). On the other hand, the high dose of Dex strongly suppressed adrenocortical activity in both genotypes (Fig. 34b, “After Dex”). The suppression was maintained in $GR^{CRF\text{-}Ctrl}$ mice even after CRF stimulation, while CRF was able to increase CORT levels in $GR^{CRF\text{-}cKO}$ mice (Fig. 34b, “After CRF”). Thus, $GR^{CRF\text{-}cKO}$ mice exhibit a weaker negative feedback at the level of the pituitary and a higher sensitivity to CRF than $GR^{CRF\text{-}Ctrl}$ mice.

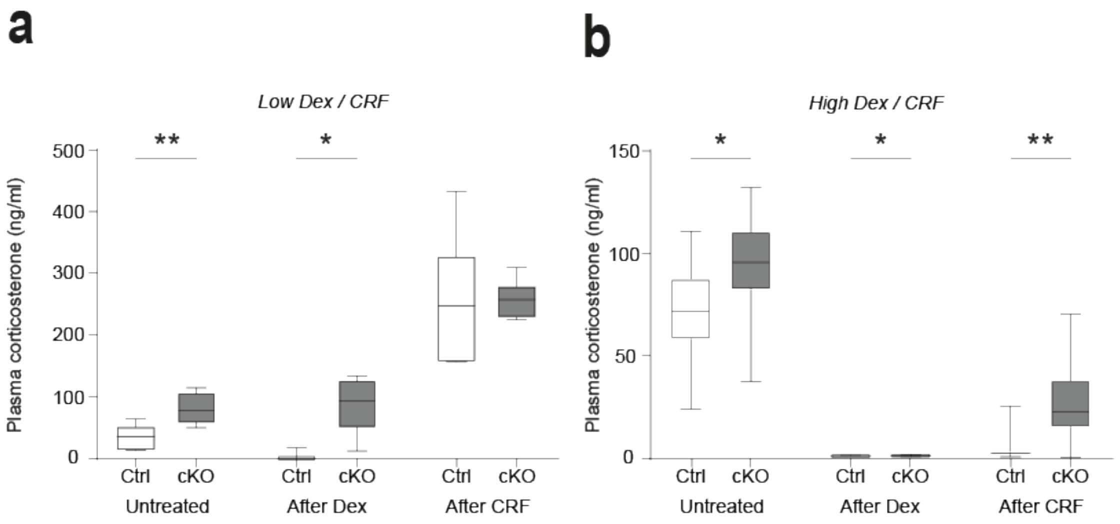

Figure 34: GR deletion in CRF+ neurons affects HPA axis negative feedback.

GR deletion in CRF expressing neurons led to a mild increase in HPA axis responsiveness. Plasma CORT levels were measured in response to a pharmacological suppression of adrenocortical activity with either a low (0.05 mg/kg, **a**) or relatively high (2 mg/kg, **b**) dose of Dex and a subsequent stimulation with CRF (0.15 mg/kg). Plasma CORT levels were measured in $GR^{CRF\text{-}Ctrl}$ and $GR^{CRF\text{-}cKO}$ mice 1 week before (Untreated, measure in the afternoon), 6 hours after Dex treatment (After Dex, Dex injection at 9 a.m.) and 30 min after CRF injection (After CRF, CRF injection at 3 p.m.). Data are given as box plots showing medians (lines in the boxes), 25% and 75% percentiles (boxes), as well as the min and max values (whiskers). Statistical differences between the groups are indicated above the columns for each time point (**a**: low dose Dex, unpaired t-test, Untreated: $t_{18} = 3.376$, $p = 0.0034$, After Dex: $t_{18} = 2.215$, $p = 0.04$, After CRF: $t_{18} = 1.096$, $p = 0.288$; **b**: high dose Dex, unpaired t-test, Untreated: $t_{24} = 2.299$, $p = 0.03$, After Dex: $t_{24} = 2.615$, $p = 0.015$, After CRF: $t_{24} = 3.511$, $p = 0.0018$). n = 10 control and 10 $GR^{CRF\text{-}cKO}$ mice in **a** and 10 control and 16 $GR^{CRF\text{-}cKO}$ mice in **b**.

5.4.2 Effect of acute stress in $GR^{CRF\text{-}cKO}$ mice

To further explore the reactivity (and recovery) of the HPA axis in a more physiological paradigm, mice were subjected to a single stress restraint and circulating CORT levels were measured (Fig. 35). Again, plasma CORT levels in the morning, prior to stressor, were indistinguishable between control and $GR^{CRF\text{-}cKO}$ mice. Surprisingly, exposure to acute stressors (15 min restraint), did not reveal any significant difference in plasma CORT levels neither right after the restraint stress nor after recovery (Fig. 35: 2-way RM-ANOVA, Genotype F(1,13) = 3.227, p = 0.096, n = 13 control and 14 $GR^{CRF\text{-}cKO}$ mice). There is also no statistically significant interaction between genotype and time points (basal, restraint stress and recovery, p=0,57) (Fig. 35 : Basal: Ctrl = 5.50 ± 3.83 ng/ml *vs.* cKO = 7.61 ± 3.38 ng/ml, U = 20.2, p =0.89; Restraint stress: Ctrl = 179.56 ± 48.42 ng/ml *vs.* cKO = 204.57 ± 78.45 ng/ml, U = 22.3, p = 0.11; Recovery: Ctrl = 48.97 ± 18 ng/ml *vs.* cKO = 59.71 ± 26.02 ng/ml, U = 20.97, p =0.5) .

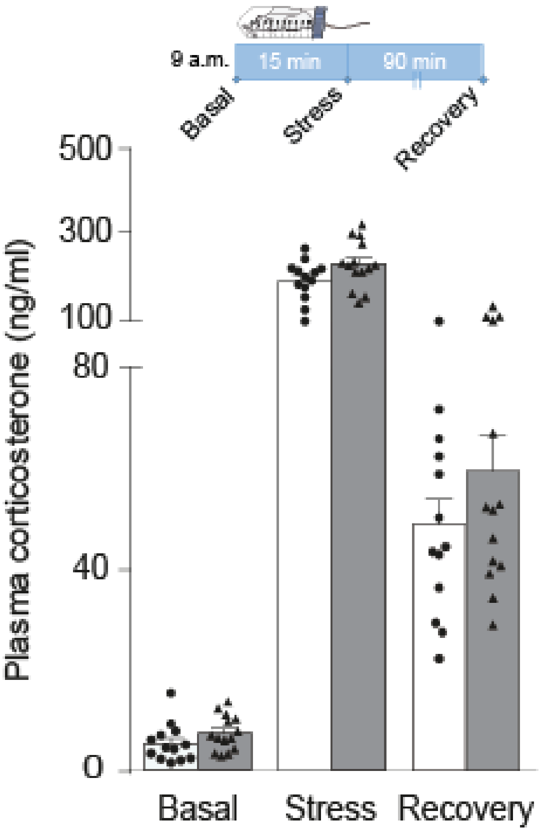

Figure 15: GR deletion in CRF+ does not affect HPA axis responsiveness to a single stressor. HPA axis responsiveness to a single restraint stress was not affected by GR deletion. Scheme of the experimental protocol: basal plasma CORT measurement was made at 9 a.m. Plasma CORT levels for the stress response were measured directly after the 15 min of restraint stress and 90 min after the end of the stressor for recovery. No difference was observed between $GR^{CRF\text{-}Ctrl}$ and $GR^{CRF\text{-}cKO}$ mice (2-way RM-ANOVA, Genotype F(1,13) = 3.227, p = 0.096). n = 13 control and 14 $GR^{CRF\text{-}cKO}$ mice. Data are shown as mean ± SEM.

Taken together, these results demonstrate that deleting GRs from CRF+ neurons impacts HPA axis rhythmicity, sensitivity, and negative feedback as expected after releasing the negative brake GRs exert on the HPA axis. Surprisingly however, this deletion does not affect HPA axis responsiveness to an acute single stressor, suggesting that GRs in CRF positive neurons are not involved in the regulation of CRF neurons' physiology in response to a single stress episode.

5.5 HPA habituation

5.5.1 Effect of repeated stress in $GR^{CRF\text{-}cKO}$ mice

To further investigate how deletion of GRs in CRF neurons impact stress response and especially the habituation of the HPA axis to a repeated homotypic stressor, mice were subjected to a Repeated Restraint Stress protocol (RRS, Fig. 16a). As shown before, $GR^{CRF\text{-}Ctrl}$ and $GR^{CRF\text{-}CKO}$ mice were indistinguishable under baseline (basal RRS1, basal RRS2, basal RRS3). No difference was found on the basal levels of CORT over the 3 RRS (Ctrl vs cKO: RRS1 $p=0.91$, RRS2 $p=0.95$, RRS3 $p=0.70$). However, upon repetition of the restraint stress (RRS), $GR^{CRF\text{-}Ctrl}$ mice exhibited a gradual decrease in plasma CORT levels compared to $GR^{CRF\text{-}cKO}$ animals (dashed orange lines, Fig. 16b). The effect of RRS depends on the genotype. A two-way repeated measures ANOVA revealed a statistically significant interaction between RRS and genotype (2-way RM-ANOVA RRS*genotype $F(2,122) = 3.36$ $p = 0.038$; Bonferroni post-hoc test $GR^{CRF\text{-}Ctrl}$ vs. $GR^{CRF\text{-}cKO}$ RRS2 and RRS3 *** $p< 0.001$). This decrease in plasma CORT levels is the result of habituation of the HPA axis response in $GR^{CRF\text{-}Ctrl}$ mice, as shown by the significant difference in CORT level between RRS1 and RRS3 (Fig. 16 c left plot: paired t-test $GR^{CRF\text{-}Ctrl}$ RRS1 *vs.* RRS3, $t29 = 3.08$, ** $p = 0.005$, $n = 30$). This habituation is, however, completely absent in $GR^{CRF\text{-}cKO}$ animals (Fig. 16c right plot: paired t-test $GR^{CRF\text{-}cKO}$ RRS1 *vs.* RRS3, $t32 = 0.911$, $p = 0.37$, $n = 33$). Taken together, those data indicate a role for GRs in CRF neurons during HPA axis habituation.

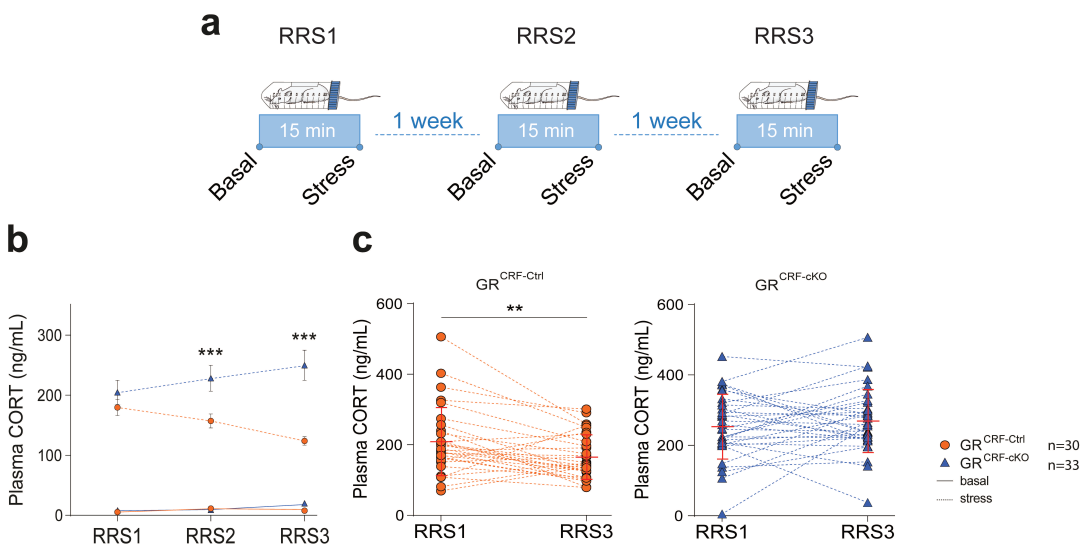

Figure 36: HPA axis habituation to repeated restraint stress (RRS).

(**a**) Scheme of the Repeated Restraint Stress (RRS) protocol. GR$^{\text{CRF-Ctrl}}$ and GR$^{\text{CRF-cKO}}$ mice were subjected to RRS 3 times with 1-week interval. Corticosterone (CORT) was measured immediately before each stress ("Basal") and at the end of the 15 minutes restraint ("Stress"). Basal plasma CORT measurement was made at 9 a.m. (**b**) CORT levels were similar under basal conditions (solid lines) between control and GR$^{\text{CRF-cKO}}$ mice for each RRS. However, upon repetition of the RRS, GR$^{\text{CRF-Ctrl}}$ mice showed a progressive decrease in plasma CORT levels after stress compared to GR$^{\text{CRF-cKO}}$ animals (dashed lines: 2-way RM-ANOVA RRS*genotype $F_{(2,122)} = 3.36$ $p = 0.038$; Bonferroni post-hoc test GR$^{\text{CRF-Ctrl}}$ *vs.* GR$^{\text{CRF-cKO}}$ RRS2 and RRS3 *** $p < 0.001$). (**c**) The decrease in CORT is the result of the habituation of the HPA axis in GR$^{\text{CRF-Ctrl}}$ mice as shown by the direct comparison of plasma CORT levels between RRS1 and RRS3 (left plot, paired t-test GR$^{\text{CRF-Ctrl}}$ RRS1 *vs.* RRS3, $t_{29} = 3.08$, ** $p = 0.005$, $n = 30$). This habituation is completely absent in GR$^{\text{CRF-cKO}}$ mice (right plot, paired t-test GR$^{\text{CRF-cKO}}$ RRS1 *vs* RRS3, $t_{32} = 0.911$, $p = 0.37$, $n = 33$). Data are shown as mean ± SEM.

5.5.2 Rescue experiment

The HPA habituation is absent in cKO mice and we have demonstrated that the region mainly affected by the GR deletion is the PVN. Since it is known that HPA stress response is regulated by different brain regions such as PVN, mPFC, CeA, HPC, NTS (Ulrich-Lai and Herman., 2009), it is important to know if the GR in CRF neurons of the PVN are the principal mediator of the stress habituation. In order to corroborate this, we examined whether the GR positive neurons of the PVN are responsible for the loss of HPA habituation in mice, by performing a rescue experiment in GR$^{\text{CRF-CKO}}$ mice to re-express GRs deleted by the transgenic construct. To explore whether GR expression levels in CRF neurons are causal in HPA habituation, we re-expressed GR, specially in CRF neurons of GR$^{CRF\text{-}cKO}$ mice using a Cre-dependent GR-expressing adeno-associated virus (AAV) vector (AAV½-EF1α-DIO-Flag-mGR: Double Floxed Inverted ORF under the control of EF1α promoter). After multiple cloning steps (see Methods 2.3.4), our plasmid was sent for sequencing to make sure that we obtained the right construct (Fig. 37) and tested on HEK cells.

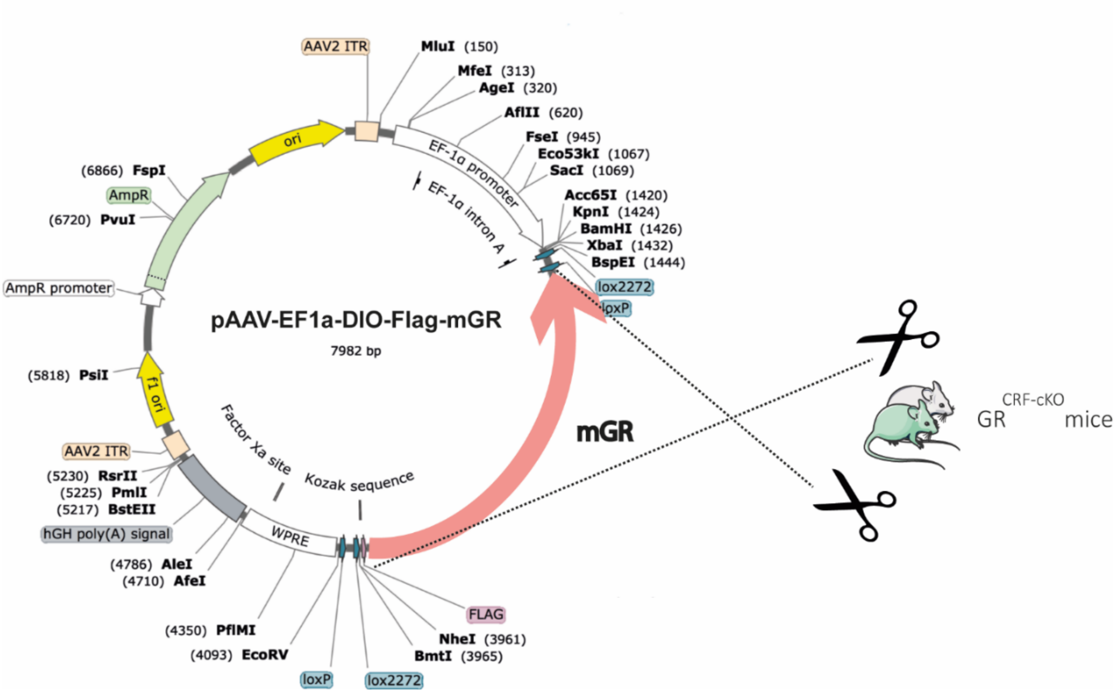
AAV2 ITR
MluI (150)
MfeI (313)
AgeI (320)
AflII (620)
FseI (945)
Eco53kI (1067)
SacI (1069)
Acc65I (1420)
KpnI (1424)
BamHI (1426)
XbaI (1432)
BspEI (1444)
lox2272
loxP
EF-1α promoter
EF-1α intron A
ori
(6866) FspI
AmpR
(6720) PvuI
AmpR promoter
pAAV-EF1a-DIO-Flag-mGR
7982 bp
(5818) PsiI
f1 ori
AAV2 ITR
(5230) RsrII
(5225) PmlI
(5217) BstEII
hGH poly(A) signal
Factor Xa site
Kozak sequence
mGR
GR CRF-cKO mice
WPRE
(4786) AleI
(4710) AfeI
(4350) PflMI
(4093) EcoRV
loxP
lox2272
FLAG
NheI (3961)
BmtI (3965)

Figure 37: Map of viral vector allowing Cre-dependent expression of murine GR: AAV1/2-EF1α-DIO-mGR (AAV-DIO-mGR).

The mGR is revealed from a flip-excision (FLEX) vector, under the control of the ubiquitous human EF1α promoter. The FLEX-switch system makes use of two pairs of heterotypic, antiparallel loxP-type recombination sites, which first undergo Cre-dependent inversion of the coding sequence, followed by excision of two of the loxP sites (Atasoy et al., 2008). Thus, each of the orthogonal recombination sites ends up reversely oriented and ineffective of further recombination. Co-expression of our gene-of-interest (mGR) and the enhanced FlagTag by the EF1α promoter takes place.

IHC was performed to validate the plasmid transfections (Fig. 38a) and see whether our plasmid can be expressed. HEK cells were co-transfected with our Cre-dependent mGR plasmid and a Cre-expressing plasmid because HEK cells do not express endogenously Cre. As a negative Ctrl we omitted the Cre plasmid and as a positive control for transfection, we transfected a Cre-independent plasmid expressing GR and FLAG (PRKmGR-Flag plasmid). Cultures were treated for IHC and the results are shown in Fig 18a where GR expression is visualized in green and FLAG expression in red.

As expected, in our negative control (Cre plasmid omitted), GR expression was not detectable, confirming the Cre-dependency of our construct. Our positive control, expresses mGR and Flag proteins, visible in the GFP and RFP channels, respectively. Our transfected cells with mGR + Cre showed GR expression (showed by GR and FLAG fluorescence). To conclude with this step of testing the validity of your plasmid construct, the plasmid was then packaged into an AAV ½ virus to create our re-expression vector AAV½-EF1-DIO. The next step requires also the use of a Ctrl virus. In our case, the mGR construct is replaced by a mCherry expressing sequence (AAV-DIO-mCherry). This means that all the Cre positive cells that will encounter the Ctrl virus will expressed mCherry instead of GR.

To validate our construct *in vivo*, we used conditional forebrain-specific *Crfr1* knockout mice (*Crfr1FB-cKO*) characterized by Muller and colleagues (Muller et al., 2003). At that time, GR$^{\text{CRF-cKO}}$ mice were used in priority for breeding, in order to generate enough pups for the rest of the experiments. This is why we used *Crfr1FB-cKO* mice, which was a relevant model for our proof of concept. The mice, characterized for they reduced expression of GR in the dHPC, were unilaterally injected in the dHPC with our mGR virus and the other half of the dHPC was injected with a control virus. After 4 weeks of expression, GR expression was measured by Western Blot from dHPC tissues. The results show that the AAV-DIO-mGR virus has a 2.5 fold increase expression of GRs compared to Ctrl virus (Fig 38b).

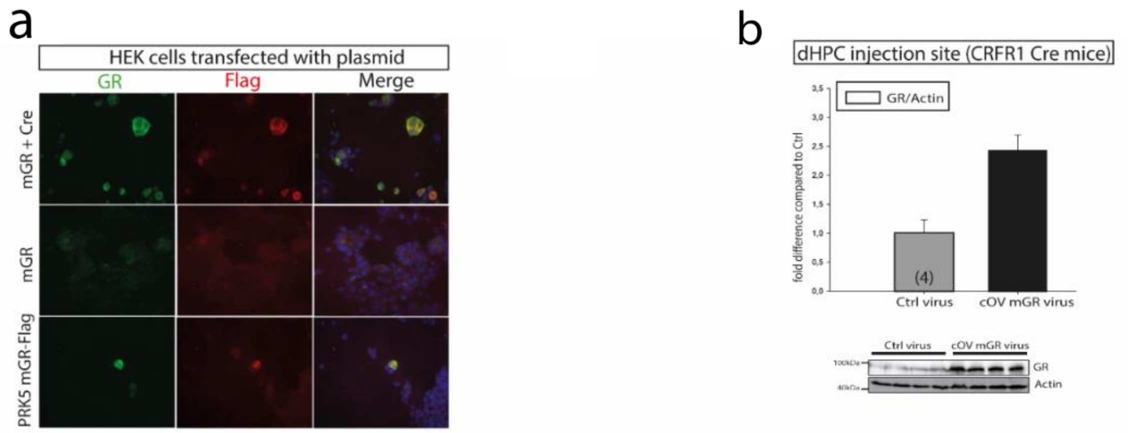

Figure 38: IHC and western blot validation of our viral vector construct.

(**a**) IHC of co-tansfected HEK cells with mGR (mouse GR) and cre plasmids, express GR and Flag protein, visible in the GFP and RFP channels, respectively. Negative control HEK cells, transfected only with mGR plasmid do not show any signal. As positive control, PRKmGR-Flag plasmid was used. mGR and Flag proteins are visible in the GFP and RFP channels, respectively. (**b**) Western Blot from dHPC tissues after injection of Ctrl and cOV mGR virus in the brain of 4 Crhf1-cKO mice. The results show that the cOV-mGR virus induces a 2.5 fold increase GR expression compared to Ctrl virus. Data are shown as mean ± SEM.

To further investigate our question, stereotactic surgery was performed on GR$^{CRF\text{-}cKO}$. Bilateral injection of AAV-DIO-mGR into the PVN of GR$^{CRF\text{-}cKO}$ mice led to the specific re-expression of GRs in PVN CRF+ neurons (Fig. 39, green fluorescence). This re-expression was not observed in GR$^{CRF\text{-}cKO}$ mice that received the control virus (AAV-DIO-mCherry, Fig. 39, red fluorescence).

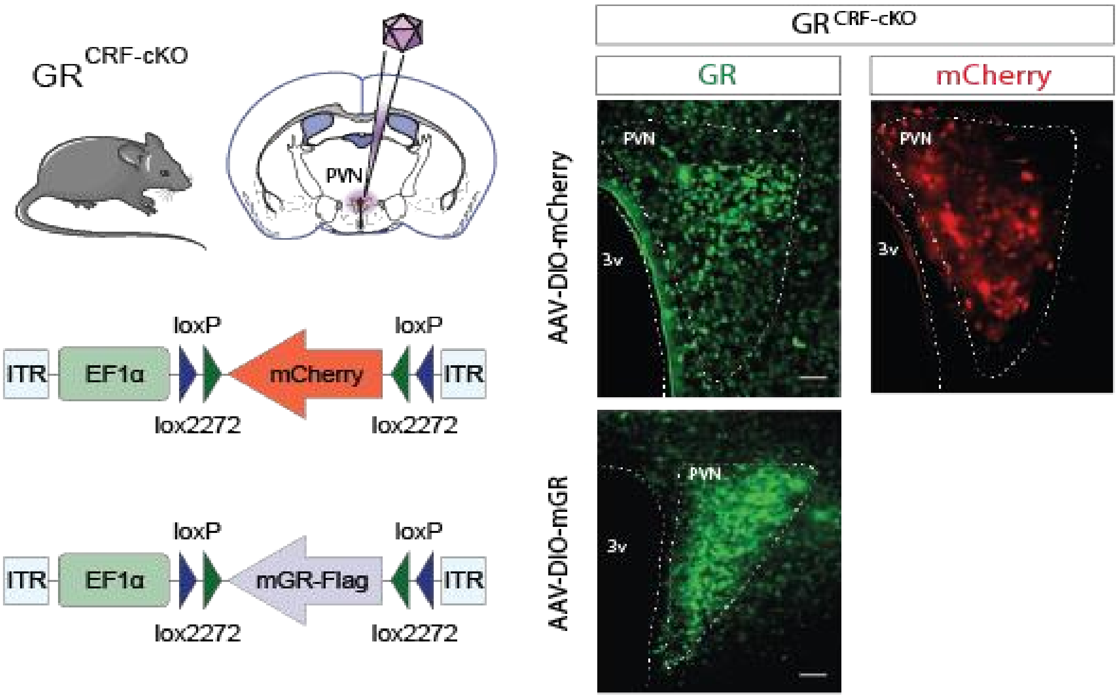
GR^CRF-cKO
PVN
loxP
loxP
ITR
EF1α
mCherry
ITR
lox2272
lox2272
loxP
loxP
ITR
EF1α
mGR-Flag
ITR
lox2272
lox2272
GR CRF-cKO
GR
mCherry
AAV-DIO-mCherry
AAV-DIO-mGR
PVN
3v
PVN
3v
PVN
3v

Figure 39: Design of the viral vector allowing Cre-dependent expression of murine GR: AAV1/2-EF1α-DIO-mGR (AAV-DIO-mGR) or control virus AAV1/2-EF1α-DIO mCherry (AAV-DIO-mCherry).

The virus was bilaterally delivered into the PVN of GR$^{CRF\text{-}cKO}$. Four weeks after viral delivery, the correct location of the injection sites was visualized by mCherry expression (AAV-DIO-mCherry) and by the re-expression of the mGR (IHC, green channel). Representative 40 µm coronal sections of PVN, scale bars, 100 µm.

In the next step, we injected another batch of $GR^{CRF\text{-}Ctrl}$ and $GR^{CRF\text{-}cKO}$ mice with either AAV-DIO-mGR or AAV-DIO-mCherry virus. 4 weeks post AAV injection; mice were subjected to our RRS protocol. As before, plasma CORT levels in basal condition (RRS1, RRS2 and RRS3) were not different between the three groups (solid lines). $GR^{CRF\text{-}Ctrl}$ mice injected with AAV-DIO-mGR showed normal HPA habituation to RRS (dashed line with orange circles) while $GR^{CRF\text{-}cKO}$ mice injected with AAV-DIO-mCherry control virus (dashed line with blue triangles) still lacked habituation. Notably, the PVN-targeted re-expression of mGR in CRF+ neurons in $GR^{CRF\text{-}cKO}$ mice (dashed line with black squares) was sufficient to restore HPA axis habituation to RRS (Fig. 40 dotted line with black squares). (2-way RM-ANOVA, Genotype effect F(2,30) =10.97, p = 0.0003; Bonferroni post hoc test $GR^{CRF\text{-}cKO}$ AAV-DIO-mGR *vs.* $GR^{CRF\text{-}cKO}$ control virus: RRS3 $$ p = 0.005; and $GR^{CRF\text{-}Ctrl}$ AAV-DIO-mGR *vs.* $GR^{CRF\text{-}cKO}$ AAV DIO-mCherry control virus: RRS2 * p = 0.041 and RRS3 *** p< 0.001).

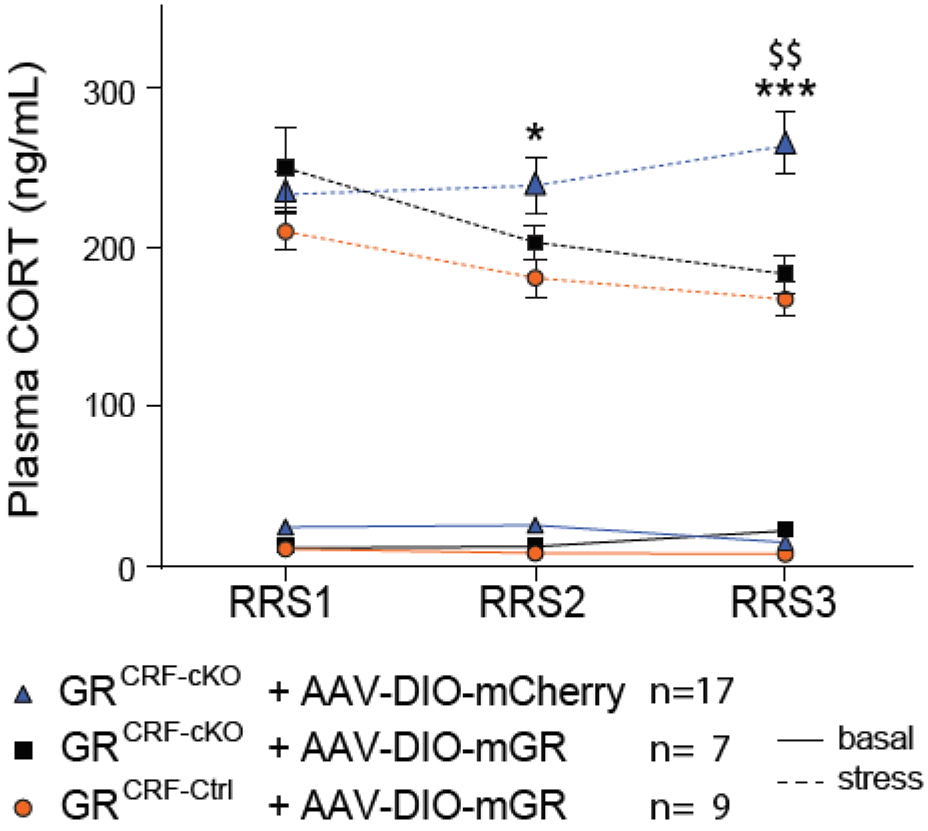

Figure 40: HPA axis habituation to repeated restraint stress (RRS) is rescued in GR$^{CRF-cKO}$ mice by bilateral GRs re-expression in the PVN.

Four weeks after AAV injections mice were subjected to our RRS protocol. As observed before, plasma CORT levels in basal condition were not different between the three groups (solid lines). GR$^{CRF-Ctrl}$ mice injected with AAV-DIO-mGR showed normal HPA habituation to RRS (dashed line with orange circles) while GR$^{CRF-cKO}$ mice injected with AAV-DIO-mCherry control virus (dashed line with blue triangles) still lacked habituation. However, the PVN-targeted re-expression of mGR in CRF+ neurons in GR$^{CRF-cKO}$ mice (dashed line with black squares) was sufficient to restore HPA axis habituation to RRS (2-way RM-ANOVA, Genotype effect F(2,30) = 10.97, p = 0.0003; Bonferroni post hoc test GR$^{CRF-cKO}$ AAV-DIO-mGR *vs.* GR$^{CRF-cKO}$ control virus: RRS3 $$ p = 0.005; and GR$^{CRF-Ctrl}$ AAV-DIO-mGR *vs.* GR$^{CRF-cKO}$ AAV DIO-mCherry control virus: RRS2 * p = 0.041 and RRS3 *** p< 0.001).

Direct comparison of plasma CORT levels between RRS1 and RRS3 showed the normal habituation of the HPA axis in GR$^{CRF-Ctrl}$ mice injected with AAV-DIO-mGR virus (Fig. 41 right plot: paired t-test, t8 = 2.899, p = 0.019, n = 9 mice), and the lack of habituation in GR$^{CRF-cKO}$ mice injected with AAV-DIO-mCherry control virus (Fig. 41 left plot: paired t-test, t16 = 1.137, p = 0.27, n = 17 mice). In GR$^{CRF-cKO}$ mice, the re-expression of mGR only in the PVN is sufficient to restore the HPA axis habituation to RRS (Fig. 41 middle plot: paired t-test, t = 2.672, p = 0.037, n = 7 mice).

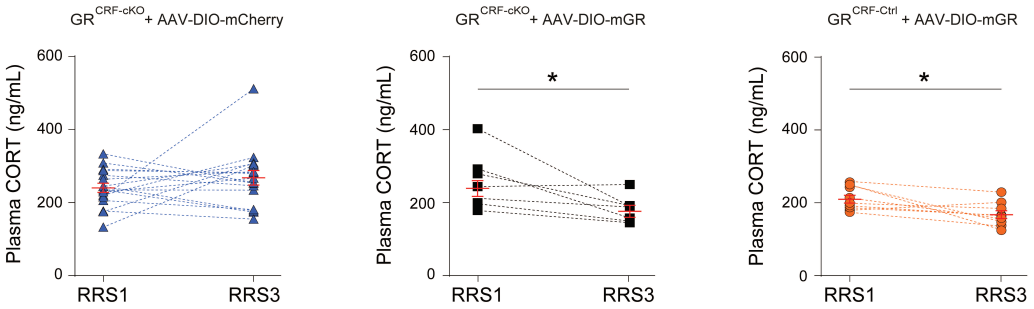

Figure 41: Comparison of plasma CORT levels between RRS1 and RRS3 after injection of AAV-DIO-mGR or AAV-DIO-mCherry

Direct comparison of plasma CORT levels between RRS1 and RRS3 showed the normal habituation of the HPA axis in GR$^{CRF\text{-}Ctrl}$ mice injected with AAV-DIO-mGR virus (right plot: paired t-test, $t_8 = 2.899$, p = 0.019, n = 9 mice), and the lack of habituation in GR$^{CRF\text{-}cKO}$ mice injected with AAV-DIO-mCherry control virus (left plot: paired t-test, $t_{16} = 1.137$, p = 0.27, n = 17 mice). In GR$^{CRF\text{-}cKO}$ mice, the re-expression of mGR only in the PVN is sufficient to restore the HPA axis habituation to RRS (middle plot: paired t-test, $t_6 = 2.672$, p = 0.037, n = 7 mice). Data are shown as mean ± SEM.

After completion of the RRS protocol, the animals were decapitated under isoflurane anesthesia and brains were removed and preserved at -80 ° C. Immunohistochemistry stainings was performed on each brain to verify the location of the virus injection. Sections were stained with GR antibody to visualize the re-expression of GR in cKO animals. All mice injected in the wrong region were excluded from analysis.

To summarize, we could reveal by measuring circulating CORT levels that GR$^{CRF\text{-}Ctrl}$ mice habituated to a repeated homotypic stressor (RRS), a phenomenon that was lost in GR$^{CRF\text{-}CKO}$ mice. This phenomenon is likely due to GRs in CRF-expressing neurons in the PVN since the injection of an AAV virus to re-express GRs in the CRF-expressing neurons of the PVN was able to rescue this phenotype. To deciphering the underlying mechanism of HPA to a repeated homotypic stressor, we tested next different hypothesis, such as the activity of CRF cells in cKO mice, the intrinsic properties of CRF neurons and the change in synaptic transmission onto PVN CRF neurons.

5.6 Impact of GR deletion in CRF+ neurons needed for the habituation of the HPA axis

5.6.1 Impact of GR deletion in CRF neurons regarding cell activity

We next studied the potential mechanisms carrying this GR-dependent habituation of the HPA axis to RRS in $GR^{CRF\text{-}Ctrl}$ mice. After RRS, $GR^{CRF\text{-}cKO}$ showed higher Crh mRNA expression in the PVN compared to $GR^{CRF\text{-}Ctrl}$ mice (Fig. 42 left bar graph: unpaired t-test, t16 = 2.429, p = 0.02; n = 10 control and 8 $GR^{CRF\text{-}cKO}$ mice), as well as cFos mRNA (Fig. 42 right bar graph: unpaired t-test, t25= 2.371, p = 0.026; n = 14 control and 13 $GR^{CRF\text{-}cKO}$ mice).

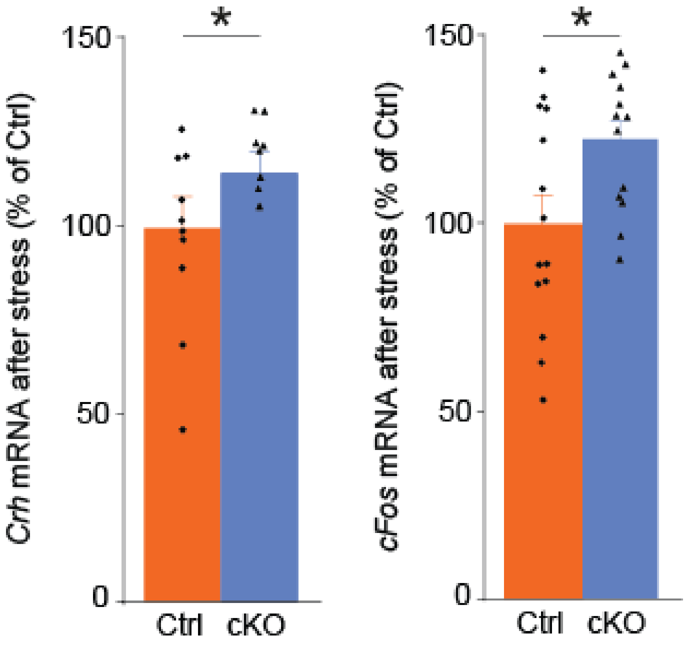

Figure 42: GR deletion in CRF+ neurons induces an increase of *Crh* and *cFos* mRNA in the PVN of cKO mice compare to Ctrl mice.

Upon repeated restraint stress (RRS), $GR^{CRF\text{-}cKO}$ mice showed higher Crh mRNA expression in the PVN (left bar graph: unpaired t-test, t16 = 2.429, p = 0.02; n = 10 control and 8 $GR^{CRF\text{-}cKO}$ mice), as well as cFos mRNA (right bar graph: unpaired t-test, t25 = 2.371, p = 0.026; n = 14 control and 13 $GR^{CRF\text{-}cKO}$ mice) compared to $GR^{CRF\text{-}Ctrl}$.

It would be relevant to check if cFos and CRF neurons colocalize in the PVN. It could be further confirm by double ISH or RNAscope. Unfortunately, we did not perform it yet. Collectively, our results can suggest higher stress-induced CRF expression and neuronal activity in the PVN, thus leading to higher plasma CORT levels. Therefore we hypothesized that a shift in intrinsic properties and/or excitability of CRF+ neurons of the PVN could lead to the reduced CORT release observed after RRS in $GR^{CRF\text{-}Ctrl}$ mice.

To further explore our hypothesis, we conducted whole-cell patch-clamp recordings of CRF-expressing neurons in acute PVN slices of control ($GR^{CRF\text{-}Ai9\text{-}Ctrl}$) and cKO ($GR^{CRF\text{-}Ai9\text{-}cKO}$) mice under basal condition or after 3 RRS. The first step was to investigate whether GRs deletion altered the intrinsic electrical properties of these neurons in basal conditions or after stress, and then to see if this deletion affected the synaptic transmission impinging onto CRF neurons.

5.6.2 GRs deletion does not affect intrinsic electrical properties or the excitability of CRF-expressing neurons of the PVN

Since we immunochemically established that 98% of CRF neurons of the PVN coexpress GRs, we could reliably record CRF-expressing neurons. CRF neurons of the PVN were visualized by the expression of tdTomato (Fig.43 left, 5X magnification). They were recorded in current-clamp mode. Bellow is shown a 40X epifluorescence picture depicting individual CRF-expressing neurons in the PVN and the recorded cell, identified by the black arrowhead (Fig. 43 right).

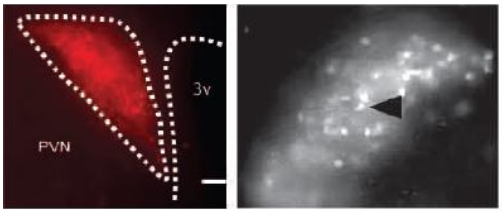

Figure 43: Coronal brain slice of the PVN from a $GR^{CRF\text{-}Ai9\text{-}Ctrl}$ mouse

Microphotograph from a 300 µm coronal acute brain slice of the PVN at 5x (left) and 40x (right) magnification. CRF neurons of the PVN were visually identified by the expression of tdTomato (black arrow shows an example of a recorded cell). PVN, hypothalamic paraventricular nucleus, 3V, third ventricle. Scale bar, 100 µm.

Several parameters were measured in these neurons in both genotypes, under basal condition or after 3 RRS: the resting membrane potential (RMP), the input resistance (Rin) and the excitability of the cell, measured by the number of action potentials (APs) fired in response to a depolarizing current injection. No significant differences were found in any of the measured parameters between control and cKO mice, nor after RRS when compared to basal conditions (Fig. 24: resting membrane potential (RMP, b), input resistance (c), and excitability (d). Thus, neither GRs deletion nor RRS affects the intrinsic electrical properties of CRF-expressing neurons of the PVN.

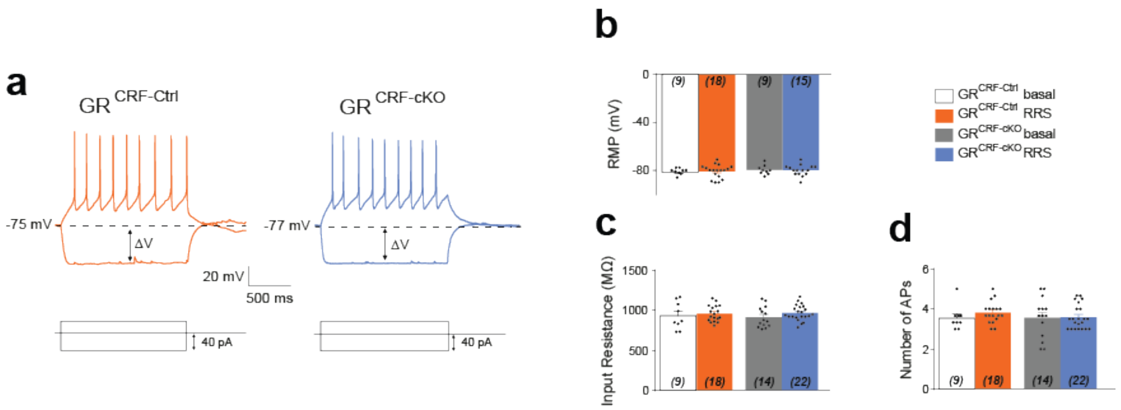

Figure 44: Intrinsic electrical properties of CRF-expressing neurons of the PVN

(**a**) Representative traces from CRF neurons recordings (current-clamp mode) from $GR^{CRF\text{-}Ai9\text{-}Ctrl}$ (orange) and $GR^{CRF\text{-}Ai9\text{-}cKO}$ (blue) mice. (**b-d**) The intrinsic membrane properties of CRF neurons from Ctrl and $GR^{CRF\text{-}Ai9\text{-}cKO}$ mice recorded under basal and stress (RRS protocol) conditions were not different (2-way ANOVAs): resting membrane potential (RMP, **b**), input resistance (**c**), and excitability (**d**). Cell numbers are indicated in brackets in each bar and were obtained from at least 7 mice.

5.6.3 GR deletion in CRF neurons impairs the RRS-induced shift in excitation / inhibition balance

Anatomical investigations have already confirmed that neurons of the PVN receive numerous synaptic inputs (both excitatory and inhibitory) from diverse brain regions (PFC, amygdala, hippocampus, for review Ulrich-Lai, and Herman, 2009). We assessed whether GRs deletion in CRF neurons would affect their synaptic inputs in basal condition and after exposure to RRS, by recording miniature excitatory postsynaptic currents (mEPSCs) and miniature inhibitory postsynaptic currents (mIPSCs).

5.6.3.1 Excitatory inputs

Under basal conditions, no significant difference was observed for the amplitude of mEPSCs between the two genotypes (Fig. 45 “-“). The exposure to RRS caused a small reduction in mEPSCs amplitude for both genotypes when compared to their corresponding basal values (Fig. 45 “+“).: 2 way ANOVA Stress F(1,94)= 10.13, p = 0.002; Postdoc Fisher LSD analysis $GR^{CRF\text{-}Ctrl}$ Basal vs RRS: 16.97 ± 0.91 pA vs 14.25 ± 1.06 pA, p=0.040 ; $GR^{CRF\text{-}cKO}$ Basal vs RRS: 17.4 ± 0.53 pA vs 14.58 ± 0.86 pA, p=0.016). Since the decrease in mEPSCs amplitude was fairly mild and kept in both genotypes, it is most likely due to a general stress effect and does not require the expression of GRs.

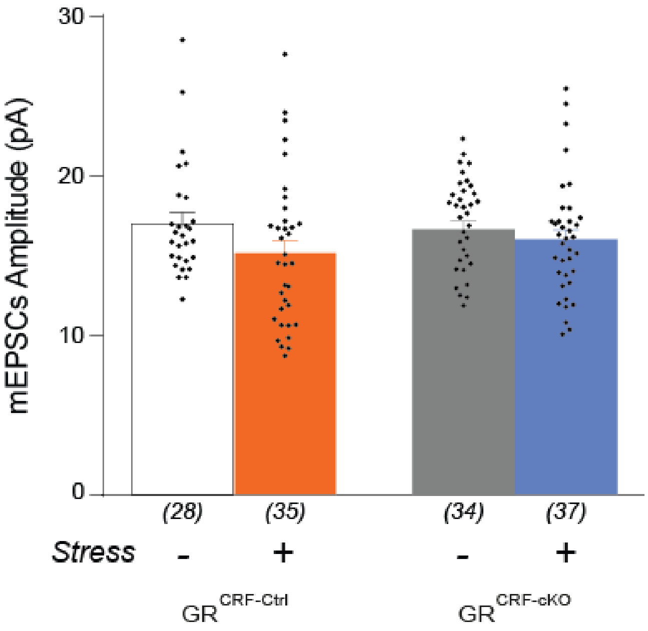

Figure 45: The amplitude of miniature excitatory post-synaptic currents (mEPSCs) is not affected by GR deletion nor by repeated restraint stress (RRS).

The amplitude of mEPSCs is not affected by GR deletion, nor by RRS (2-way ANOVA Stress*Genotype F(1,126) = 0.922, p = 0.338: $GR^{CRF\text{-}Ai9\text{-}Ctrl}$ basal = 16.99 ± 0.67 pA; $GR^{CRF\text{-}Ai9\text{-}Ctrl}$ RRS = 15.16 ± 0.79 pA; $GR^{CRF\text{-}Ai9\text{-}cKO}$ basal = 16.57 ± 0.45 pA; $GR^{CRF\text{-}Ai9\text{-}cKO}$ RRS = 16.00 ± 0.59 pA).

However, RRS induced a significant decrease in mEPSCs frequency in control mice (Fig. 46b: see recording traces and the rightward shift in the cumulative probability plot). This effect was not observed in $GR^{CRF\text{-}Ai9\text{-}cKO}$ mice (Fig. 46a: 2-way ANOVA Stress effect F(1,130) = 6.335, p = 0.013; Bonferroni post-hoc test $GR^{CRF\text{-}Ai9\text{-}Ctrl}$ Basal

$\text{GR}^{\text{CRF-Ai9-cKO}}$ RRS: 0.75 ± 0.07 Hz *vs.* 0.47 ± 0.05 Hz, p = 0.02; $\text{GR}^{\text{CRF-Ai9-cKO}}$ Basal *vs.* RRS: 0.83 ± 0.06 Hz *vs.* 0.80 ± 0.08 Hz, p = 0.9. Cell numbers are indicated in brackets under each bar and were obtained from at least 7 mice). Taken together, these results suggest that exposure to RRS induces a GR-mediated decrease in excitatory drive onto CRF-expressing neurons of the PVN.

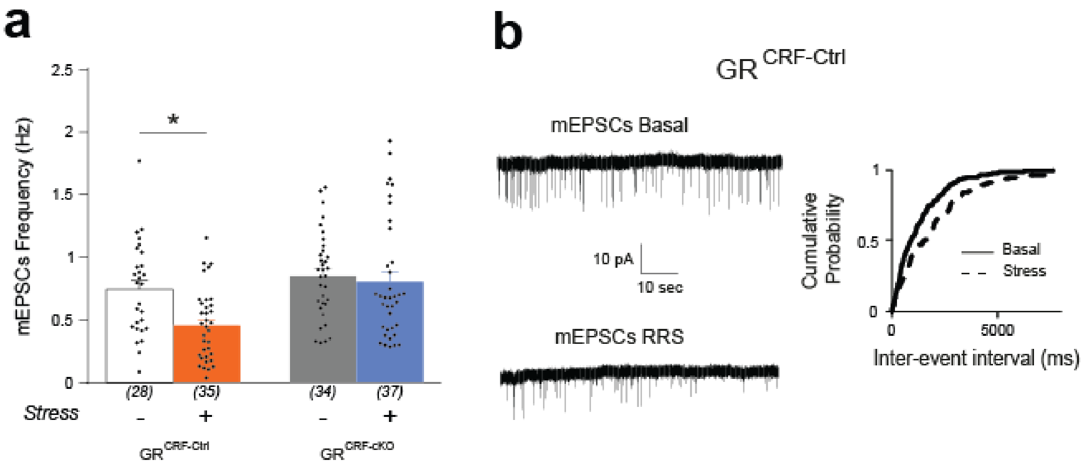

Figure 46: The frequency of miniature excitatory post-synaptic currents (mEPSCs) is decreased under stress in Ctrl mice but not in cKO mice.

(**a**) RRS induced a strong decrease in miniature excitatory post-synaptic currents (mEPSCs) frequency in $\text{GR}^{\text{CRF-Ai9-Ctrl}}$ but not in $\text{GR}^{\text{CRF-Ai9-cKO}}$ (2-way ANOVA Stress effect F$_{(1,130)}$ = 6.335, p = 0.013, Bonferroni post-hoc test $\text{GR}^{\text{CRF-Ai9-Ctrl}}$ Basal *vs.* RRS: 0.75 ± 0.07 Hz *vs.* 0.47 ± 0.05 Hz, p = 0.02; $\text{GR}^{\text{CRF-Ai9-cKO}}$ Basal *vs.* RRS: 0.83 ± 0.06 Hz *vs.* 0.80 ± 0.08 Hz, p = 0.9). Cell numbers are indicated in brackets under each bar and were obtained from at least 7 mice. (**b**) Representative traces and cumulative plot of inter-event interval distribution of mEPSCs in $\text{GR}^{\text{CRF-Ai9-Ctrl}}$ mice under basal (black line) and stress (dotted line) conditions. Stress induced a rightward shift of the distribution reflecting a decrease in mEPSCs frequency.

5.6.3.2 Inhibitory inputs

Concerning the inhibitory inputs, the amplitude of mIPSCs was not significantly different under basal conditions between the genotypes. Furthermore, exposure to RRS did not induce any significant changes (Fig. 47: 2-way ANOVA Stress*Genotype F$_{(1,70)}$ = 0.902, p = 0345: $\text{GR}^{\text{CRF-Ai9-Ctrl}}$ basal = 65.55 ± 3.5 pA; $\text{GR}^{\text{CRF-Ai9-Ctrl}}$ RRS = 72.59 ± 3.28 pA; GRCRF-Ai9-cKO basal = 66.87 ± 4.32 pA; GRCRF-Ai9-cKO RRS = 66.70 ± 3.45 pA).

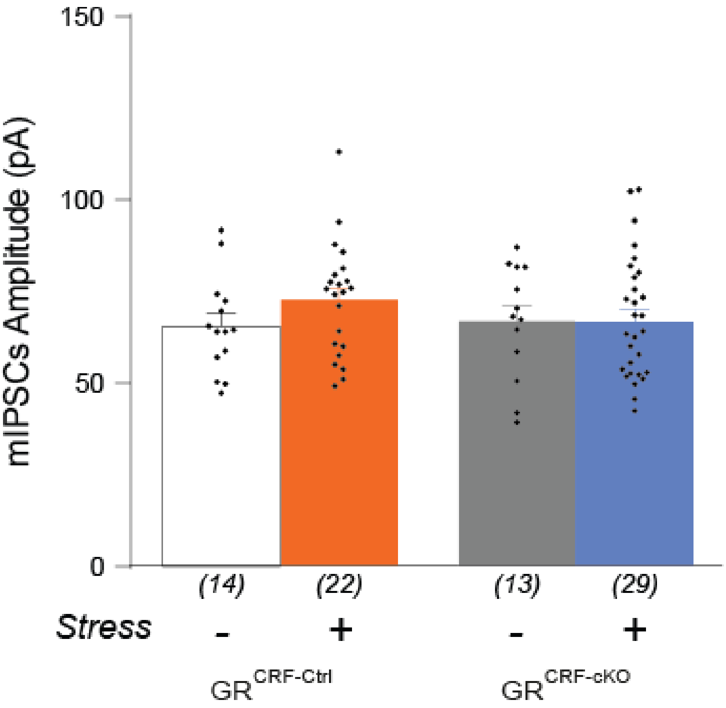

Figure 47: The amplitude of miniature inhibitory post-synaptic currents (mIPSCs) is not affected by GR deletion nor by repeated restraint stress (RRS).

The amplitude of mIPSCs is not affected by GR deletion, nor by RRS (2-way ANOVA Stress*Genotype $F_{(1,70)} = 0.902$, p = 0345: $GR^{CRF\text{-}Ai9\text{-}Ctrl}$ basal = 65.55 ± 3.5 pA; $GR^{CRF\text{-}Ai9\text{-}Ctrl}$ RRS = 72.59 ± 3.28 pA; $GR^{CRF\text{-}Ai9\text{-}cKO}$ basal = 66.87 ± 4.32 pA; $GR^{CRF\text{-}Ai9\text{-}cKO}$ RRS = 66.70 ± 3.45 pA).

However, the frequency of mIPSCs was strongly enhanced by RRS in control mice (Fig. 48b: see recording traces and the leftward shift in the cumulative probability plot). Again, this effect was not present in $GR^{CRF\text{-}Ai9\text{-}cKO}$ mice (Fig. 48a: 2-way ANOVA Stress*Genotype $F_{(1,74)} = 8.76$, p = 0.004, Bonferroni post-hoc test $GR^{CRF\text{-}Ai9\text{-}Ctrl}$ Basal *vs.* RRS: 8.42 ± 0.94 Hz *vs.* 17.50 ± 1.51 Hz, *** $p < 0.001$; $GR^{CRF\text{-}Ai9\text{-}cKO}$ Basal *vs.* RRS: 9.38 ± 1.18 Hz *vs.* 10.69 ± 0.98 Hz, p = 0.9). Taken collectively, these results suggest that exposure to RRS induces a GR-mediated increase in inhibitory drive onto CRF-expressing neurons of the PVN.

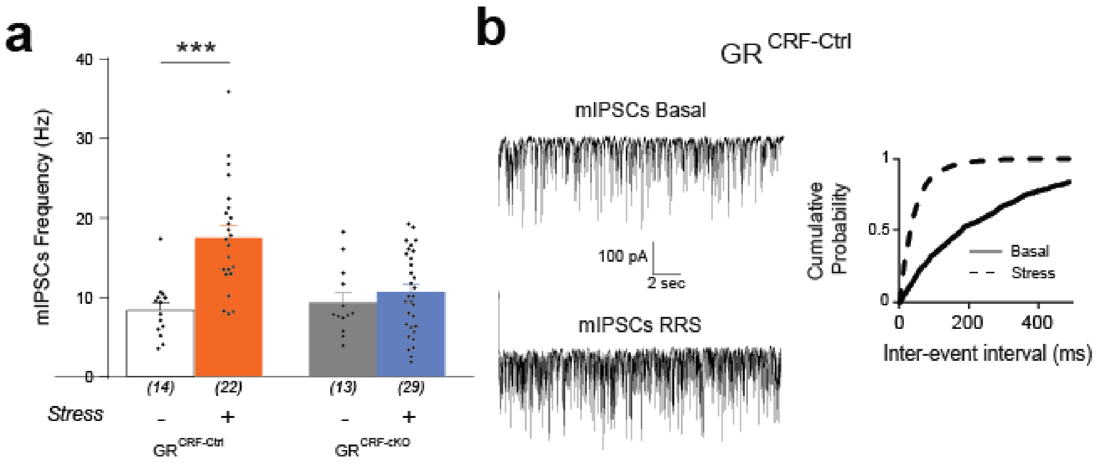

Figure 48: The frequency of miniature inhibitory post-synaptic currents (mIPSCs) is increased by stress in Ctrl mice but not in cKO mice.

(**a**) RRS induced a strong increase in miniature inhibitory post-synaptic currents (mIPSCs) frequency in $GR^{CRF\text{-}Ai9\text{-}Ctrl}$ but not in $GR^{CRF\text{-}Ai9\text{-}cKO}$ mice (2-way ANOVA Stress*Genotype $F_{(1,74)} = 8.76$, $p = 0.004$, Bonferroni post-hoc test $GR^{CRF\text{-}Ai9\text{-}Ctrl}$ Basal *vs.* RRS: 8.42 ± 0.94 Hz *vs.* 17.50 ± 1.51 Hz, *** $p < 0.001$; $GR^{CRF\text{-}Ai9\text{-}cKO}$ Basal *vs.* RRS: 9.38 ± 1.18 Hz *vs.* 10.69 ± 0.98 Hz, $p = 0.9$). Cell numbers are indicated in brackets under each bar and were obtained from at least 7 mice. (**b**) Representative traces and cumulative plot of inter-event interval distribution of mIPSCs in $GR^{CRF\text{-}Ai9\text{-}Ctrl}$ mice under basal (black line) and stress (dotted line) conditions. Stress induced a leftward shift of the distribution reflecting an increase in mIPSCs frequency. Data are shown as mean ± SEM.

To summarize, under basal conditions, CRF neurons of the PVN – with or without GRs expression – exhibit the same intrinsic electrical properties, and a similar glutamatergic and GABAergic synaptic drive in both genotypes, suggesting that GRs deletion does not affect all these parameters. However and more interestingly, when subjected to a repeated stressful challenge (here an exposure to RRS), control mice show a decreased excitatory and an increased inhibitory drive.

GRs are expressed post-synaptically but modulate synaptic transmission in the context of RRS. This suggests the involvement of a retrograde messenger, which is released from the post-synapse in a GR-dependent manner to act at the presynaptic level to change the release probability of neurotransmitters (Wamsteeker Cusulin, Fuzesi et al. 2013). We next investigated different hypotheses to understand what retrograde messenger could lead to this change in excitatory/inhibitory balance in Ctrl mice after repeated exposure to stress. We studied the GR-mediated post-synaptic release of neuromediators, which could in turn act pre-synaptically and modify the release probability of neurotransmitter. Previous studies have already shown that the endocannabinoid (eCB) and the nitric oxide (NO) systems are very potent retrograde modulators of synaptic transmission in the PVN (Nahar et al, 2015).

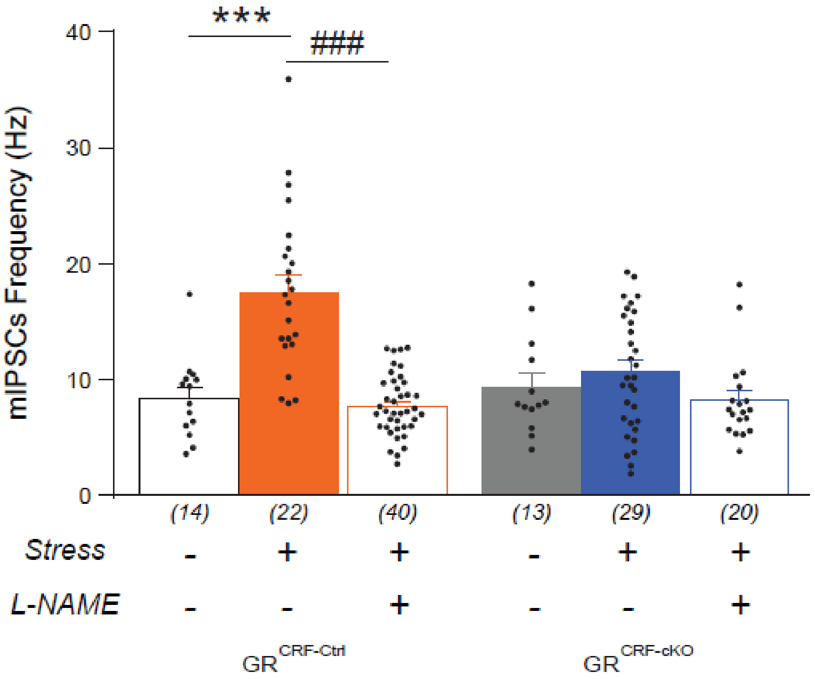

Figure 49: The inhibitory inputs in presence of nitric oxide synthase 1 inhibitor L-NAME are normalized.

The incubation of PVN slices from GR$^{\text{CRF-Ai9-Ctrl}}$ mice in the nitric oxide synthase 1 inhibitor L-NAME was able to completely reverse the RRS-induced increase in mIPSCs frequency (GR$^{\text{CRF-Ai9-Ctrl}}$ RRS = 17.50 ± 1.51 Hz vs. GR$^{\text{CRF-Ai9-Ctrl}}$ RRS + L-NAME = 7.63 ± 0.41 Hz, unpaired t test, t60 = 7.92, ### $p < 0.001$), without affecting the mIPSCs frequency in GR$^{\text{CRF-Ai9-cKO}}$ mice (GR$^{\text{CRF-Ai9-cKO}}$ RRS = 10.69 ± 0.98 Hz vs. GR$^{\text{CRF-Ai9-cKO}}$ RRS + L-NAME = 8.19 ± 0.78 Hz, unpaired t-test, t47 = 1.84, p = 0.072). (*** See Fig. 48) Cell numbers are indicated in brackets under each bar and were obtained from at least 7 mice.

Thus, the incubation of PVN slices from GR$^{\text{CRF-Ai9-Ctrl}}$ mice in the nitric oxide synthase 1 inhibitor L-NAME (100 µM) was able to completely reverse this RRS-induced increase in mIPSCs frequency (Fig. 49: GR$^{\text{CRF-Ai9-Ctrl}}$ RRS = 17.50 ± 1.51 Hz *vs.* GR$^{\text{CRF-}}$$_{\text{Ai9-Ctrl}}$ RRS + L-NAME = 7.63 ± 0.41 Hz, unpaired t-test, t60 = 7.92, ### $p < 0.001$), without affecting the amplitude of mIPSCs (Fig. 50: GRCRF-Ai9-Ctrl RRS = 72.59 ± 3.28 pA *vs.* GR$^{\text{CRF-Ai9-Ctrl}}$ RRS + L-NAME = 75.73 ± 2.25 pA, unpaired t-test, t60 = 0.81, p = 0.417; and GR$^{\text{CRF-Ai9-cKO}}$ RRS = 66.70 ± 3.45 pA *vs.* GR$^{\text{CRF-Ai9-cKO}}$ RRS + L-NAME

= 72.60 ± 3.16 pA, unpaired t-test, t47 = 1.194, p = 0.239), nor exerting any effect on mIPSCs frequency in $GR^{CRF-Ai9-cKO}$ RRS mice ($GR^{CRF-Ai9-cKO}$ RRS = 10.69 ± 0.98 Hz *vs*. $GR^{CRF-Ai9-cKO}$ RRS + L-NAME = 8.19 ± 0.78 Hz, unpaired t-test, t47 = 1.84, p = 0.072). This suggests an RRS-mediated GR-dependent release of NO, which acts retrogradely at the presynaptic terminal to enhance the release probability of GABA onto CRF+ neurons of the PVN.

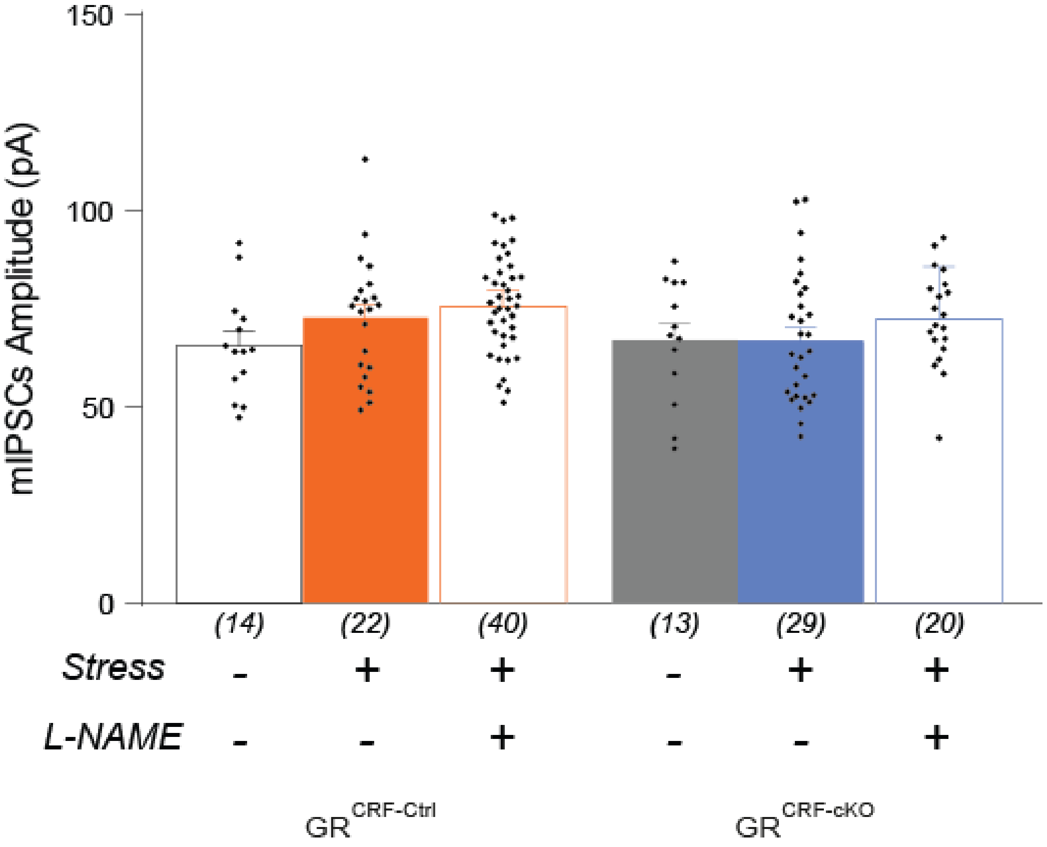

Figure 50: L-NAME has no effect on the amplitude of miniature inhibitory post-synaptic currents (mIPSCs) in basal and stress condition (RRS), nor in Ctrl mice, neither in cKO mice.

The amplitude of mIPSCs is not affected by GR deletion, nor by RRS (2-way ANOVA Stress*Genotype $F_{(1,70)}$ = 0.902, p = 0345: $GR^{CRF-Ai9-Ctrl}$ basal = 65.55 ± 3.5 pA; $GR^{CRF-Ai9-cKO}$ RRS = 72.59 ± 3.28 pA; $GR^{CRF-Ai9-cKO}$ basal = 66.87 ± 4.32 pA; $GR^{CRF-Ai9-cKO}$ RRS = 66.70 ± 3.45 pA). Moreover, slice incubation in the nitric oxide synthase 1 inhibitor L-NAME also has no effect on mIPSCs amplitude ($GR^{CRF-Ai9-Ctrl}$ RRS = 72.59 ± 3.28 pA *vs.* $GR^{CRF-Ai9-Ctrl}$ RRS + L-NAME = 75.73 ± 2.25 pA, unpaired t-test, t_{60} = 0.81, p = 0.417; and $GR^{CRF-Ai9-cKO}$ RRS = 66.70 ± 3.45 pA *vs.* $GR^{CRF-Ai9-cKO}$ RRS + L-NAME = 72.60 ± 3.16 pA, unpaired t-test, t_{47} = 1.194, p = 0.239). Cell numbers are indicated in brackets under each bar and were obtained from at least 7 mice. Data are shown as mean ± SEM.

To summarize, GR deletion from CRF$^+$ neurons does not affect their intrinsic electrical properties nor the HPA axis response to a single stressor. However, we showed that, upon repetition of the same stressor (RRS), control mice exhibit habituation of the HPA axis, as shown by reduced plasma CORT levels. The HPA axis habituation is dependent on GR expression in CRF neurons of the PVN and does not involve changes in the intrinsic electrical properties of these neurons. These findings contrast with a recently published study showing CORT-independent fast adaptation of CRF neurons excitability to repeated white-noise presentation, measured by *in vivo* calcium imaging. In our study, the HPA habituation is likely mediated by a change in the excitation / inhibition balance, towards a stronger inhibitory tone onto CRF$^+$ neurons of the PVN, leading to lower CORT release from the adrenals (Fig. 51). Although the mechanism underlying the decreased excitation has yet to be determined, we showed that the increased inhibition is mediated by the GR-dependent retrograde action of NO at the presynaptic side, leading to an increased release probability of GABA.

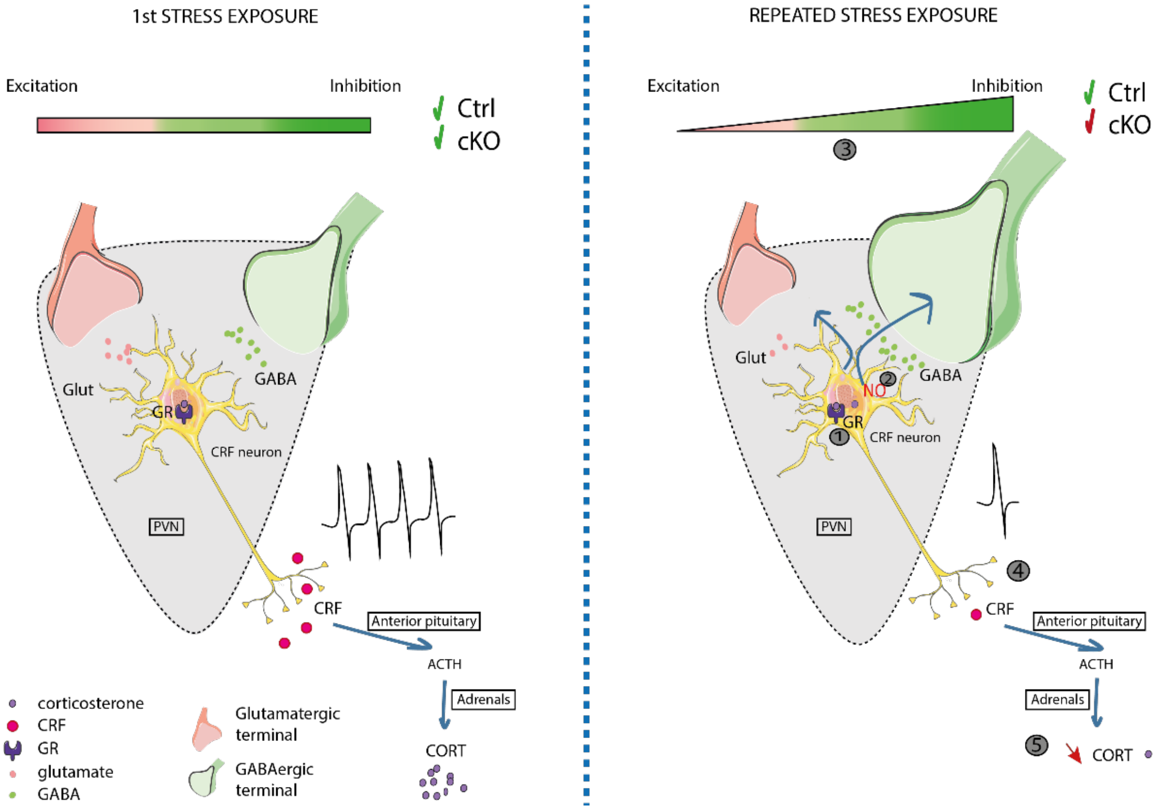
1st STRESS EXPOSURE
Excitation
Inhibition
✓ Ctrl
✓ cKO
Glut
GABA
GR
CRF neuron
PVN
CRF
Anterior pituitary
ACTH
Adrenals
CORT
corticosterone
CRF
GR
glutamate
GABA
Glutamatergic terminal
GABAergic terminal
REPEATED STRESS EXPOSURE
Excitation
Inhibition
✓ Ctrl
✓ cKO
③
Glut
GABA
②
NO
GR
①
CRF neuron
PVN
④
CRF
Anterior pituitary
ACTH
Adrenals
⑤
CORT

Figure 51: Proposed mechanism underlying habituation to homotypic stressor in mice.

Left part: The PVN is highly innervated by GABAergic inputs, which provide a global inhibitory tone in normal condition. After perception of a first stressor (1st stress EXPOSURE), the parvocellular neurons in the PVN secrete CRF into the portal vein to the median eminence of the pituitary gland, where they trigger the release of ACTH into the bloodstream to stimulate the synthesis and release of CORT from the cortex of the adrenal glands. **Right part**: Upon perception of a repeated stressor (REPEATED STRESS EXPOSURE), HPA habituation takes place, likely mediated by a change in the excitation / inhibition balance, towards a stronger inhibitory tone onto CRF+ neurons of the PVN, leading to lower CORT release from the adrenals. The increased inhibition is mediated by GR dependent retrograde action of NO at the presynaptic side, leading to an increased release probability of GABA.

6 Discussion

A recent study conducted in 121 countries, investigated the role of stress in people's life (Ortiz & Roser, 2013). A stress index was calculated and correlated to other health indicators, such as life expectancy, Gross Domestic Product (GDP), global happiness, or personal satisfaction. The results were the exact opposite of the researchers' expectations. The higher the stress index of the nation, the higher the GDP and life span, the happier they are with their life, their work, their communities, with their own health. This odd correlation was defined as "Stress Paradox". Although we perceive stress as distressing at the time and always think of it as negative, harmful, detrimental, counterproductive, it can be a gauge for how committed we are to reach happiness, joy and professional development. This is an uncommon way of thinking about stress. Stress could become an indicator of engagement to achieve the tasks that someone is pursuing, and facing obstacles. Stress is usually defined as harmful and associated to depression, anxiety-related disorders, burnout, and heart disease (Gill et al., 2020). However, a more modern approach is that stressful events lead to greater wellbeing and resilience. That is why it becomes evident to study better the mechanisms underlying stress coping strategies, resilience, desensitization, and habituation.

Modern life style is a very dynamic plot pervaded by cultural, social, emotional, and biological experiences, some of which that ultimately endanger our lifestyle and affect our physiology and behaviour. Consequently, during our daily lives, we are exposed to various stressors, ranging from mild to robust, sporadic to chronic. Indeed, many work experiences combine elevated levels of stress with high responsibility, vigorously calling for executive behavioral control and cognition (Jakobsson, 2014). Those very situations place a high demand on our coping strategies, always demanding cognitive agility and executive functions, and trigger a series of adaptive responses that eventually enable us to deal more or less successfully with these stressors. For health and survival, adequate regulatory control of the HPA stress axis is essential. The extrinsic and intrinsic pathways responsible for regulating the hypothalamic paraventricular nucleus' stress-responsive CRF neurons, which sum excitatory and inhibitory inputs into a pure secretory signal in the pituitary, have been extensively studied (Herman, 2003). Brain structures that directly innervate those neurons are designed to transmit sensory information, such as visceral afferents, nociceptors, while supporting stress responses to new homeostatic challenges. Secondary inputs from the limbic-associated areas are capable of activating these same neurons when no direct physiological challenges are detected. Crucially, anticipatory circuits are integrated with neural pathways which support multi-level reactive responses. The resulting centralized organization of stress-responsive neurocircuits can compare information from various limbic inputs with data internally and peripherally sensed, thereby tuning the adrenal cortex's relative action (Herman *et al.*, 2016). Hypothalamic – pituitary – adrenocortical dysfunction linked with multiple disease processes is likely to underlie imbalances between these limbic systems and homeostatic sensors.

Over the years, chronic stress has been frequently involved in altered brain function, leading to mental illnesses such as anxiety, depression, mania, schizophrenia (Ulrich-Lai & Herman, 2009). As a consequence, many studies focused primarily on evaluating stress-related neurocircuits. Particular variations in the expression of CRF and its high-affinity receptor (CRFR1) are linked with mood and anxiety disorders (Holsboer, 1999; De Kloet et al., 2005; Deussing & Wurst, 2005). CRF acts in this respect as both a neuroendocrine hormone through the HPA axis (Vale et al., 1981) and a neuromodulator via neuronal hypothalamic and extra-hypothalamic pathways (Gallagher et al., 2008).

Among patients with MDD, recurrent findings include elevated levels of CRF in the cerebrospinal fluid, hypersecretion of CRF from the PVN, systemic cortisol elevation and reduced glucocorticoid (GR)-mediated negative feedback (Lowy et al., 1984; Nemeroff et al., 1984; Fossey et al., 1996; Holsboer, 2000; Binder & Nemeroff, 2010). Intracerebroventricular administration of CRF in rodents causes behavioral effects similar to those generated by stress, including hyperlocomotion, anxiety-related behavior, anorexia, changes in sexual behavior, and impaired cognitive performance (Sutton et al., 1982; Butler et al., 1990; Menzaghi et al., 1993; Koob & Heinrichs, 1999; Zorrilla & Koob, 2010). Genetic and pharmacological studies have implicated GR in the modulation of stress-related behaviors (Muller & Holsboer, 2006) and therefore mice with changes in the HPA axis as relevant models of depression-like symptoms (Tronche et al., 1999). At the level of the brain, disruption of the GR gene (Nr3c1) diminishes anxiety (Wei et al., 2004). A conditional Knock-out (KO) approach allows the engineering of a mouse model with a reduced expression of GRs, thus avoiding well-known complications due to classical transgenesis such as many integration copies or sites of modification (Lu et al., 2008). In the generated mouse line, the spatial and/or temporal properties of GRs expression depends only on the added Cre recombinases. In contrast, transcriptional regulation via the endogenous CRF promoter ensures permanent and reproducible rates of expression. Studies have shown that CNS- and forebrain-specific GR deletion result in reduced anxiety (Tronche et al., 1999; Boyle, 2005). Nevertheless, the underlying brain areas and distinct cell types that modulate GR effects on HPA control and anxiety remain still to be elucidated. Several previous GR conditional KO mouse studies have helped us to understand GR-mediated HPA-axis control. Notably, conditional loss of GR function in the CNS, under the Nestin promoter (GR-Nes-Cre mice) induces hyperactivity of HPA axis, followed by an increase in glucocorticoid release, which leads to symptoms similar to those observed in Cushing syndrome, possibly due to GR deletion in the PVN (Tronche et al., 1999). In those animals, both anxiety and despair were reduced. The use of the GR-Nes-Cre mice has a major limitation since the Nestin is expressed all over the brain, making it difficult to decipher the contribution of HPA axis versus forebrain structures. To overcome this difficulty, Boyle and colleagues (Boyle, 2005) generated a forebrain forebrain-specific GR knockout, using the FKBP5 promotor, under the α-calcium/calmodulin-dependent protein kinase II (αCaMKII) promoter. GRs in the PVN remain unaffected and those mice show a robust depression-like phenotype, which was normalized after chronic injection of imipramine, a tricyclic antidepressant (Boyle, 2005). Lately, mice with a specific GR deletion in the hypothalamus (Sim1-Cre-GRe3Δ mice) demonstrated hypersecretion of glucocorticoids, and mice lacking GR in the CeA showed no alterations in anxiety-related or despair behavior, respectively (Laryea et al., 2013a, Laryea et al., 2013b respectively). Scientists at our institute have recently shown that GR removal in forebrain glutamatergic (Nex-Cre), but not GABAergic (Dlx5/6-Cre) neurons mediate anxiogenic effects of the glucocorticoid receptor (Hartmann et al., 2017).

This research aims to use genetic loss-of-function approaches to explore further stress-related GR / CRF neurocircuits. The first intention was to discriminate between direct effects of reduced expression of GRs from those, resulting from HPA axis. Thus, we generated for the first time a mouse line where GRs are specifically deleted from CRF expressing neurons of the brain (GR$^{CRF\text{-}cKO}$). The effects on basal and stress-induced emotional behaviour were analysed in *GR*$^{CRF\text{-}cKO}$ and *GR*$^{CRF\text{-}Ctrl}$ *control* littermates. Consequently, influences on emotional activity induced by basal and stress conditions were studied in GR$^{CRF\text{-}cKO}$ mice. Potential physiological, neuroendocrine, and behavioural alterations were investigated in this conditional mouse model. The conditional *GR*-knockout mice were used to locate the receptors controlling habituation of the HPA axis to repeated homotypic stress. Eventually, the study aimed to assess the synaptic transmission impinging on the CRF neurons that could explain the change in the inhibitory/excitatory balance essential for HPA habituation.

6.1 PVN anatomy

Here we describe and characterize the physiological function of a distinct population of HPA axis-initiating PVN neurons, coexpressing GR and CRF. Based on our expression quantification between GR and CRF, we showed that almost all CRF neurons of the PVN (98%) express GR, while GRs are also expressed in other neuronal types (i.e., OT, VP Fig. 24). ~70% of GRs are expressed in CRF+ neurons (Fig. 22). Thus, our mouse line is a potent model for studying GR's role in the regulation of CRF release. The validation of our knockout shows ~30% less expression of GRs in the cKO mice compared to the Ctrl mice. Moreover, the data show that the deletion is specific to CRF expressing cells in the PVN and CeA (percentage of deletion, ~70% (Fig. 25), corresponds to the percentage of co-expression, ~70% for mRNA expression mRNA (Fig. 22), ~50% for scRNA expression (Fig. 24). It has to be noted nevertheless that the colocalization percentage obtained with the scRNA sequencing is slightly lower than the results obtained by IHC. This is likely due to the dissection method used for scRNA sequencing. The isolated area is larger than the actual PVN (Fig. 23), and GRs are strongly expressed in this region, leading to the observed "dilution" of the GR/CRF colocalization. However, the cKO isn't specific to the PVN, and for example, CeA also shows a certain degree of co-expression between GR and CRF (around 30% Fig. 6). Thus the effects observed might not be entirely specific to the deletion in the PVN.

6.2 Effect of GRs deletion in CRF-expressing neurons in mice

Mice displaying GRs deletion in CRF-expressing neurons show a normal circadian rhythm, with a rise of CORT before the beginning of the active phase of the mice (dark phase), and a drop of CORT few hours before the start of the rest period (light phase). The circadian rhythm is not affected by the deletion, only its intensity is changed. When the mice approach the dark phase, the CORT levels increase more importantly in the cKO mice than in the Ctrl mice (Fig. 29). A decrease in GC-negative feedback sensitivity is the most likely explanation for the changes in HPA axis settings assessed here. Those findings emphasizes that normal HPA axis rhythmicity does not require GRs in CRF-expressing neurons. Further more, cKO mice have similar body weight compared to Ctrl mice, bigger adrenal glands and smaller thymus. The last two findings reflect the chronic higher CORT exposure in cKO mice described above. Daily higher CORT levels exposure commonly increases adrenal weight, in Human and in rodents (Carroll et al., 1976; Ulrich-Lai et al., 2006).

Impaired function of the GR and consequently an altered negative feedback regulation of the HPA axis have regularly been shown to be critical features in the progress, evolution and resolution of psychiatric disorders (Anacker et al., 2011). GR deletion in CRF-expressing neurons did not alter locomotion, anxiety, and stress-coping behaviour. $GR^{CRF\text{-}cKO}$ mice displayed no behavioural distortion, which could be expected considering that the deletion mostly affects the PVN, a brain structure that is rarely involved in emotional behaviour, although we cannot rule out the fact that the deletion of GR in the CeA can have effects, as some of the neurocircuits responsible for emotional behaviour and anxiety involve the CeA. On the the contrary, Boyle and colleagues showed that removal of GR in forebrain structures (GR-αCaMKII-cKO) but not in the hypothalamic PVN induced a robust depression-like phenotype (Boyle, 2005). Since GRs do not need to be recruited for normal anxiety-related behavior in basal conditions (Oitzl et al., 2001), it would appear relevant to submit our cKO mice to a more chronic form of stress. In the scenario of repeated stress and/or prolonged stress, the exacerbated corticosterone phenotype of $GR^{CRF\text{-}cKO}$ mice might also be able to alter the behavioral outcome. Indeed, we believe that GRs are necessary for long term recruitment and not to cope with an acute stress response.

Next, HPA axis responsiveness was assessed in $GR^{CRF\text{-}Ctrl}$ and $GR^{CRF\text{-}cKO}$ mice by means of the dexamethasone (Dex)/CRF test (Fig. 33). Two independent tests were performed using either a low or a relatively high dose of Dex to assess GR negative feedback at the level of the pituitary alone or at the level of pituitary and brain, respectively. In both tests, $GR^{CRF\text{-}cKO}$ mice showed significantly higher afternoon CORT levels under basal conditions compared to $GR^{CRF\text{-}Ctrl}$ mice. This difference is similar to what we previously observed when we investigated the physiology of the mice. As expected, the low dose of Dex strongly suppressed adrenocortical activity in $GR^{CRF\text{-}Ctrl}$ mice, but was ineffective in $GR^{CRF\text{-}cKO.}$ Both genotypes responded to stimulation with CRF with a similar increase in CORT levels. On the other hand, the high dose of Dex strongly suppressed adrenocortical activity in both genotypes. The suppression was maintained in $GR^{CRF\text{-}Ctrl}$ mice even after CRF stimulation, while CRF was able to increase CORT levels in $GR^{CRF\text{-}cKO}$ mice. Thus $GR^{CRF\text{-}cKO}$ mice exhibit a weaker negative feedback at the level of the pituitary and a higher sensitivity to CRF than $GR^{CRF\text{-}Ctrl}$ mice.

6.3 Response to acute stress in *GR*$^{CRF\text{-}cKO}$ mice

Restraint is among the most frequently applied stressors in mice and rats to elicit a stress response. There is a broad variation between the different methods, including duration of the restraint and type of restraint (including restraint in tubes or wire mesh, or immobilization of the limbs with tape to a surface; see Glavin et al. for review, 1994; Buynitsky & Mostofsky, 2009). Surely these factors affect the magnitude of the response in the animals (Armario et al., 1984; Blanchard et al., 1997; Van Pett et al., 2000). Variations in measurements after stress (such as circulating CORT levels or behavioral tests) and how long after the stress they happen have also been reported in the literature, making the comparison of outcomes from different studies very challenging. The length of behavioural tests, in particular, varies greatly, i.e. several studies check for emotionality immediately after the stress period (Katz et al., 1981; Nosek et al., 2008) others include periods of differing length (Armario et al., 2008).

Furthermore, the duration of the test itself may affect the result. In a pilot experiment, we assessed different time point measurements to collect blood and measure CORT levels. We tested 5, 10, 15, and 20 min restraint. In our case, the peak was after 15 min restraint, so we decided to pursue our investigation with that time point. In rats, restraint stress has been successfully used to produce a habituation response (Akana, 1992; Dhabhar et al., 1997) in contrast to mice, where no protocols are available to the best of our knowledge and researchers have failed to model HPA habituation. NB: Since the end of our *in vivo* investigation, Kim and colleagues have shown habituation to white noise in mice (Kim, Joon S. *et al.*, 2019).

When exploring the HPA axis function of $GR^{CRF\text{-}cKO}$ mice, we demonstrated that circulating CORT levels after exposing mice to 15 min restraint stress were not different in Ctrl and cKO mice. It indicated that the stress response was not affected by the impaired GRs expression. Since the primary deletion was identified in the PVN, this indicates that PVN GRs are not necessary for the regulation of HPA axis activity under acute stress conditions. One hypothesis to explain the absence of a specific phenotype of $GR^{CRF\text{-}cKO}$ mice under basal conditions and after a single stress exposure might be the involvement and/or compensation of the other glucocorticoid receptor, MR. The discovery inside the brain of such stress-responsive membrane MRs has put forward the MR as an essential regulator of stress. Throughout the last decade, numerous reviews reported on a role of the MR in the behavior and activity of the HPA axis (Reul *et al.*, 2000; Joëls *et al.*, 2008). Researchers suggest that the association between the expression of MR and stress reactivity is bidirectional, since a response to stress can also influence the expression of MR (Groeneweg *et al.*, 2012). Both results seem to depend on the stressor's length. Acute stress raised the production of hippocampal MR that peaked after 24 h and then decreased over 48h (Gesing et al., 2001). Nonetheless, the GR deficiency in $GR^{CRF\text{-}cKO}$ was greater in the PVN, which is not a prevalent area for MR expression (Reul & De Kloet, 1985; Seckl et al., 1991). Alternatively, cKO mice may be able to compensate for the loss of PVN GR by alternative regulatory mechanisms, due to increased PVN-level signaling of the estrogen receptor (ER) (Lund et al., 2006).

Our results show no difference between cKO and Ctrl animals on CORT responses after the first episode of acute restraint stress. The response of glucocorticoids in interfering with the solicited circuitry during such conditions might, therefore, depends on the intensity and duration of the stimuli as well as the physiological request.

6.4 Role of GRs in habituation of the HPA axis

6.4.1 Effect of repeated homotypic stress in cKO mice

To further investigate how deletion of GRs in CRF neurons impact stress response and especially if the mice are able to reach habituation of the HPA axis, they were subjected to a Repeated Restraint Stress protocol (RRS, Fig. 36a). $GR^{CRF\text{-}Ctrl}$ mice exhibited a gradual decrease in plasma CORT levels compared to $GR^{CRF\text{-}cKO}$ animals and the effect of the RRS was dependent on the genotype. This decrease in plasma CORT levels is the result of habituation of the HPA axis response in $GR^{CRF\text{-}Ctrl}$ mice, as shown by the significant difference in CORT level between RRS1 and RRS3 (Fig. 36 c left plot). This habituation is, however, completely absent in $GR^{CRF\text{-}cKO}$ animals. It indicates that GRs in the PVN are likely not needed for primo stress response but essential for regulating the stress response over time, especially in case of repeated stressful events. Control mice were able to habituate to a homotypic stressor while $GR^{CRF\text{-}cKO}$ mice lost this ability. Taken together, these findings suggest that the mechanisms of glucocorticoid signaling vary significantly between the types of stress exposure.

HPA habituation was observed in rats after repeated exposure to moderate stressors (Dhabhar et al., 1994). In these situations, the intensity of the response decreases with each exposure, even as novel stressors facilitate the responses. A decreased activation of Fos is linked to the lowered physiological responses. Paraventricular thalamus lesions suppress CORT reaction habituations to repetitive restraints without influencing acute responsiveness (Bhatnagar et al., 2002; Fernandes, 2002). Combined with the facilitation effects of lesions in this area, paraventricular thalamus tends to be critical in transmitting information about the chronicity of stress exposure. This region receives dense afferences from the ventral subiculum and the mPFC (Sesack et al., 1989; Cullinan et al., 1993) and projects densely to the CeA (Li & Kirouac, 2008) presenting a potential intermediary relay between stress-inhibitory and stress-excitatory brain areas. According to our GR / CRF colocalization studies and the rescue experiment performed by AAV injection in the PVN, our data showed that, in mice, the mechanisms underlying HPA habituation involve GR expression in CRF neurons of the PVN. It contradicts with a study done in rats, where the habituation process appears to require MRs, because systemic therapy with MR antagonists reverses the decreased CORT responses to repeated restraint in rats (Cole, 2000). However, we did not tested if MR antagonists could also blocked HPA habituation in our model. This could be added to future experiments.

While there is a wealth of literature explaining HPA axis habituation in rats, very little is known in mice. In the laters, chronic social stress produces limited habituation of heart-rate responses to attack in submissive, but not dominant mice (Bartolomucci, 2003). Thus, chronic social defeat might not be the most adapted paradigm to study HPA habituation since it is a strong and traumatic stressor and usually repeated daily over a long period. We believe that habituation can take place if a mild stress is presented with sufficient time between two exposures. Otherwise, a strong exposure of stress does not allow the stress response system to relapse and makes memory traces impossible. Chronic stress produces long-lasting alterations in autonomic functions, such as decreased blood pressure variability (Farah et al., 2004). Chronic stress in rats may recruit distinct pathways from those participating in acute responses. It was shown that lesions of the paraventricular thalamus prevent the development of chronic-stress induced facilitation of HPA-axis activation but do not impact responses to acute exposure of stress (Bhatnagar & Dallman, 2002) indicating the role of this region during repeated, chronic stress exposure. On the opposite, hippocampal lesions do not affect chronic stress-related HPA-axis responses (Herman & Mueller, 2006) suggesting that the role of the hippocampus in HPA-axis regulation is decreased upon repeated stress exposure. The neuronal pathways influencing the habituation of autonomic changes caused by chronic stress have yet to be investigated, as was the case with response facilitation.

6.4.2 Targeted re-expression of GRs can restore HPA habituation in $GR^{CRF\text{-}cKO}$ mice

HPA habituation to RRS is absent in cKO mice. Since GRs are removed from every CRF neurons of the brain with the mean of the Cre/LoxP system, we aimed to assess whether GR in CRF neurons of the PVN accurately could mediate the HPA habituation.

We choose to specifically investigate the PVN region since it is an essential structure for HPA habituation, and CRF is strongly expressed within this region.

To ask whether the absence of habituation depends exclusively on the removal of GR from the PVN's CRF+ neurons, we produced a viral vector that allows for Cre-dependent expression of murine GR (AAV1/2-Ef1α-DIO-Flag-mGR). Bilateral injection of AAV-DIO-mGR into the PVN of GRCRF-cKO mice led to the specific re-expression of GRs in PVN CRF+ neurons (Fig. 38). Four weeks after virus injection, when the mice were subjected to our RRS protocol, plasma CORT levels in all three groups of mice were indistinguishable under baseline conditions (RRS1, RRS2 and RRS3). $GR^{CRF\text{-}Ctrl}$ mice injected with AAV-DIO-mGR showed a normal habituation to RRS, comparable to the one observed in non-injected $GR^{CRF\text{-}Ctrl}$ mice (Fig 39). Conversely, $GR^{CRF\text{-}cKO}$ mice injected with control AAV-DIO-mCherry confirmed the previously observed absence of HPA axis habituation. Notably, the re-expression of GRs alone in the PVN of $GR^{CRF\text{-}cKO}$ mice was sufficient to restore the habituation of the HPA axis to the RRS.

6.5 Electrophysiological characterization of GR / CRF neurons and impact on HPA habituation

We next investigated the possible mechanisms underlying this GR-dependent habituation of the HPA axis to RRS in GRCRF-Ctrl mice. After RRS, $GR^{CRF\text{-}cKO}$ showed higher Crh mRNA expression in the PVN compared to GRCRF-Ctrl mice, as well as higher levels of stress-induced cFos mRNA (Fig. 4a), suggesting higher stress induced CRF expression and neuronal activity in the PVN, thus leading to higher plasma CORT levels. Thus, we hypothesized that a change in intrinsic properties and/or excitability of CRF+ neurons of the PVN could lead to the decreased CORT release observed after RRS in GRCRF-Ctrl mice.

Taken together, our data highlight the role of GR in CRF-expressing neurons in HPA habituation. The changes in mEPSCs and mIPSCs frequency suggest that RRS induced a decrease in excitation and an increase in inhibition in Ctrl mice that is lost in cKO mice, explained by changes in presynaptic properties. Our findings are supported by

Nahar and colleagues, who demonstrated that in PVN magnocellular neurons, glucocorticoids affect synaptic transmission in a postsynaptic G protein-dependent mechanism. They proposed the involvement of eCB as a retrograde messenger for modulating presynaptic glutamate release and that the glucocorticoid-induced facilitation of GABA synaptic inputs onto magnocellular neurons is mediated by the retrograde action of NO (Nahar et al., 2015), in rats.

The RRS-induced inhibitory/excitatory shift was romved in slices from cKO mice in which the classical nuclear GR was removed in a tissue-specific manner. Thereby, the absence of these effects in slices from cKO mice uncovers the loss in the glucocorticoid signaling mechanism of a major element with the deletion of exon 3 of GR. Our data show that under basal conditions, CRF neurons of the PVN exhibit the same intrinsic electrical properties – with or without GRs-, and a similar glutamatergic and GABAergic synaptic drive in both genotypes, suggesting that GRs deletion does not affect all these parameters. However and more interestingly, when subjected to a stressful challenge (here an exposure to RRS), control mice show a decreased excitatory and an increased inhibitory drive. This shift in excitatory/inhibitory balance towards more inhibition is likely to explain the decrease in circulating CORT level observed in control mice exposed to RRS. Indeed a stronger inhibitory drive onto CRF neurons of the PVN would prevent these neurons from being activated upon exposition to a stressor, impairing the activation of the HPA at the first level and thus decreasing CORT release by the adrenals, leading to the observed habituation. It is also interesting to note that this effect seems to be mediated by GRs since their deletion in CRF neurons is sufficient to entirely abolish both the effects on circulating CORT levels and synaptic inputs after stress exposure.

To sum up, GR deletion from CRF+ neurons does not affect their intrinsic electrical properties nor the HPA axis response to a single stressor. Nevertheless, we showed that, upon repetition of the same stressor (RRS), control mice exhibit habituation of the HPA axis, as confirmed by reduced plasma CORT levels. The HPA axis habituation is dependent on GR expression in CRF neurons of the PVN and does not require changes in the intrinsic electrical properties of these neurons. Such results contrast with the recently published study showing CORT-independent rapid adaptation of CRF neurons to repeated white-noise applications, reported by *in vivo* calcium imaging (Kim et al., 2019). In our research, HPA habituation is likely to be mediated by changing the excitation / inhibition balance towards a more potent inhibitory tone to the PVN CRF+ neurons, leading to lower CORT release from the adrenal glands. Although the mechanism behind reduced excitation has yet to be discovered, we have shown that increased inhibition is mediated by GR-dependent retrograde NO activity on the presynaptic side, leading to an increased release probability of GABA. Another likely possibility, which could explain our results is that exposure to RRS could decrease the number of glutamatergic and increase the number of GABAergic synapses onto CRF neurons, leading to the previously-mentioned effects.

As mentioned above, repetitive immobilization induced a genomic GR-dependent impairment of eCB signaling in GABAergic and glutamatergic synapses on parvocellular PVN neurons; however, without discriminating among the different populations of parvocellular neurons. Other studies have shown a fast non-genomic and synapse-specific GC effect driven by retrograde eCB signaling to glutamatergic synapses and NO signaling to GABAergic synapses to magnocellular and parvocellular PVN neurons. This modulation causes significant changes in the electrical activity of these neurons and, therefore, in the release of peptides (i.e., oxytocin, vasopressin, thyrotropin-releasing hormone, and CRF). In addition, it has been shown that the rapid non-genomic GC effect involves the expression of the classical nuclear GR, since its deletion in the PVN fully removes the effect on synaptic transmission. It is nonetheless unclear whether this mechanism takes place endogenously. Because Dex was bath-applied to brain slices, it is hard to draw final conclusions about the physiological regulation of the neural networks that underlie stress reactions. Here, we have demonstrated that GR-dependent retrograde signaling is an endogenous, essential component of the PVN's HPA axis habituation to a repeated stressor by dampening synaptic transmission onto CRF+ neurons.

We may conclude from our study that GRs in CRF-expressing neurons of the PVN has a significant role in facilitating the negative feedback on the HPA axis leading to the habituation process.

Collectively, our data highlights a role for GRs in CRF-expressing neurons in controlling repeated neuroendocrine responses to stressful exposure, and further illustrate the propensity for differential involvement of brain regions that regulate the HPA axis responses under acute vs. repeated stress paradigm. Moreover, these data indicate that the rapid inhibition of the HPA axis, a crucial step towards limiting the magnitude and length of fast stress responses to glucocorticoids, is largely regulated by local, perhaps nongenomic glucocorticoid behavior.

6.6 Conclusion and future directions

Thus, the current research study provides a new set of data that positions the GR-CRF system confidently as a crucial player in the executive function following repeated stress exposure, thus offering a molecular mechanism through which this effect occurs. It hence shows a possible pharmacological target which could support in the production of active measures to mitigate the deleterious effects of repeated stress exposure. Further studies can be considered, such as the eCB hypothesis and the investigation of the number of glutamatergic and GABAergic synapses onto CRF neurons following RRS. It will be beneficial to also explore different types of stressors and different combinations of repeated stressors.

7 References

Akana, S. F. Feedback and facilitation in the adrenocortical system: unmasking facilitation by partial inhibition of the glucocorticoid response to prior stress. Endocrinology, v. 131, p. 57-68, // 1992.

Anderzhanova, E.; Kirmeier, T.; Wotjak, C. T. Animal models in psychiatric research: The RDoC system as a new framework for endophenotype-oriented translational neuroscience. Neurobiol Stress, v. 7, p. 47-56, Dec 2017. ISSN 2352-2895 (Print) 2352-2895.

Armario, A.; Castellanos, J. M.; Balasch, J. Adaptation of anterior pituitary hormones to chronic noise stress in male rats. Behav Neural Biol, v. 41, n. 1, p. 71-6, May 1984. ISSN 0163-1047.

Armario, A.; Escorihuela, R. M.; Nadal, R. Long-term neuroendocrine and behavioural effects of a single exposure to stress in adult animals. Neurosci Biobehav Rev, v. 32, n. 6, p. 1121-35, Aug 2008. ISSN 0149-7634.

Bale, T. L., & Chen, A. (2012). Minireview: CRF and Wylie Vale: a story of 41 amino acids and a Texan with grit. Endocrinology, 153(6), 2556-2561. doi:10.1210/en.2012-1273.

Bale, T. L., Anderson, K. R., Roberts, A. J., Lee, K. F., Nagy, T. R., & Vale, W. W. (2003). Corticotropin-releasing factor receptor-2-deficient mice display abnormal homeostatic responses to challenges of increased dietary fat and cold. Endocrinology, 144(6), 2580-2587. doi:10.1210/en.2002-0091.

Bali, B., Ferenczi, S., & Kovacs, K. J. (2008). Direct inhibitory effect of glucocorticoids on corticotrophin-releasing hormone gene expression in neurones of the paraventricular nucleus in rat hypothalamic organotypic cultures. J Neuroendocrinol, 20(9), 1045-1051. doi:10.1111/j.1365-2826.2008.01759.x.

Bamberger, C. M., Bamberger, A. M., de Castro, M., & Chrousos, G. P. (1995). Glucocorticoid receptor beta, a potential endogenous inhibitor of glucocorticoid action in humans. J Clin Invest, 95(6), 2435-2441. doi:10.1172/jci117943.

Baram, T. Z., & Lerner, S. P. (1991). Ontogeny of corticotropin releasing hormone gene expression in rat hypothalamus--comparison with somatostatin. Int J Dev Neurosci, 9(5), 473-478.

Bartolomucci, A. Chronic psychosocial stress persistently alters autonomic function and physical activity in mice. Physiol. Behav., v. 80, p. 57-67, // 2003.

Beck, I. M., De Bosscher, K., & Haegeman, G. (2011). Glucocorticoid receptor mutants: man-made tools for functional research. Trends Endocrinol Metab, 22(8), 295-310. doi:10.1016/j.tem.2011.03.009.

Behan, D. P., De Souza, E. B., Lowry, P. J., Potter, E., Sawchenko, P., & Vale, W. W. (1995). Corticotropin releasing factor (CRF) binding protein: a novel regulator of CRF and related peptides. Front Neuroendocrinol, 16(4), 362-382. doi:10.1006/frne.1995.1013.

Belzung, C., & Lemoine, M. (2011). Criteria of validity for animal models of psychiatric disorders: focus on anxiety disorders and depression. Biol Mood Anxiety Disord, 1(1), 9. doi:10.1186/2045-5380-1-9.

Berridge, C. W., & Waterhouse, B. D. (2003). The locus coeruleus-noradrenergic system: modulation of behavioral state and state-dependent cognitive processes. Brain Res Brain Res Rev, 42(1), 33-84.

Berton, O., McClung, C. A., Dileone, R. J., Krishnan, V., Renthal, W., Russo, S. J., . . . Nestler, E. J. (2006). Essential role of BDNF in the mesolimbic dopamine pathway in social defeat stress. Science, 311(5762), 864-868. doi:10.1126/science.1120972.

Bhatnagar, S. et al. Lesions of the posterior paraventricular thalamus block habituation of hypothalamic-pituitary-adrenal responses to repeated restraint. J Neuroendocrinol, v. 14, n. 5, p. 403-10, May 2002. ISSN 0953-8194.

Bhatnagar, S., & Meaney, M. J. (1995). Hypothalamic-pituitary-adrenal function in chronic intermittently cold-stressed neonatally handled and non-handled rats. J Neuroendocrinol, 7(2), 97-108.

Bhatnagar, S., Lee, T. M., & Vining, C. (2005). Prenatal stress differentially affects habituation of corticosterone responses to repeated stress in adult male and female rats. Horm Behav, 47(4), 430-438. doi:10.1016/j.yhbeh.2004.11.019.

Bhatnagar, S.; Dallman, M. Neuroanatomical basis for facilitation of hypothalamic-pituitary-adrenal responses to a novel stressor after chronic stress. Neuroscience, v. 84, n. 4, p. 1025-39, Jun 1998. ISSN 0306-4522.

Biag, J., Huang, Y., Gou, L., Hintiryan, H., Askarinam, A., Hahn, J. D., Dong, H. W. (2012). Cyto- and chemoarchitecture of the hypothalamic paraventricular nucleus in the C57BL/6J male mouse: a study of immunostaining and multiple fluorescent tract tracing. J Comp Neurol, 520(1), 6-33. doi:10.1002/cne.22698.

Binder, E. B.; Nemeroff, C. B. The CRF system, stress, depression and anxiety-insights from human genetic studies. Mol Psychiatry, v. 15, n. 6, p. 574-88, Jun 2010. ISSN 1359-4184.

Blanchard, R. J. et al. Differentiation of anxiolytic and panicolytic drugs by effects on rat and mouse defense test batteries. Neurosci Biobehav Rev, v. 21, n. 6, p. 783-9, Nov 1997. ISSN 0149-7634.

Boyle, M. P. Acquired deficit of forebrain glucocorticoid receptor produces depression-like changes in adrenal axis regulation and behavior. Proc. Natl Acad. Sci. Usa, v. 102, p. 473-478, // 2005.

Buijs, R. M.; Kalsbeek, A. Hypothalamic integration of central and peripheral clocks. Nat Rev Neurosci, v. 2, n. 7, p. 521-6, Jul 2001. ISSN 1471-003X (Print) 1471-003x

Butler, P. D. et al. Corticotropin-releasing factor produces fear-enhancing and behavioral activating effects following infusion into the locus coeruleus. J Neurosci, v. 10, n. 1, p. 176-83, Jan 1990. ISSN 0270-6474.

Buynitsky, T.; Mostofsky, D. I. Restraint stress in biobehavioral research: Recent developments. Neurosci Biobehav Rev, v. 33, n. 7, p. 1089-98, Jul 2009. ISSN 0149-7634.

Cannon, W. B. (1929). Bodily Changes in Pain, Hunger, Fear and Rage: An Account of Recent Researches into the Function of Emotional Excitement.

Chadman, K. K., Yang, M., & Crawley, J. N. (2009). Criteria for validating mouse models of psychiatric diseases. Am J Med Genet B Neuropsychiatr Genet, 150b(1), 1-11. doi:10.1002/ajmg.b.30777.

Chen, A. et al. Mouse corticotropin-releasing factor receptor type 2alpha gene: isolation, distribution, pharmacological characterization and regulation by stress and glucocorticoids. Mol Endocrinol, v. 19, n. 2, p. 441-58, Feb 2005. ISSN 0888-8809 (Print)0888-8809.

Chen, R., Lewis, K. A., Perrin, M. H., & Vale, W. W. (1993). Expression cloning of a human corticotropin-releasing-factor receptor. Proc Natl Acad Sci U S A, 90(19), 8967-8971.

Cole, M. A. Selective blockade of the mineralocorticoid receptor impairs hypothalamic-pituitary-adrenal axis expression of habituation. J. Neuroendocrinol., v. 12, p. 1034-1042, // 2000.

Cole, M. A., Kalman, B. A., Pace, T. W., Topczewski, F., Lowrey, M. J., & Spencer, R. L. (2000). Selective blockade of the mineralocorticoid receptor impairs hypothalamic-pituitary-adrenal axis expression of habituation. J Neuroendocrinol, 12(10), 1034-1042.

Cole, R. L., & Sawchenko, P. E. (2002). Neurotransmitter regulation of cellular activation and neuropeptide gene expression in the paraventricular nucleus of the hypothalamus. J. Neurosci., 22, 959-969.

Collins, P. Y., Patel, V., Joestl, S. S., March, D., Insel, T. R., Daar, A. S., . . . Stein, D. J. (2011). Grand challenges in global mental health. Nature, 475(7354), 27-30. doi:10.1038/475027a.

Conrad, C. D., LeDoux, J. E., Magarinos, A. M., & McEwen, B. S. (1999). Repeated restraint stress facilitates fear conditioning independently of causing hippocampal CA3 dendritic atrophy. Behav Neurosci, 113(5), 902-913.

Cooney, R. E., Joormann, J., Eugene, F., Dennis, E. L., & Gotlib, I. H. (2010). Neural correlates of rumination in depression. Cogn Affect Behav Neurosci, 10(4), 470-478. doi:10.3758/cabn.10.4.470.

Cullinan, W. E.; Herman, J. P.; Watson, S. J. Ventral subicular interaction with the hypothalamic paraventricular nucleus: evidence for a relay in the bed nucleus of the stria terminalis. J. Comp. Neurol., v. 332, p. 1-20, // 1993.

Dallman, M. F., Akana, S. F., Bell, M. E., Bhatnagar, S., Choi, S., Chu, A., Viau, V. (1999). Warning! Nearby construction can profoundly affect your experiments. Endocrine, 11(2), 111-113. doi:10.1385/endo:11:2:111.

Dallman, M. F., Akana, S. F., Cascio, C. S., Darlington, D. N., Jacobson, L., & Levin, N. (1987). Regulation of ACTH secretion: variations on a theme of B. Recent Prog Horm Res, 43, 113-173.

Dautzenberg, F. M., & Hauger, R. L. (2002). The CRF peptide family and their receptors: yet more partners discovered. Trends Pharmacol Sci, 23(2), 71-77.

De Bellis, M. D. et al. Association of fluoxetine treatment with reductions in CSF concentrations of corticotropin-releasing hormone and arginine vasopressin in patients with major depression. Am J Psychiatry, v. 150, n. 4, p. 656-7, Apr 1993. ISSN 0002-953X (Print) 0002-953x.

de Kloet, E. R. (2000). Stress in the brain. Eur J Pharmacol, 405(1-3), 187-198.

de Kloet, E. R., Joels, M., & Holsboer, F. (2005). Stress and the brain: from adaptation to disease. Nat Rev Neurosci, 6(6), 463-475. doi:10.1038/nrn1683.

De Kloet, E. R., Vreugdenhil, E., Oitzl, M. S., & Joels, M. (1998). Brain corticosteroid receptor balance in health and disease. Endocr. Rev., 19, 269-301.

De Kloet, E. R.; Joels, M.; Holsboer, F. Stress and the brain: from adaptation to disease. Nat Rev Neurosci, v. 6, n. 6, p. 463-75, Jun 2005. ISSN 1471-003X.

Decavel, C., & Van Den Pol, A. N. (1990). GABA: a dominant neurotransmitter in the hypothalamus. J. Comp. Neurol., 302, 1019-1037.

Dedic, N. et al. Chronic CRH depletion from GABAergic, long-range projection neurons in the extended amygdala reduces dopamine release and increases anxiety. Nat Neurosci, v. 21, n. 6, p. 803-807, Jun 2018. ISSN 1097-6256.

Dedic, N., Chen, A., & Deussing, J. M. (2018). The CRF Family of Neuropeptides and their Receptors - Mediators of the Central Stress Response. Curr Mol Pharmacol, 11(1), 4-31. doi:10.2174/1874467210666170302104053.

Dedic, N., Touma, C., Romanowski, C. P., Schieven, M., Kuhne, C., Ableitner, M., Deussing, J. M. (2012). Assessing behavioural effects of chronic HPA axis activation using conditional CRH-overexpressing mice. Cell Mol Neurobiol, 32(5), 815-828. doi:10.1007/s10571-011-9784-0.

Deussing, J. M.; Wurst, W. Dissecting the genetic effect of the CRH system on anxiety and stress-related behaviour. C R Biol, v. 328, n. 2, p. 199-212, Feb 2005. ISSN 1631-0691.

Dhabhar, F. S. et al. Diurnal and Acute Stress-Induced Changes in Distribution of Peripheral Blood Leukocyte Subpopulations. Brain, Behavior, and Immunity, v. 8, n. 1, p. 66-79, 1994/03/01/ 1994. ISSN 0889-1591.

Dhabhar, F. S.; McEwen, B. S.; Spencer, R. L. Adaptation to prolonged or repeated stress–comparison between rat strains showing intrinsic differences in reactivity to acute stress. Neuroendocrinology, v. 65, p. 360-368, // 1997.

Dobrakovova, M., Kvetnansky, R., Oprsalova, Z., & Jezova, D. (1993). Specificity of the effect of repeated handling on sympathetic-adrenomedullary and pituitary-adrenocortical activity in rats. Psychoneuroendocrinology, 18(3), 163-174.

Dostert, A., & Heinzel, T. (2004). Negative glucocorticoid receptor response elements and their role in glucocorticoid action. Curr Pharm Des, 10(23), 2807-2816.

DSM-5. DSM-5 the Mental Illness Manual on Diagnostics and Statistics p. http:/www.dsm5.org/Pages/Default.aspx, 2013.

Elenkov, I. J. et al. The sympathetic nerve--an integrative interface between two supersystems: the brain and the immune system. Pharmacol Rev, v. 52, n. 4, p. 595-638, Dec 2000. ISSN 0031-6997 (Print) 0031-6997.

Emmert, M. H., & Herman, J. P. (1999). Differential forebrain c-fos mRNA induction by ether inhalation and novelty: evidence for distinctive stress pathways. Brain Res, 845(1), 60-67.

Esteban Ortiz-Ospina and Max Roser. Happiness and Life Satisfaction, 2013. Published online at OurWorldInData.org. 2013. Retrieved from: 'https://ourworldindata.org/happiness-and-life-satisfaction'.

Evans, R. T.; Seasholtz, A. F. Soluble corticotropin-releasing hormone receptor 2alpha splice variant is efficiently translated but not trafficked for secretion. Endocrinology, v. 150, n. 9, p. 4191-202, Sep 2009. ISSN 0013-7227.

Evanson, N. K. et al. Fast feedback inhibition of the HPA axis by glucocorticoids is mediated by endocannabinoid signaling. Endocrinology, v. 151, n. 10, p. 4811-9, Oct 2010. ISSN 0013-7227.

Farah, V. M. et al. Acute and chronic stress influence blood pressure variability in mice. Physiol. Behav., v. 83, p. 135-142, // 2004.

Fernandes, G. A. Habituation and cross-sensitization of stress-induced hypothalamic-pituitary-adrenal activity: effect of lesions in the paraventricular nucleus of the thalamus or bed nuclei of the stria terminalis. J. Neuroendocrinol., v. 14, p. 593-602, // 2002.

Fossey, M. D. et al. Cerebrospinal fluid corticotropin-releasing factor concentrations in patients with anxiety disorders and normal comparison subjects. Biol Psychiatry, v. 39, n. 8, p. 703-7, Apr 15 1996. ISSN 0006-3223.

Fritzsche, A., Dahme, B., Gotlib, I. H., Joormann, J., Magnussen, H., Watz, H., . . . von Leupoldt, A. (2010). Specificity of cognitive biases in patients with current depression and remitted depression and in patients with asthma. Psychol Med, 40(5), 815-826. doi:10.1017/s0033291709990948.

Gabr, R. W., Gladfelter, W. E., Birkle, D. L., & Azzaro, A. J. (1994). In vivo microdialysis of corticotropin releasing factor (CRF): calcium dependence of depolarization-induced neurosecretion of CRF. Neurosci Lett, 169(1-2), 63-67.

Gallagher, J. P. et al. Synaptic physiology of central CRH system. Eur J Pharmacol, v. 583, n. 2-3, p. 215-25, Apr 7 2008. ISSN 0014-2999.

Gallagher, J. P., Orozco-Cabal, L. F., Liu, J., & Shinnick-Gallagher, P. (2008). Synaptic physiology of central CRH system. Eur J Pharmacol, 583(2-3), 215-225. doi:10.1016/j.ejphar.2007.11.075.

Garcia, A., Marti, O., Valles, A., Dal-Zotto, S., & Armario, A. (2000). Recovery of the hypothalamic-pituitary-adrenal response to stress. Effect of stress intensity, stress duration and previous stress exposure. Neuroendocrinology, 72(2), 114-125. doi:10.1159/000054578.

Gesing, A. et al. Psychological stress increases hippocampal mineralocorticoid receptor levels: involvement of corticotropin-releasing hormone. The Journal of neuroscience: the official journal of the Society for Neuroscience, v. 21, n. 13, p. 4822-4829, 2001. ISSN 1529-2401.

Gill, H. et al. The Association Between Adverse Childhood Experiences and Inflammation in Patients with Major Depressive Disorder: A Systematic Review. J Affect Disord, v. 272, p. 1-7, Apr 5 2020. ISSN 0165-0327.

Girotti, M., Pace, T. W., Gaylord, R. I., Rubin, B. A., Herman, J. P., & Spencer, R. L. (2006). Habituation to repeated restraint stress is associated with lack of stress-induced c-fos expression in primary sensory processing areas of the rat brain. Neuroscience, 138(4), 1067-1081. doi:10.1016/j.neuroscience.2005.12.002.

Givalois, L., Arancibia, S., & Tapia-Arancibia, L. (2000). Concomitant changes in CRH mRNA levels in rat hippocampus and hypothalamus following immobilization stress. Brain Res Mol Brain Res, 75(1), 166-171.

Glavin, G. B. et al. Restraint stress in biomedical research: an update. Neurosci Biobehav Rev, v. 18, n. 2, p. 223-49, Summer 1994. ISSN 0149-7634.

Glavin, G. B., Pare, W. P., Sandbak, T., Bakke, H. K., & Murison, R. (1994). Restraint stress in biomedical research: an update. Neurosci Biobehav Rev, 18(2), 223-249.

Golier, J. A., Schmeidler, J., Legge, J., & Yehuda, R. (2007). Twenty-four hour plasma cortisol and adrenocorticotropic hormone in Gulf War veterans: relationships to posttraumatic stress disorder and health symptoms. Biol Psychiatry, 62(10), 1175-1178. doi:10.1016/j.biopsych.2007.04.027.

Grissom, N., & Bhatnagar, S. (2009). Habituation to repeated stress: get used to it. Neurobiol Learn Mem, 92(2), 215-224. doi:10.1016/j.nlm.2008.07.001.

Grissom, N., Iyer, V., Vining, C., & Bhatnagar, S. (2007). The physical context of previous stress exposure modifies hypothalamic-pituitary-adrenal responses to a subsequent homotypic stress. Horm Behav, 51(1), 95-103. doi:10.1016/j.yhbeh.2006.08.011.

Guardiola-Diaz, H. M., Boswell, C., & Seasholtz, A. F. (1994). The cAMP-responsive element in the corticotropin-releasing hormone gene mediates transcriptional regulation by depolarization. J Biol Chem, 269(20), 14784-14791.

Gunnar, M. R. (1992). Reactivity of the hypothalamic-pituitary-adrenocortical system to stressors in normal infants and children. Pediatrics, 90(3 Pt 2), 491-497.

Gunnar, M. R., & Donzella, B. (2002). Social regulation of the cortisol levels in early human development. Psychoneuroendocrinology, 27(1-2), 199-220.

Gunnar, M. R., & Nelson, C. A. (1994). Event-related potentials in year-old infants: relations with emotionality and cortisol. Child Dev, 65(1), 80-94.

Hartmann, J. et al. Forebrain glutamatergic, but not GABAergic, neurons mediate anxiogenic effects of the glucocorticoid receptor. Mol Psychiatry, v. 22, n. 3, p. 466-475, Mar 2017. ISSN 1359-4184.

Hartmann, J. et al. The involvement of FK506-binding protein 51 (FKBP5) in the behavioral and neuroendocrine effects of chronic social defeat stress. Neuropharmacology, v. 62, n. 1, p. 332-9, Jan 2012. ISSN 0028-3908.

Hennessy, J. W., Levin, R., & Levine, S. (1977). Influence of experiential factors and gonadal hormones on pituitary-adrenal response of the mouse to novelty and electric shock. J Comp Physiol Psychol, 91(4), 770-777.

Herman, J. P. Central mechanisms of stress integration: hierarchical circuitry controlling hypothalamo-pituitary-adrenocortical responsiveness. Front. Neuroendocrinol., v. 24, p. 151-180, // 2003.

Herman, J. P., & Cullinan, W. E. (1997). Neurocircuitry of stress: central control of the hypothalamo-pituitary-adrenocortical axis. Trends Neurosci, 20(2), 78-84.

Herman, J. P.; Mueller, N. K. Role of the ventral subiculum in stress integration. Behav. Brain Res., v. 174, p. 215-224, // 2006.

Hodges, J. R., & Mitchley, S. (1970). The effect of 'training' on the release of corticotrophin in response to minor stressful procedures in the rat. J Endocrinol, 47(2), 253-254.

Hollenberg, S. M., Weinberger, C., Ong, E. S., Cerelli, G., Oro, A., Lebo, R., . Evans, R. M. (1985). Primary structure and expression of a functional human glucocorticoid receptor cDNA. Nature, 318(6047), 635-641.

Holsboer F. The corticosteroid receptor hypothesis of depression. Neuropsychopharmacology, v. 23, n. 5, p. 477-501, Nov 2000. ISSN 0893-133X.

Holsboer, F. The rationale for corticotropin-releasing hormone receptor (CRH-R) antagonists to treat depression and anxiety. J Psychiatr Res, v. 33, n. 3, p. 181-214, May-Jun 1999. ISSN 0022-3956 (Print) 0022-3956.

Holsboer, F. The rationale for corticotropin-releasing hormone receptor (CRH-R) antagonists to treat depression and anxiety. J Psychiatr Res, v. 33, n. 3, p. 181-214, May-Jun 1999. ISSN 0022-3956.

Howell, M. P., & Muglia, L. J. (2006). Effects of genetically altered brain glucocorticoid receptor action on behavior and adrenal axis regulation in mice. Front Neuroendocrinol, 27(3), 275-284. doi:10.1016/j.yfrne.2006.05.001.

Hsu, D. T., Chen, F. L., Takahashi, L. K., & Kalin, N. H. (1998). Rapid stress-induced elevations in corticotropin-releasing hormone mRNA in rat central amygdala nucleus and hypothalamic paraventricular nucleus: an in situ hybridization analysis. Brain Res, 788(1-2), 305-310.

Hsu, S. Y., & Hsueh, A. J. (2001). Human stresscopin and stresscopin-related peptide are selective ligands for the type 2 corticotropin-releasing hormone receptor. Nat Med, 7(5), 605-611. doi:10.1038/87936.

Imaki, T., Nahan, J. L., Rivier, C., Sawchenko, P. E., & Vale, W. (1991). Differential regulation of corticotropin-releasing factor mRNA in rat brain regions by glucocorticoids and stress. J Neurosci, 11(3), 585-599.

Irwin, M.; Hauger, R.; Brown, M. Central corticotropin-releasing hormone activates the sympathetic nervous system and reduces immune function: increased responsivity of the aged rat. Endocrinology, v. 131, n. 3, p. 1047-53, Sep 1992. ISSN 0013-7227 (Print) 0013-7227.

Ising, M., & Holsboer, F. (2006). Genetics of stress response and stress-related disorders. Dialogues Clin Neurosci, 8(4), 433-444.

Jaferi, A., & Bhatnagar, S. (2006). Corticosterone can act at the posterior paraventricular thalamus to inhibit hypothalamic-pituitary-adrenal activity in animals that habituate to repeated stress. Endocrinology, 147(10), 4917-4930. doi:10.1210/en.2005-1393.

Jakobsson K, G. P. Occupational exposure and stroke - A critical review of shift work, and work-related psychosocial risk factors. Occup Environ Med, v. 71 Suppl 1:A100-A101, 2014.

Jeanneteau, F. D., Lambert, W. M., Ismaili, N., Bath, K. G., Lee, F. S., Garabedian, M. J., & Chao, M. V. (2012). BDNF and glucocorticoids regulate corticotrophin-releasing hormone (CRH) homeostasis in the hypothalamus. Proc Natl Acad Sci U S A, 109(4), 1305-1310. doi:10.1073/pnas.1114122109.

Joels, M., & Baram, T. Z. (2009). The neuro-symphony of stress. Nat Rev Neurosci, 10(6), 459-466. doi:10.1038/nrn2632.

Joormann, J., Gilbert, K., & Gotlib, I. H. (2010). Emotion identification in girls at high risk for depression. J Child Psychol Psychiatry, 51(5), 575-582. doi:10.1111/j.1469-7610.2009.02175.x.

Kadmiel, M., & Cidlowski, J. A. (2013). Glucocorticoid receptor signaling in health and disease. Trends Pharmacol Sci, 34(9), 518-530. doi:10.1016/j.tips.2013.07.003.

Kalueff, A. V.; Murphy, D. L. The importance of cognitive phenotypes in experimental modeling of animal anxiety and depression. Neural Plast, v. 2007, p. 52087, 2007. ISSN 1687-5443.

Katz, R. J.; Roth, K. A.; Carroll, B. J. Acute and chronic stress effects on open field activity in the rat: implications for a model of depression. Neurosci Biobehav Rev, v. 5, n. 2, p. 247-51, Summer 1981. ISSN 0149-7634.

Keen-Rhinehart, E., Michopoulos, V., Toufexis, D. J., Martin, E. I., Nair, H., Ressler, K. J., . . . Wilson, M. E. (2009). Continuous expression of corticotropin-releasing factor in the central nucleus of the amygdala emulates the dysregulation of the stress and reproductive axes. Mol Psychiatry, 14(1), 37-50. doi:10.1038/mp.2008.91.

Kendler, K. S., Karkowski, L. M., & Prescott, C. A. (1999). Causal relationship between stressful life events and the onset of major depression. Am J Psychiatry, 156(6), 837-841. doi:10.1176/ajp.156.6.837.

Kendler, K. S., Kessler, R. C., Walters, E. E., MacLean, C., Neale, M. C., Heath, A. C., & Eaves, L. J. (1995). Stressful life events, genetic liability, and onset of an episode of major depression in women. Am J Psychiatry, 152(6), 833-842. doi:10.1176/ajp.152.6.833.

Kim, J. S.; Han, S. Y.; Iremonge R, K. J. Stress experience and hormone feedback tune distinct components of hypothalamic CRH neuron activity. Nat Commun, v. 10, n. 1, p. 5696, Dec 13 2019. ISSN 2041-1723.

Kino, T.; SU, Y. A.; Chrousos, G. P. Human glucocorticoid receptor isoform beta: recent understanding of its potential implications in physiology and pathophysiology. Cell Mol Life Sci, v. 66, n. 21, p. 3435-48, Nov 2009. ISSN 1420-682x.

Klengel, T., & Binder, E. B. (2015). Epigenetics of Stress-Related Psychiatric Disorders and Gene x Environment Interactions. Neuron, 86(6), 1343-1357. doi:10.1016/j.neuron.2015.05.036

Koob, G. F.; Heinrichs, S. C. A role for corticotropin releasing factor and urocortin in behavioral responses to stressors. Brain Res, v. 848, n. 1-2, p. 141-52, Nov 27 1999. ISSN 0006-8993.

Koolhaas, J. M., Bartolomucci, A., Buwalda, B., de Boer, S. F., Flugge, G., Korte, S. M., . . . Fuchs, E. (2011). Stress revisited: a critical evaluation of the stress concept. Neurosci Biobehav Rev, 35(5), 1291-1301. doi:10.1016/j.neubiorev.2011.02.003.

Koolhaas, J. M., De Boer, S. F., De Rutter, A. J., Meerlo, P., & Sgoifo, A. (1997). Social stress in rats and mice. Acta Physiol Scand Suppl, 640, 69-72.

Kovacs, K. J. (2013). CRH: the link between hormonal-, metabolic- and behavioral responses to stress. J Chem Neuroanat, 54, 25-33. doi:10.1016/j.jchemneu.2013.05.003.

Kovács, K. J., & Sawchenko, P. E. (1996). Regulation of stress-induced transcriptional changes in the hypothalamic neurosecretory neurons. Journal of Molecular Neuroscience, 7(2), 125-133. doi:10.1007/bf02736792

Kraepelin, E. Textbook of Psychiatry. Abstracted and adapted from the 6th German edition of Lehrbuch der Psychiatrie [1899] by Defendorf (New York: A. R. Macmillan and Co.). 1902.

Kretz, O., Reichardt, H. M., Schutz, G., & Bock, R. (1999). Corticotropin-releasing hormone expression is the major target for glucocorticoid feedback-control at the hypothalamic level. Brain Res, 818(2), 488-491.

Kuperman, Y.; Chen, A. Urocortins: emerging metabolic and energy homeostasis perspectives. Trends Endocrinol Metab, v. 19, n. 4, p. 122-9, May-Jun 2008. ISSN 1043-2760 (Print) 1043-2760.

Laryea, G.; Schütz, G.; Muglia, L. J. Disrupting Hypothalamic Glucocorticoid Receptors Causes HPA Axis Hyperactivity and Excess Adiposity. Molecular Endocrinology, v. 27, n. 10, p. 1655-1665, 2013. ISSN 0888-8809.

Levine, S. (2001). Primary social relationships influence the development of the hypothalamic--pituitary--adrenal axis in the rat. Physiol Behav, 73(3), 255-260.

Levine, S., Huchton, D. M., Wiener, S. G., & Rosenfeld, P. (1991). Time course of the effect of maternal deprivation on the hypothalamic-pituitary-adrenal axis in the infant rat. Dev Psychobiol, 24(8), 547-558. doi:10.1002/dev.420240803.

Levine, S., Smotherman, W. P., & Hennessy, J. W. (1977). Pituitary-adrenal hormones and learned taste aversion. Adv Biochem Psychopharmacol, 17, 163-177.

Lewis, K., Li, C., Perrin, M. H., Blount, A., Kunitake, K., Donaldson, C.,Vale, W. W. (2001). Identification of urocortin III, an additional member of the corticotropin-releasing factor (CRF) family with high affinity for the CRF2 receptor. Proc Natl Acad Sci U S A, 98(13), 7570-7575. doi:10.1073/pnas.121165198.

Lewis-Tuffin, L. J., Jewell, C. M., Bienstock, R. J., Collins, J. B., & Cidlowski, J. A. (2007). Human glucocorticoid receptor beta binds RU-486 and is transcriptionally active. Mol Cell Biol, 27(6), 2266-2282. doi:10.1128/mcb.01439-06.

Li, S.; Kirouac, G. J. Projections from the paraventricular nucleus of the thalamus to the forebrain, with special emphasis on the extended amygdala. J. Comp. Neurol., v. 506, p. 263-287, // 2008.

Lister, R. G. The use of a plus-maze to measure anxiety in the mouse. Psychopharmacology (Berl), v. 92, n. 2, p. 180-5, 1987. ISSN 0033-3158.

Lovenberg, T. W., Chalmers, D. T., Liu, C., & De Souza, E. B. (1995). CRF2 alpha and CRF2 beta receptor mRNAs are differentially distributed between the rat central nervous system and peripheral tissues. Endocrinology, 136(9), 4139-4142. doi:10.1210/endo.136.9.7544278.

Lowy, M. T. et al. Glucocorticoid resistance in depression: the dexamethasone suppression test and lymphocyte sensitivity to dexamethasone. Am J Psychiatry, v. 141, n. 11, p. 1365-70, Nov 1984. ISSN 0002-953X.

Lu, A. et al. Conditional mouse mutants highlight mechanisms of corticotropin-releasing hormone effects on stress-coping behavior. Mol Psychiatry, v. 13, n. 11, p. 1028-42, Nov 2008. ISSN 1359-4184.

Lund, T. D.; Hinds, L. R.; Handa, R. J. The Androgen 5α-Dihydrotestosterone and Its Metabolite 5α-Androstan-3β, 17β-Diol Inhibit the Hypothalamo–Pituitary–Adrenal Response to Stress by Acting through Estrogen Receptor β-Expressing Neurons in the Hypothalamus. The Journal of Neuroscience, v. 26, n. 5, p. 1448-1456, 2006.

Lunga, P., & Herbert, J. (2004). 17Beta-oestradiol modulates glucocorticoid, neural and behavioural adaptations to repeated restraint stress in female rats. J Neuroendocrinol, 16(9), 776-785. doi:10.1111/j.1365-2826.2004.01234.x.

Lupien, S. J., McEwen, B. S., Gunnar, M. R., & Heim, C. (2009). Effects of stress throughout the lifespan on the brain, behaviour and cognition. Nat Rev Neurosci, 10(6), 434-445. doi:10.1038/nrn2639.

Ma, X. M., Camacho, C., & Aguilera, G. (2001). Regulation of corticotropin-releasing hormone (CRH) transcription and CRH mRNA stability by glucocorticoids. Cell Mol Neurobiol, 21(5), 465-475.

Makino, S., Asaba, K., Nishiyama, M., & Hashimoto, K. (1999). Decreased type 2 corticotropin-releasing hormone receptor mRNA expression in the ventromedial hypothalamus during repeated immobilization stress. Neuroendocrinology, 70(3), 160-167. doi:10.1159/000054472.

Marin, M. T., Cruz, F. C., & Planeta, C. S. (2007). Chronic restraint or variable stresses differently affect the behavior, corticosterone secretion and body weight in rats. Physiol Behav, 90(1), 29-35. doi:10.1016/j.physbeh.2006.08.021.

McEwen, B. S. (2004). Protection and damage from acute and chronic stress: allostasis and allostatic overload and relevance to the pathophysiology of psychiatric disorders. Ann N Y Acad Sci, 1032, 1-7. doi:10.1196/annals.1314.001.

McEwen, B. S. (2007). Physiology and neurobiology of stress and adaptation: central role of the brain. Physiol Rev, 87(3), 873-904. doi:10.1152/physrev.00041.2006.

McEwen, B. S.; Gianaros, P. J. Central role of the brain in stress and adaptation: links to socioeconomic status, health, and disease. Ann N Y Acad Sci, v. 1186, p. 190-222, Feb 2010. ISSN 0077-8923.

MCIlwain, K. L. et al. The use of behavioral test batteries: effects of training history. Physiol Behav, v. 73, n. 5, p. 705-17, Aug 2001. ISSN 0031-9384.

Menzaghi, F. et al. Functional impairment of hypothalamic corticotropin-releasing factor neurons with immunotargeted toxins enhances food intake induced by neuropeptide Y. Brain Res, v. 618, n. 1, p. 76-82, Jul 30 1993. ISSN 0006-8993.

Merchenthaler, I. (1984). Corticotropin releasing factor (CRF)-like immunoreactivity in the rat central nervous system. Extrahypothalamic distribution. Peptides, 5 Suppl 1, 53-69.

Muller, M. B. et al. Limbic corticotropin-releasing hormone receptor 1 mediates anxiety-related behavior and hormonal adaptation to stress. Nat Neurosci, v. 6, n. 10, p. 1100-7, Oct 2003. ISSN 1097-6256.

Muller, M. B., & Holsboer, F. (2006). Mice with mutations in the HPA-system as models for symptoms of depression. Biol Psychiatry, 59(12), 1104-1115. doi:10.1016/j.biopsych.2006.02.008

Muller, M. B.; Holsboer, F. Mice with mutations in the HPA-system as models for symptoms of depression. Biol Psychiatry, v. 59, n. 12, p. 1104-15, Jun 15 2006. ISSN 0006-3223.

Myers B, Mark Dolgas C, Kasckow J, Cullinan WE, Herman JP. Central stress-integrative circuits: forebrain glutamatergic and GABAergic projections to the dorsomedial hypothalamus, medial preoptic area, and bed nucleus of the stria terminalis. Brain Struct Funct. 2014;219(4):1287-1303. doi:10.1007/s00429-013-0566-y

Nahar, J. et al. Rapid Nongenomic Glucocorticoid Actions in Male Mouse Hypothalamic Neuroendocrine Cells Are Dependent on the Nuclear Glucocorticoid Receptor. Endocrinology, v. 156, n. 8, p. 2831-42, Aug 2015. ISSN 0013-7227.

Natelson, B. H., Ottenweller, J. E., Cook, J. A., Pitman, D., McCarty, R., & Tapp, W. N. (1988). Effect of stressor intensity on habituation of the adrenocortical stress response. Physiol Behav, 43(1), 41-46.

Nemeroff, C. B. et al. Elevated concentrations of CSF corticotropin-releasing factor-like immunoreactivity in depressed patients. Science, v. 226, n. 4680, p. 1342-4, Dec 14 1984. ISSN 0036-8075.

Nestler, E. J., & Hyman, S. E. (2010). Animal models of neuropsychiatric disorders. Nat Neurosci, 13(10), 1161-1169. doi:10.1038/nn.2647

Nosek, K. et al. Context and strain-dependent behavioral response to stress. Behav Brain Funct, v. 4, p. 23, Jun 2 2008. ISSN 1744-9081.

Oakley, R. H., & Cidlowski, J. A. (2011). Cellular processing of the glucocorticoid receptor gene and protein: new mechanisms for generating tissue-specific actions of glucocorticoids. J Biol Chem, 286(5), 3177-3184. doi:10.1074/jbc.R110.179325

Otto, C., Reichardt, H. M., & Schutz, G. (1997). Absence of glucocorticoid receptor-beta in mice. J Biol Chem, 272(42), 26665-26668.

Pacak, K., Palkovits, M., Makino, S., Kopin, I. J., & Goldstein, D. S. (1996). Brainstem hemisection decreases corticotropin-releasing hormone mRNA in the paraventricular nucleus but not in the central amygdaloid nucleus. J Neuroendocrinol, 8(7), 543-551.

Palkovits, M., Brownstein, M. J., & Vale, W. (1985). Distribution of corticotropin-releasing factor in rat brain. Fed Proc, 44(1 Pt 2), 215-219.

Park, J. B., Skalska, S., Son, S., & Stern, J. E. (2007). Dual GABAA receptor-mediated inhibition in rat presympathetic paraventricular nucleus neurons. J. Physiol., 582, 539-551.

Pearce, D. (1994). A mechanistic basis for distinct mineralocorticoid and glucocorticoid receptor transcriptional specificities. Steroids, 59(2), 153-159.

Perrin, M. H., Donaldson, C. J., Chen, R., Lewis, K. A., & Vale, W. W. (1993). Cloning and functional expression of a rat brain corticotropin releasing factor (CRF) receptor. Endocrinology, 133(6), 3058-3061. doi:10.1210/endo.133.6.8243338

Perrin, M., Donaldson, C., Chen, R., Blount, A., Berggren, T., Bilezikjian, L., Vale, W. (1995). Identification of a second corticotropin-releasing factor receptor gene and characterization of a cDNA expressed in heart. Proc Natl Acad Sci U S A, 92(7), 2969-2973.

Pfister, H. P. (1979). The glucocorticosterone response to novelty as a psychological stressor. Physiol Behav, 23(4), 649-652.

Pilpel, N. et al. Rapid, reproducible transduction of select forebrain regions by targeted recombinant virus injection into the neonatal mouse brain. Journal of neuroscience methods, v. 182, n. 1, p. 55-63, 2009/08// 2009. ISSN 0165-0270.

Plotsky, P. M. (1985). Hypophyseotropic regulation of adenohypophyseal adrenocorticotropin secretion. Fed Proc, 44(1 Pt 2), 207-213.

Porsolt, R. D.; Bertin, A.; Jalfre, M. Behavioral despair in mice: a primary screening test for antidepressants. Arch Int Pharmacodyn Ther, v. 229, n. 2, p. 327-36, Oct 1977. ISSN 0003-9780.

Ramot, A. et al. Hypothalamic CRFR1 is essential for HPA axis regulation following chronic stress. Nat Neurosci, v. 20, n. 3, p. 385-388, Mar 2017. ISSN 1097-6256.

Reul, J. M., & de Kloet, E. R. (1985). Two receptor systems for corticosterone in rat brain: microdistribution and differential occupation. Endocrinology, 117, 2505-2511.

Reul, J. M.; De Kloet, E. R. Two receptor systems for corticosterone in rat brain: microdistribution and differential occupation. Endocrinology, v. 117, p. 2505-2511, // 1985.

Reyes, T. M., Lewis, K., Perrin, M. H., Kunitake, K. S., Vaughan, J., Arias, C. A., Sawchenko, P. E. (2001). Urocortin II: a member of the corticotropin-releasing factor (CRF) neuropeptide family that is selectively bound by type 2 CRF receptors. Proc Natl Acad Sci U S A, 98(5), 2843-2848. doi:10.1073/pnas.051626398

Roland, B. L., & Sawchenko, P. E. (1993). Local origins of some GABAergic projections to the paraventricular and supraoptic nuclei of the hypothalamus of the rat. J. Comp. Neurol., 332, 123-143.

Romanov, R. A., Alpar, A., Zhang, M. D., Zeisel, A., Calas, A., Landry, M., Harkany, T. (2015). A secretagogin locus of the mammalian hypothalamus controls stress hormone release. Embo j, 34(1), 36-54. doi:10.15252/embj.201488977

Rosenfeld, P., Gutierrez, Y. A., Martin, A. M., Mallett, H. A., Alleva, E., & Levine, S. (1991). Maternal regulation of the adrenocortical response in preweanling rats. Physiol Behav, 50(4), 661-671.

Rosenfeld, P., Wetmore, J. B., & Levine, S. (1992). Effects of repeated maternal separations on the adrenocortical response to stress of preweanling rats. Physiol Behav, 52(4), 787-791.

Sandi, C., & Pinelo-Nava, M. T. (2007). Stress and memory: behavioral effects and neurobiological mechanisms. Neural Plast, 2007, 78970. doi:10.1155/2007/78970

Sapolsky, R. M., Romero, L. M., & Munck, A. U. (2000). How do glucocorticoids influence stress responses? Integrating permissive, suppressive, stimulatory, and preparative actions. Endocr Rev, 21(1), 55-89. doi:10.1210/edrv.21.1.0389

Sawchenko, P. E. (1987). Evidence for differential regulation of corticotropin-releasing factor and vasopressin immunoreactivities in parvocellular neurosecretory and autonomic-related projections of the paraventricular nucleus. Brain Res, 437(2), 253-263.

Schmidt, M. V., Enthoven, L., van der Mark, M., Levine, S., de Kloet, E. R., & Oitzl, M. S. (2003). The postnatal development of the hypothalamic-pituitary-adrenal axis in the mouse. Int J Dev Neurosci, 21(3), 125-132.

Schmidt, M. V., Sterlemann, V., Wagner, K., Niederleitner, B., Ganea, K., Liebl, C., . . . Muller, M. B. (2009). Postnatal glucocorticoid excess due to pituitary glucocorticoid receptor deficiency: differential short- and long-term consequences. Endocrinology, 150(6), 2709-2716. doi:10.1210/en.2008-1211

Seasholtz, A. F., Burrows, H. L., Karolyi, I. J., & Camper, S. A. (2001). Mouse models of altered CRH-binding protein expression. Peptides, 22(5), 743-751.

Seasholtz, A. F., Valverde, R. A., & Denver, R. J. (2002). Corticotropin-releasing hormone-binding protein: biochemistry and function from fishes to mammals. J Endocrinol, 175(1), 89-97.

Seckl, J. R. et al. Distribution of glucocorticoid and mineralocorticoid receptor messenger RNA expression in human postmortem hippocampus. Brain Research, v. 561, n. 2, p. 332-337, 1991/10/11/ 1991. ISSN 0006-8993.

Selye, H. (1980). Changing Distress Into Eustress. Tex. Med. 1980;, 76, 78–80.

Sesack, S. R. et al. Topographical organization of the efferent projections of the medial prefrontal cortex in the rat: an anterograde tract-tracing study with Phaseolus vulgaris leucoagglutinin. J. Comp. Neurol., v. 290, p. 213-242, // 1989.

Simeon, D., Knutelska, M., Yehuda, R., Putnam, F., Schmeidler, J., & Smith, L. M. (2007). Hypothalamic-pituitary-adrenal axis function in dissociative disorders, post-traumatic stress disorder, and healthy volunteers. Biol Psychiatry, 61(8), 966-973. doi:10.1016/j.biopsych.2006.07.030

Slattery, D. A.; Cryan, J. F. Using the rat forced swim test to assess antidepressant-like activity in rodents. Nat Protoc, v. 7, n. 6, p. 1009-14, May 3 2012. ISSN 1750-2799.

Solomon, M. B. et al. Neuroendocrine Function After Hypothalamic Depletion of Glucocorticoid Receptors in Male and Female Mice. Endocrinology, v. 156, n. 8, p. 2843-53, Aug 2015. ISSN 0013-7227.

Steckler, T., & Holsboer, F. (1999). Corticotropin-releasing hormone receptor subtypes and emotion. Biol Psychiatry, 46(11), 1480-1508.

Strack, A. M. et al. CNS cell groups regulating the sympathetic outflow to adrenal gland as revealed by transneuronal cell body labeling with pseudorabies virus. Brain Res, v. 491, n. 2, p. 274-96, Jul 10 1989. ISSN 0006-8993 (Print) 0006-8993.

Sutton, R. E. et al. Corticotropin releasing factor produces behavioural activation in rats. Nature, v. 297, n. 5864, p. 331-3, May 27 1982. ISSN 0028-0836.

Swanson, L. W., & Sawchenko, P. E. (1980). Paraventricular nucleus: a site for the integration of neuroendocrine and autonomic mechanisms. Neuroendocrinology, 31(6), 410-417. doi:10.1159/000123111

Taniguchi, H. et al. A resource of Cre driver lines for genetic targeting of GABAergic neurons in cerebral cortex. Neuron, v. 71, n. 6, p. 995-1013, Sep 22 2011. ISSN 0896-6273.

Thompson, R. F., & Spencer, W. A. (1966). Habituation: a model phenomenon for the study of neuronal substrates of behavior. Psychol Rev, 73(1), 16-43.

Thomson, F., & Craighead, M. (2008). Innovative approaches for the treatment of depression: targeting the HPA axis. Neurochem Res, 33(4), 691-707. doi:10.1007/s11064-007-9518-3

Touma, C. et al. FK506 binding protein 5 shapes stress responsiveness: modulation of neuroendocrine reactivity and coping behavior. Biol Psychiatry, v. 70, n. 10, p. 928-36, Nov 15 2011. ISSN 0006-3223.

Touma, C. et al. Mice selected for high versus low stress reactivity: a new animal model for affective disorders. Psychoneuroendocrinology, v. 33, n. 6, p. 839-62, Jul 2008. ISSN 0306-4530.

Tronche, F. et al. Disruption of the glucocorticoid receptor gene in the nervous system results in reduced anxiety. Nat Genet, v. 23, n. 1, p. 99-103, Sep 1999. ISSN 1061-4036.

Tsagarakis, S.; Grossman, A. Corticotropin-Releasing Hormone: Interactions with the Immune System. Neuroimmunomodulation, v. 1, n. 6, p. 329-334, 1994. ISSN 1021-7401

Uht, R. M., McKelvy, J. F., Harrison, R. W., & Bohn, M. C. (1988). Demonstration of glucocorticoid receptor-like immunoreactivity in glucocorticoid-sensitive vasopressin and corticotropin-releasing factor neurons in the hypothalamic paraventricular nucleus. J Neurosci Res, 19(4), 405-411, 468-409. doi:10.1002/jnr.490190404

Urani, A., Chourbaji, S., & Gass, P. (2005). Mutant mouse models of depression: candidate genes and current mouse lines. Neurosci Biobehav Rev, 29(4-5), 805-828. doi:10.1016/j.neubiorev.2005.03.020

Vale, W. et al. Characterization of a 41-residue ovine hypothalamic peptide that stimulates secretion of corticotropin and beta-endorphin. Science, v. 213, n. 4514, p. 1394-7, Sep 18 1981. ISSN 0036-8075.

Vale, W., Spiess, J., Rivier, C., & Rivier, J. (1981). Characterization of a 41-residue ovine hypothalamic peptide that stimulates secretion of corticotropin and beta-endorphin. Science, 213(4514), 1394-1397.

Valentino, R. J., & Van Bockstaele, E. (2008). Convergent regulation of locus coeruleus activity as an adaptive response to stress. Eur J Pharmacol, 583(2-3), 194-203. doi:10.1016/j.ejphar.2007.11.062

Valentino, R. J.; Page, M. E.; Curtis, A. L. Activation of noradrenergic locus coeruleus neurons by hemodynamic stress is due to local release of corticotropin-releasing factor. Brain Res, v. 555, n. 1, p. 25-34, Jul 26 1991. ISSN 0006-8993 (Print) 0006-8993.

Van pett, K. et al. Distribution of mRNAs encoding CRF receptors in brain and pituitary of rat and mouse. J Comp Neurol, v. 428, n. 2, p. 191-212, Dec 11 2000. ISSN 0021-9967.

Vaughan, J., Donaldson, C., Bittencourt, J., Perrin, M. H., Lewis, K., Sutton, S., et al. (1995). Urocortin, a mammalian neuropeptide related to fish urotensin I and to corticotropin-releasing factor. Nature, 378(6554), 287-292. doi:10.1038/378287a0

Vita, N., Laurent, P., Lefort, S., Chalon, P., Lelias, J. M., Kaghad, M., Ferrara, P. (1993). Primary structure and functional expression of mouse pituitary and human brain corticotrophin releasing factor receptors. FEBS Lett, 335(1), 1-5.

Vogel, W. H., & Jensh, R. (1988). Chronic stress and plasma catecholamine and corticosterone levels in male rats. Neurosci Lett, 87(1-2), 183-188.

Walker, C. D., Sapolsky, R. M., Meaney, M. J., Vale, W. W., & Rivier, C. L. (1986). Increased pituitary sensitivity to glucocorticoid feedback during the stress nonresponsive period in the neonatal rat. Endocrinology, 119(4), 1816-1821. doi:10.1210/endo-119-4-1816

Wamsteeker Cusulin, J. I., T. Fuzesi, W. Inoue and J. S. Bains (2013). Glucocorticoid feedback uncovers retrograde opioid signaling at hypothalamic synapses. Nat Neurosci 16(5): 596-604.

Wang, X. D., Su, Y. A., Wagner, K. V., Avrabos, C., Scharf, S. H., Hartmann, J., . . . Schmidt, M. V. (2013). Nectin-3 links CRHR1 signaling to stress-induced memory deficits and spine loss. Nat Neurosci, 16(6), 706-713. doi:10.1038/nn.3395

Watts, A. G. (2005). Glucocorticoid regulation of peptide genes in neuroendocrine CRH neurons: a complexity beyond negative feedback. Front Neuroendocrinol, 26(3-4), 109-130. doi:10.1016/j.yfrne.2005.09.001

Wei, Q. et al. Glucocorticoid receptor overexpression in forebrain: a mouse model of increased emotional lability. Proc Natl Acad Sci U S A, v. 101, n. 32, p. 11851-6, Aug 10 2004. ISSN 0027-8424.

WHO. World Health Organization. 2017.

Woolley, C. S., Gould, E., Frankfurt, M., & McEwen, B. S. (1990). Naturally occurring fluctuation in dendritic spine density on adult hippocampal pyramidal neurons. J Neurosci, 10(12), 4035-4039.

Yehuda, R., Teicher, M. H., Trestman, R. L., Levengood, R. A., & Siever, L. J. (1996). Cortisol regulation in posttraumatic stress disorder and major depression: a chronobiological analysis. Biol Psychiatry, 40(2), 79-88. doi:10.1016/0006-3223(95)00451-3

Yudt, M. R., Jewell, C. M., Bienstock, R. J., & Cidlowski, J. A. (2003). Molecular origins for the dominant negative function of human glucocorticoid receptor beta. Mol Cell Biol, 23(12), 4319-4330.

Zorn JV, Schür RR, Boks MP, Kahn RS, Joëls M, Vinkers CH. Cortisol stress reactivity across psychiatric disorders: A systematic review and meta-analysis. Psychoneuroendocrinology.2017;77:25-36.

Zorrilla, E. P.; Koob, G. F. Progress in corticotropin-releasing factor-1 antagonist development. Drug Discov Today, v. 15, n. 9-10, p. 371-83, May 2010. ISSN 1359-6446.

8 Appendix

8.1 Abbreviations

35S	Isotope 35 of sulphur
3v	third ventricle
5-HT	5-hydroxytryptamine (serotonin)
AAc	Alpha-actinin-2
AAV	Adeno-associated virus
AAV-DIO-mCherry	control virus
AAV-DIO-mGR	over-expressing mouse glucocorticoid receptor virus: over-expressing virus
AC	Anterior Cingulate
AcbSh	Nucleus accumbens shell
ACSF	Artificial Cerebrospinal Fluid
ACTH	Adreno-Corticotropic Hormone
AKAP	A-Kinase Anchoring Proteins
AMP	Adenosine monophosphate
Amy	Amygdala
ANOVA	Analysis of Variance
AOL	Anterior olfactory area
Apit	Anterior pituitary
aRNA	Amplified ribonucleic acid
ATP	Adenosine triphosphate
AUC	Area under the Curve

avBNST	anterior part of the BNST
AVP	Arginine vasopressin
Bar	Barrington’s nucleus
BDI	Beck depression inventory
BDNF	Brain-derived neurotrophic factor
BLA	Basolateral nucleus of the amygdala
BNST	Bed Nucleus of the Stria Terminalis
bp	Base pairs
BPD	Bipolar disorder
Ca2+	Calcium
CAMK2α	Calcium/calmodulin-dependent protein kinase type II alpha
CaMKII	Ca+/calmodulin-dependent protein kinase II
cAMP	cyclic Adenosine Monophosphate
CAR	Cortisol Awakening Response
Cas	CRISP-associated protein
cDNA	Copy DNA
CeA	Central nucleus of the amygdala
CGS	central gray, spinal cord
cKO	Conditional knockout
CLOCK	(gene) Circadian Locomotor Output Cycles Kaput (transcription factor)
CMV	Cytomegalovirus
CNS	Central Nervous System
COE	Conditional overexpression
CoIP	Co-immunoprecipitation
CORT	Corticosterone

cOV-mGR	conditional over-expressing mouse glucocorticoid receptor (plasmid or virus)
Cp	Crossing point
Cpm	Counts per minute
CPu	Caudate putamen
Cre	Cyclization recombination
CREB	cAMP Response Element Binding Protein
CRF	Corticotropin Releasing Factor
CRF-BP	CRF binding protein
CRFR1	Corticotropin Releasing Factor Receptor 1
CRFR2	Corticotropin Releasing Factor Receptor 2
CRH	Corticotrophin-Releasing Hormone
Crh+	Crf expressing
CRHBP	Corticotropin-releasing hormone binding protein
CRHR	Corticotropin-releasing hormone receptor
CRISP	Clustered regulatory interspaced short palindromic repeats
CSDS	Chronic social defeat stress
CSF	Cerebrospinal fluid
Ctrl	Control
Ctx	cortex
D1/DRP1	Dopamine receptor 1
DA	Dopamine
DAG	Diacylglycerol
DaLi	Dark-light box
DAOA	D-Amino acid oxidase activator
DAPI	4’,6-diamidino-2-phenylindole

DAT/SLC6A3	Dopamine transporter
dB	Decibel
dDG	Dorsal Dentate Gyrus
Del	Deleter
DEPC	Diethyl Pyrocarbonate
DEX	Dexamethasone
DG	Dentate Gyrus
dHip	Dorsal Hippocampus
dHPC	dorsal hipocampus
DIO	Double-floxed inverted open reading frame
DISC1	Disrupted in schizophrenia 1
DLPFC	Dorsolateral Preforntal Cortex
DLX5/6	Homeodomain transcription factor (s) related to the Drosophila distalles (Dll) gene
DMH	dorsomedial hypothalamus
DMSO	Dimethyl sulfoxide
DMX	dorsal motor nucleus of the vagus nerve
DNA	Deoxyribonucleic acid
dNTP	Desoxyribonucleotide triphosphate
Dock 10	Dedicator of cytokinesis protein 10
DOPAC	3,4-dihydroxyphenylacetic acid
Dox	Doxycycline
DSB	Double strand break
DSM	Diagnostic and Statistical Manual of Mental Disorders
DTT	1,4-dithiothreitol
E	Embryonic

E. Coli	Escherichia coli
e.g.	exempli gratia, meaning “for example"
eCB	endocanabinoid
EDTA	Ethylenediaminetetraacetic acid
EF1α	Expression of elongation factor 1α
ELS	Early-life Stress
EPM	Elevated plus-maze
ER	Estrogen receptor
ERK	Extracellular-signal-regulated kinase
ES	cells Embryonic stem cells
EtOH	Ethanol
eYFP	enhanced Yellow fluorescent protein
FB	Forebrain
fEPSP	Field excitatory post-synaptic potential
FGF	Fibroblast growth factor
Fig.	figure
FKBP5	FK506 binding protein 5
FLEX	Flip-excision
flop	Floxed stop
Flp	Flipase
FR	Fixed ratio
frt	Flp recognition target
FST	Forced swim test
g	Gram
GABA	Gamma-Aminobutyric Acid

Gad65	Glutamic acid decarboxylase (molecular weight 65 kDa)
Gad67	Glutamic acid decarboxylase (molecular weight 67 kDa)
GC	Glucocorticoids
GCs	Glucocorticoids
GEF	Guanyl-nucleotide Exchange Factor
GFAP	Glial fibrillary acidic protein
GFP	Green fluorescent protein
Gl	Glomerular layer of the olfactory bulb
Glu	Glutamate
Glur6	Glutamate receptor, ionotropic, kainite 2
GPCR	G-protein coupled receptor
GR	Glucocorticoid receptor
$GR^{CRF\text{-}cKO}$	conditional knock out mice: cKO mice
$GR^{CRF\text{-}Ctrl}$	Control mice
GRE	Glucocorticoid Response Element
GRs	glucocorticoid receptors
GSK-3β	Glycogen synthase kinase 3β
GWAS	Genom-wide association study
GxE	Gene × Environment
h	Hour
H2O	water
HB	Habenula nucleus
HDR	Homology directed repair
HEK	Human embryonic kidney cells
Het	Heterozygous
HFS	High frequency stimulation

Hip	Hippocampus
Hom	Homozygous
HPA	Hypothalamic-pituitary-adrenocortical
HPRT	Hypoxanthine-Guanine Phosphoribosyltransferase
HR	High Reactivity
HVA	Homovanilic acid
HY	Hypothalamus
Hz	Hertz
IC	Inferior colliculus
ICS	Intracellular calcium stores
ICV/i.v.c	Intracerebroventricular
iDA	Inducible dopaminergic (Cre)
IEG	Immediate early gene
iFB	Inducible forebrain-specific (Cre)
Ifitm1	Interferon-induced transmembrane protein
IHC	Immunohistochemistry
IL	Infralimbic
IML	intermediolateral column, spinal cord
IO	Inferior olive
IP3	Inositol 1,4,5-trisphosphate
IR	Intermediate Reactivity
IRES	Internal ribosome entry site
ISH	In situ hybridization
ITI	Inter-trial Interval
kb	Kilobasepairs

kDa	Kilodalton
KO	Knockout
KW	Kruskal Wallis test
LacZ	Gene encoding β-galactosidase
LBD	Ligand binding domain
LC	Locus Coeruleus
LGE	Lateral ganglionic eminence
LHA	Lateral hypothalamic area
LiCl	Lithium chloride
Lmol	Stratum lacunosum
L-NAME	nitric oxide synthase 1 inhibitor
loxP	Locus of crossover [x] of P1
LR	Low Reactivity
LTCC	L-type calcium channel
LTD	Long-term depression
LTP	Long-Term Potentiation
L-type	Long-lasting type
LV	Lentivirus
M	Molar
MAOA	Monoamine Oxidase A
MAOI	Monoamine Oxidase Inhibitor
MAPK	Mitogen Activated Protein Kinase
MDD	Major Depressive Disorder
MeA	Medial nucleus of the amygdala
mEPSCs	miniature excitatory synaptic currents
mEPSP	Miniature excitatory post-synaptic potential

MgCl2	Magnesium chloride
MGM	Medial ganglionic eminence
mGR	mouse glucocorticoid receptor
MHB	Mid/hindbrain
Mi	Mitral layer of the olfactory bulb
min	Minute
mIPSCs	miniature inhibitory postsynaptic currents
MM	Mammillary nucleus
MoDG	moleculare layer of the dentate gyrus
mPFC	medial Prefrontal Cortex
mPOA	medial preoptic region
MR	Mineralocorticoid receptor
mRNA	Messenger ribonucleic acid
MSN	Medium spiny neurons
Mt1	Metallothionine 1
MWM	Morris water-maze
Myk	Myshkin
NA	Noradrenaline
NAc	Nucleus accumbens
Neo	Neomycin
NET/SLC6A2	Norepinephrine transporter
Nex	Helix-loop-helix transcription factor
Nfib	Nuclear factor I/B
NHEJ	Non-homologous end joining
NHS	N-hydroxysuccinimid

NMDA	N-Methyl-D-aspartic acid
NMDAR	N-Methyl-D-aspartic acid receptor
NO	nitric oxide
NPY	Neuropeptide Y
Nr3c1	GR gene
NRG1	Neuregulin 1
ns	non significant
NT	Neurotransmitter
o.n.	Over night
OB	Olfactory bulb
OCD	Obsessive Compulsive Disorder
OD	Optical density
OE	Overexpression
OF	Open field
OFT	Open Field Test
ONPG	Ortho-nitrophenyl-β-galactoside
ORF	Open reading frame
ORT	Object Recognition Test
oxy	oxytocin
P	Postnatal Day
P/S	Penicillin/streptomycin
pA	pico ampere
PAG	Periaqueductal grey
PB	Parabrachial nucleus
pBNST	BNST's posterior areas
PBS	Phosphate buffered saline

PCP	Phencyclidine
PCR	Polymerase chain reaction
PFA	Paraformaldehyde
PFC	Prefrontal Cortex
Pir	Piriform cortex
PKA	Protein Kinase A
PKA-C	Protein Kinase A Catalytic subunit
PKA-R	Protein Kinase A Regulatory subunit
PKB	Protein Kinase B
PKC	Protein Kinase C
PL	Prelimbic
PN	Pontine nucleus
PoDG	Polymorph DG
POMC	Proopiomelanocortin
PPI	Prepulse inhibition
pPVN	peri-PVN
PR	Progressive ratio
PSD-95	Pos-tsynaptic density protein 95
PTSD	Posttraumatic Stress Disorder
PV	parvalbumin
PVC	Polyvinyl chloride
PVN	Paraventricular nucleus of the hypothalamus
PVNam	paraventricular hypothalamic nucleus, anterior magnocellular part
PVNdp	paraventricular hypothalamic nucleus, descending division, dorsal parvocellular part

PVNf	paraventricular hypothalamic nucleus, descending division, forniceal part
PVNlp	paraventricular hypothalamic nucleus, lateral parvocellular
PVNmm	paraventricular hypothalamic nucleus medial magnocellular
PVNmpd	paraventricular hypothalamic nucleus, medial parvicellular part, dorsal zone
PVNmpv	paraventricular hypothalamic nucleus, medial parvicellular part, ventral zone
PVNpml	paraventricular hypothalamic nucleus, posterior magnocellular part, lateral zone
PVNpmm	paraventricular hypothalamic nucleus, posterior magnocellular part, medial zone
PVNpv	paraventricular hypothalamic nucleus, periventricular part
qRT-PCR	Quantitative real-time polymerase chain reaction
REM	Rapid-Eye Movement
RGN	RNA-guided endonucleases
rIPFC	Right Inferior Prefrontal Cortex
RM-ANOVA	Repeated measures analysis of variance
RN	Raphe nucleus
RNA	Ribonucleic acid
Rpm	Rounds per minute
RRS	repeated restraint stress
RRS1	first repeated restraint stress
RRS2	second repeated restraint stress
RRS3	third repeated restraint stress
Rt	Room temperature
RyR	Ryanodine receptor
s	Second

SA	Social avoidance
SAM	Sympathetic Adrenal Medullary Axis
SC	Superior colliculus
SCP	Stresscopin
scRNA	single cell RNA
SCZ	Schizophrenia
SEM	Standard error of mean
SFO	step-function opsins
SHANK3	SH3 and multiple ankyrin repeat domains 3
shRNA	short hairpin RNA
Sim1GR−/−	Single minded 1 , is a transcription factor involved in brain patterning and control of energy balance
SN	Substantia nigra
SNP	Single nucleotide polymorphism
SOC	Super optimal broth
Sp	Septum
SS	somatostatin
TAE	Tris acetate EDTA
TALEN	transcription activator-like effector nucleases
Taq	T. aquaticus: Taq polymerase
TB	Tubulin
TEA	Triethanolamine
TEI	Traumatic events inventory
tetO	Tetracycline operator
tg	Transgenic
TH	Thalamus

TH	Tyrosine hydroxylase
Thy1	Also known as CD90 (cluster of differentiation 90)
TRAP	Targeted recombination in active populations
TRH	thyrotropin-releasing hormone
Tris	Trisaminomethane
TRKB	Tyrosine kinase B receptor
TST	Tail suspension test
tTA	Tetracycline transactivator
U	Unit(s)
UCN	Urocortins
um	micrometer
UMAP	Uniform Manifold Approximation and Projection
UTP	Uridine triphosphate
UV	Ultra violet
VDCC	Voltage-dependent calcium channel
Vglut (1-3)	Vesicular glutamate transporter (1-3)
vHip	Ventral hippocampus
VIP	Vasoactive intestinal peptide
vlDMH	ventrolateral portion of the dorsomedial hypothalamus
VMPFC	Ventromedial Prefrontal Cortex
vs.	versus
VTA	Ventral tegmental area
WB	Western blot
WCM	Water-cross maze
wt	Wild-type
αCaMKII	α-calcium/calmodulin-dependent protein kinase II

8.2 Acknowledgements

Without the help and support of many people, the work comprised in this thesis would not have been possible. It was a long journey since my first day as a PhD student until now. Especially, I would like to sincerely thank:

The jury members, Dr Mathias Schmidt, Prof. Laura Busse, Prof. Anja Horn-Bochtler, Prof. Thomas Nägele, Prof. Heinrich Leohnardt and Prof. Nils Dingemanse for generously offering their time, support and good will, throughout the re-view of this document.

My supervisor, **Alon Chen,** for accepting me as one of his students and always finding time to meet with me to discuss my project, guide my experiments into fruitful directions, and provide me with all the means and motivation to move this research forward. Thank you for enabling me to develop, pursue this project, and establish my professional life. Thank you also for opening my eyes and mind to a different culture and continent.

Jan Deussing, for his great co-supervision, guidance, and support during this project. Thank you for always having your door open and advising me.

Mathias Schmidt for his permanent support, his advice and expertise regarding behavioural experiments, for being my Doktorvater and member of my Thesis Advisory Committee. Some of your inputs and comments helped me a lot to get a clearer picture of my project and decide on the next steps.

Guy Griebel, for being my supervisor and mentor when I started my master's thesis. You helped me to develop my scientific mind and made me realized how much I like to work in Science. Thank you for being a member of my Thesis Advisory Committee and see me growing, scientifically.

I also want to thank **Heike Junkert** for her never-failing help in many administrative matters.

My friend, collaborator, co-author, scientific big brother, **Julien Dine**, without your help, many of the projects would not have been possible.

Silja McIlwrick, my fashion queen, **Georgia Balsevich,** my favorite Canadian that I miss a lot**,** **Suellen Almeida,** my good-vibe-girl, **Alec Dick,** my favorite hipster**,** thank you guys for many coffee breaks and relaxing lunch times, for jumping in to help me with sample collections when needed, for always being there to share methods, to check presentation, and to discuss ideas, for being real friends along those years. I am very grateful for having you by my side during those years.

My parents, who gave me the two most beautiful gifts: roots, to always remember where I come from, and wings to explore the world. **Mes parents**, pour m'avoir donné les deux plus beaux cadeaux qui existent: de solides racines et des ailes pour explorer le monde.

Quirin, for showing up on my road one day, and never leaving. Thank you for caring and believing in me. Thank you for this fantastic little monster that makes our life more fun (and sleep-deprived!) for almost 3 years and without whom this work would have been finished yeeeeaaaaars ago! but family first <3

To all these individuals that I have mentioned and to everyone else who supported me throughout this journey, Vielen herzlichen Dank!

8.3 Affidavit

I hereby declare, that the submitted thesis entitled “STRESS, A MATTER OF BALANCE" is my own work. I have only used the sources indicated and have not made unauthorised use of services of a third party. Where the work of others has been quoted or reproduced, the source is always given.

I further declare that the submitted thesis or parts thereof have not been presented as part of an examination degree to any other university.

Munich, 05/10/2020 Carine Dournes

8.4 Declaration of author contributions

The work of this thesis is summarized in a manuscript, submitted to the journal Nature Neuroscience, and currently under revision. Additional experiments are ongoing.

All listed authors contributed to this manuscript: Carine Dournes, Julien Dine, Juan-Pablo Lopez, Elena Brivio, Elmira Anderzhanova, Simone Roeh, Claudia Kuehne, Maria Holzapfel, Rosa-Eva Huett, Rainer Stoffe, Lisa Tietze, Carola Eggert, Marcel Schieven, Mira Jakovcevski, Jan M. Deussing & Alon Chen.

Carine Dournes, Alon Chen, Jan M. Deussing and Julien Dine designed the study. Carine Dournes conducted all the experiments except the electrophysiology part that was performed by Julien Dine. Carine Dournes and Julien Dine prepared the manuscript. Alon Chen and Jan M. Deussing edited the manuscript and supervised the study. All authors approved to all modifications and approval of the final version of the manuscript.

8.5 Curriculum vitae

MY EDUCATION

Ph.D candidate
Max Planck Institute, Department of Stress Neurobiology and Neurogenetics Munich, GER | Jan 2014 - April 2018. graduation ***March 2021***

Certificate of Laboratory Animal Science Course B314
(FELASA cat B), *Munich, Germany | 2014 - LTK validation 2018*

M.Sc in Neuropsychopharmacology, major in R&D, clinical trial and addiction
Bordeaux University, FR | 2011

Maitrise (4th-year college degree) of Biology and Health
University Paul Sabatier, Toulouse, FR | 2010

B.Sc in Cell biology and Physiology
Limoges, FR | 2009